NASA CONTRACTOR REPORT

NASA CR-2363

NASA CR-2363

EXPERIMENTAL INVESTIGATION OF A $4\frac{1}{2}$-STAGE TURBINE WITH VERY HIGH STAGE LOADING FACTOR

II - Turbine Performance

by N. D. Walker and M. W. Thomas

Prepared by
GENERAL ELECTRIC COMPANY
Cincinnati, Ohio 45215
for Lewis Research Center

NATIONAL AERONAUTICS AND SPACE ADMINISTRATION • WASHINGTON, D. C. • FEBRUARY 1974

1. Report No. NASA CR-2363	2. Government Accession No.	3. Recipient's Catalog No.
4. Title and Subtitle EXPERIMENTAL INVESTIGATION OF A $4\frac{1}{2}$-STAGE TURBINE WITH VERY HIGH STAGE LOADING FACTOR II - TURBINE PERFORMANCE		5. Report Date January 1974
		6. Performing Organization Code
7. Author(s) N.D. Walker and M.W. Thomas		8. Performing Organization Report No. GE 73 AEG 163
		10. Work Unit No.
9. Performing Organization Name and Address General Electric Company 1 Jimson Road Cincinnati, Ohio 45215		11. Contract or Grant No. NAS 3-15322
		13. Type of Report and Period Covered Contractor Report
12. Sponsoring Agency Name and Address National Aeronautics and Space Administration Washington D.C. 20546		14. Sponsoring Agency Code

15. Supplementary Notes

Final Report. Project Manager, Warren J. Whitney, Fluid System Components Division, NASA Lewis Research Center, Cleveland, Ohio

16. Abstract

The experimental test program results of a $4\frac{1}{2}$-stage turbine with a very high stage loading factor are presented. A four-stage turbine was tested with and without outlet turning vanes. The $4\frac{1}{2}$-stage turbine achieved a design point total-to-total efficiency of 0.853. The outlet turning vane design point performance was 0.4 percent of the overall $4\frac{1}{2}$-stage turbine efficiency. Tests were conducted at various levels of Reynolds number and indicated decreases in turbine efficiency and equivalent weight flow with decreasing Reynolds number.

17. Key Words (Suggested by Author(s))	18. Distribution Statement
Turbine, Very high stage loading factor, Lift fan engine system, Outlet turning vane	Unclassified - unlimited Cat.28

19. Security Classif. (of this report)	20. Security Classif. (of this page)	21. No. of Pages	22. Price*
Unclassified	Unclassified	94	$3.75

* For sale by the National Technical Information Service, Springfield, Virginia 22151

TABLE OF CONTENTS

LIST OF TABLES

LIST OF ILLUSTRATIONS

LIST OF ILLUSTRATIONS (Continued)

LIST OF ILLUSTRATIONS (Concluded)

SUMMARY

The experimental results of the program are presented. The object of this program was to provide technology for fan drive turbines utilizing very high stage loading. A four-stage turbine was tested with and without outlet turning vanes.

The four and one-half stage turbine achieved a total-to-total efficiency of 0.853 at the design equivalent speed ($N/\sqrt{\theta_{cr}}$ = 2171.2 rev/min) and design total-to-total pressure ratio (P_{T_1}/P_{T_3} = 2.66).

The outlet turning vanes were successful in turning the turbine exit flow to axial at all of the operating conditions investigated. The test results indicate that approximately 0.5 percent loss in overall 4-1/2-stage turbine efficiency at 100% speed and design work is attributed to the outlet turning vane performance when based on measured turbine exhaust total pressures. However, a difference of only 0.08 percent loss in performance was indicated when based on calculated exhaust total pressure.

The 4-1/2-stage turbine radial efficiency profile showed high efficiency in the pitchline region with a slight decrease toward the tip and a heavy loss in the hub region.

Reynolds number testing, accomplished by varying the inlet pressure (density level), indicated decreases in efficiency and equivalent weight flow with decreasing Reynolds number. Radial efficiency profiles indicated the hub region sustained the greatest increase in loss with decreasing Reynolds number.

INTRODUCTION

A twenty-one month analytical and experimental investigation program was conducted to provide technology for fan drive turbines utilizing very high stage loading. The technology is specifically applicable to multi-stage configurations for advanced high bypass ratio, direct lift turbofan propulsion system applications.

The expanding role of the turbofan engine stems from its inherent design flexibility to exploit the cycle advantage afforded through a small gas generator core in conjunction with a fan selected to provide improved fuel consumption and thrust characteristics. Advanced research investigations of the propulsion requirements for direct lift fan engine systems indicate these systems will have high bypass ratio turbofan engines.

The size of a lift engine is as important as its weight. A V/STOL airplane will require twelve to fourteen of these engines to be mounted, involving considerable pod area and weight. If twelve or more lift engines are installed per airplane, it is apparent that engine cost will be a significant factor in the total airplane cost. Since number of parts and components has an effect on cost, there is an incentive to reduce the number of stages in a fan drive turbine.

The foregoing considerations of V/STOL engine requirements suggest the following fan drive turbine requirements:

1. Minimum number of stages (short, less cost)

2. Some SFC penalty acceptable (relative to cruise engine)

Combined with the low rotor speed (non-geared), these requirements imply a fan drive turbine with meanline average loading ($gJ\Delta h/2\Sigma U_p^2$) in the 2-2.5 range and efficiencies in the 80% to 85% range for lift engine operation. A fan drive turbine design of this type can save two to three stages with minimum impact on lift engine fuel consumption, while having a beneficial effect on installation weight, drag, and cost.

The specific objective of this program was to design, build, and test a very highly loaded four-stage fan drive turbine with outlet turning vanes.

The program was divided into two phases encompasssing eight task items of activity. The first phase covered Task Items I and II. The purpose of Task I was to investigate parametric turbine velocity diagram studies. Task II involved selecting one turbine design for which detailed aerodynamic, mechanical, and rig modification sub-tasks were performed. The results of Tasks I and II were reported in Reference 1.

The second phase covered the remaining tasks of this program including the following: (a) fabrication and procurement of turbine blading, casing

pieces, and running gear, (b) vibration bench testing and fatigue endurance testing of rotor blades, (c) modification of turbine rig, (d) instrumentation of turbine test section, (e) performance test of turbine, and (f) analysis of performance tests and writing of performance report. The purpose of this report is to present the results of the task items completed in Phase Two of this program.

AERODYNAMIC EVALUATION

TURBINE

Requirements - The analysis and design of the 4-1/2-stage fan drive turbine which was investigated are presented in Reference 1. The turbine design requirements are presented below:

• Constant pitch diameter	19.00 in. (48.26 cm.)
• Number of stages	4-1/2
• Equivalent weight flow	25.07 lbm/sec (11.37 kg/sec.)
• Inlet swirl angle	0.0 degrees
• Exit swirl angle with turning vanes	0.0 degrees
• Velocity leaving outlet turning vanes related to inlet critical velocity	0.376
• D-Factor of outlet turning vanes at mean radius	0.4
• Average mean radius loading ($gJ\Delta h/2\Sigma U_p{}^2$)	2.5
• Equivalent specific work	25.88 BTU/lbm (60242.32 joules/kg
• $W\sqrt{T_T}/P_T$ at inlet	38.85 lbm-$\sqrt{°R}$/(sec-lbf/in^2 (25.55 kg-$\sqrt{°R}$/[sec-n/cm^2])
• $N/\sqrt{T_T}$	95.33
• Equivalent mean blade speed (constant for all stages)	180 ft/sec (54.86 m/sec)

Configurations Tested - A 4-1/2-stage turbine with constant pitchline diameter was tested in an air turbine facility to obtain detailed design and off design aerodynamic performance data of the Very Highly Loaded Turbine reported in Reference 1. The design percent total energy produced by each stage ($\Delta h_{stage}/\Delta h_{turbine}$) was 28.5% on stage one, 26.5% on stage two, 26.0% on stage three, and 19% on stage four. The corresponding aerodynamic pitchline loadings ($gJ\Delta h/2\Sigma U_p{}^2$) for each stage were 2.85, 2.65, 2.60, and 1.9 for stages one, two, three, and four respectively. The turbine design velocity diagram is presented in Figure 1 and the flowpath is shown in Figure 2.

The turbine was also tested as a four stage configuration in order to assess the design and off design performance of the Outlet Turning Vanes.

Photographs of the turbine blading used in the test program are presented in Figures 3 through 16.

TEST APPARATUS AND INSTRUMENTATION

Test Facility - The two turbine configurations were tested in the General Electric Company's Evendale Air Turbine Test Facility, which is a dual purpose facility capable of evaluating either single stage high pressure turbine or multistage fan drive turbine performance. Figure 17 shows a typical test facility configuration.

Turbine air is supplied from the Central Air Supply System of the Component Test Complex, which consists of an arrangement of five multistage centrifugal compressors driven by synchronous motors through speed increasing gears. Staging these compressors in series or parallel or using them as exhaustors provides the various modes of operation normally required for the turbine operation. The compressor discharge air is then directed through various auxiliary systems in order to provide air that is filtered to ten micron particle size, dried to minus 70° F dewpoint, and indirectly heated to the desired temperature by passing it through a heat exchanger. Flow enters the test section through a specially shaped scroll which smoothes out flow disturbances and provides a uniform stream to the turbine inlet. Air enters the first stage nozzle through a convergent bellmouth section and a constant annular passage approximately three inches long. Turbine discharge air leaves through a constant annular passage approximately nine inches long and expands into the exhaust plenum.

The generated turbine horsepower is extracted by means of a low speed waterbrake, specifically designed for this test series, which was directly coupled to the turbine shaft by flexible couplings and a short spool piece. This waterbrake design provides excellent speed stability throughout the entire turbine operating map.

A two-level trip system is used to guard against overspeed and excessive temperature or vibrations. The level 1 trip is signaled by an overspeed or bearing over-temperature. Level 2 is signaled by excessive vibrations or critical support system temperatures or pressures.

The turbine facility control console is located in the Test Cell Control Room, illustrated in Figure 18. All the necessary controls and critical turbine or facility monitoring instrumentation are strategically located to enable one man control of the entire test facility. This feature is a direct result of the utilization of analog closed-loop control circuits for setting and maintaining all prime turbine variables. Turbine parameters of inlet temperature, inlet pressure, speed, discharge pressure, and rotor thrust bearing load can all be maintained automatically at pre-set values.

Data Acquisition System - The data acquisition system consists of a digital recorder linked to a paper tape and paper punch tape printer. A total of 61 temperatures and 236 pressures, as well as other specific turbine performance parameters, were recorded by the digital recording system.

Temperature measurements were obtained with precision manufactured Chromel-Alumel thermocouple wire. Sensors in any one plane of measurements use wire from one spool. Calibration samples of wire were cut from each sensor lead and both samples and sensor leads were oven cured for 28 hours at approximately 400° F. The wire samples were then calibrated over the expected temperature range against a Platinum Resistance Thermocouple which is traceable to the National Bureau of Standards, resulting in correction curves which were applied to the temperature measurements in the data reduction program.

Calibration curves were also established to determine temperature recovery at various expected Mach number ranges and flow incidence angles using a specially designed calibration stand with a 2.5 inch free jet nozzle capable of a Mach number range from 0.2 to 1.0. Corrections were made in the data reduction program using the calibration curves.

The thermocouple leads terminate in a Copper Alloy Thermal Sink (CATS), which is thermally insulated to minimize temperature gradients. To arrive at the absolute value of any temperature sensor, the absolute temperature of the CATS block was measured, using both a water-ice bath reference and an electronically controlled Ice Point Reference System. The latter was used to determine absolute temperature levels, but both systems were continually compared. The electrical output of each thermocouple was measured at this CATS block and the signal was amplified and directed to the digital recorder.

Turbine rig pressure measurements were obtained by the use of precision strain gage pressure transducers which convert pneumatic signals to electrical outputs. The pressures enter the control room pneumatically and terminate in electrically controlled scanners which systematically direct each pressure signal to a transducer. The transducer electrical outputs were amplified and directed to the digital recorder. All transducers of this type have a common excitation and output amplification. Each data reading contains the excitation voltage sensed at the transducer, the transducer zero, and a known calibration signal which was recorded through all its associated electrical circuitry. The repeatability of these parameters was continually monitored to preclude any measurement errors.

Pressure calibrations were performed prior to each test run using a precision dead weight tester for above-atmospheric calibrations, and a quartz manometer for sub-atmospheric calibrations. Both units were frequently calibrated and their precisions are directly traceable to the National Bureau of Standards. All pressure transducers used have characteristic curves compiled in a computer library file, to which each pre-run calibration was compared for discrepancies.

The digital recording system is linked to the General Electric 635 Computer by means of a GE Terminet 300 located in the Control Room. This feature enabled reduced data to be printed out in the Control Room within five minutes of the reading of a test point.

Instrumentation - Figure 19 shows the location of the instrumentation used in the testing of the two turbine configurations.

Temperature and pressure instrumentation was mounted on the leading edge of the inlet strut frame, station 0, Figure 19, on each of ten struts which were spaced 36 degrees apart, and located approximately 12 inches upstream of the first stage stator. Temperature was measured with 25 Chromel-Alumel thermocouples mounted in high recovery stagnation tubes affixed to five of the struts 72 degrees apart. The thermocouples were grouped five to a strut and were located radially at the area center of five equal annular areas. Total pressure was measured by 25 Kiel-type probes located on five alternate struts, also 72 degrees apart, and located in an identical manner as the thermocouples. These pressures were measured independently by means of the scanner-transducer system and then arithmetically averaged in the data reduction program. They were also pneumatically averaged, using a specially designed averaging block, measuring an average output on a single pressure transducer. The temperatures at this station were used for turbine inlet temperature.

Inlet static pressure was measured with five equally spaced static pressure taps located on both the inner and outer casings in a straight annular section about 2-1/2 chord lengths upstream of the first stage stator, Station 1.0, Figure 19. These static pressure taps were used to check the circumferential uniformity of the flow and to calculate the turbine inlet total pressure. Five Kiel-type total pressure probes were also installed in the inlet plane and spaced 72 degrees apart to serve as a check of the circumferential uniformity of the flow.

Interstage static pressures were measured with four static pressure taps installed 90 degrees apart at the leading and trailing edge planes of the stator blade rows on both the inner and outer bands, Station 1.2 through 1.8. The circumferential location of the pressure taps was selected to coincide with the position of the mean streamline. A similar arrangement of static pressure taps was used at the leading edge plane of the outlet turning vanes, Station 1.9 and 1.95.

Four turbine outlet static pressures were measured on both the inner and outer casings at Station 2 and approximately one inch downstream of the outlet turning vanes. These static pressure taps were spaced 90 degrees apart. Turbine outlet total temperature, total pressure, and flow angle were also measured at Station 2 over an angle subtending about 11 degrees by a radially and circumferentially traversing combination probe. A fast response pressure differential servo-system aligned the probe with the flow and provided an electrical output proportional to the flow angle. Total temperature, total pressure, and flow angle were recorded on X-Y chart recorders as functions of either radial immersion or circumferential position. The instrumentation at Station 2 was used to calculate outlet total pressure as described in Appendix A.

At Station 3, approximately four inches downstream of the outlet turning vanes, turbine outlet total temperature and total pressure were measured with six fixed circumferential arc rakes 60 degrees apart, located radially at the centers of six equal annular areas. A total of 36 total temperatures and 72 total pressures were measured. Each rake contained twelve Kiel-type pressure elements located side-by-side and six shielded thermocouple probes side-by-side. The total pressures were averaged both arithmetically and pneumatically in the same manner as the inlet pressure measurements. Six static pressure taps were also installed on the inner and outer walls at this station and were located 60 degrees apart.

Four turbine outlet static pressures were measured on both the inner and outer casings immediately aft of the outlet turning vanes and approximately one inch downstream of the outlet turning vanes. These static pressure taps were spaced 90 degrees apart. Six static pressure taps were also installed on the inner and outer walls about four inches downstream of the turning vanes and were located 60 degrees apart.

Air flow to the turbine was measured using a calibrated circular arc venturi which was operated at critical flow conditions. The venturi inlet pressure and temperature were measured using wall static pressure taps and Chromel-Alumel air thermocouple probes, respectively, located upstream of the venturi throat.

Three independent speed measurements were provided by an indicating system consisting of a 60-tooth gear attached to the turbine shafting and three stationary magnetic sensors located very close to the gear teeth. Electrical impulses resulting from the passing of each tooth provided an electrical frequency proportional to turbine speed. Electrically time integrating this signal provided the speed indication, accurate within $\pm$ 1 rpm. During the course of each data reading, twelve different samples of speed were recorded and arithmetically averaged.

Two independent techniques were employed for the measurement of shaft torque. The primary system consisted of a dual bridged shaft-mounted torque sensor. The strain sensitive spool section was located between the turbine shaft and the waterbrake shaft with a specially designed slip ring mounted behind the waterbrake to transmit electrical signals to the digital recorder. Each bridge was excited with its own independent electronics system and read out or displayed through the digital data acquisition system. The secondary torque measurement was obtained by means of a load cell located beneath a lever arm attached to the cradled waterbrake stator housing. The load cell also employed independent signal conditioning and readout electronics.

Torque calibrations were performed in place using a precision torque arm and dead weights, whose weight values are traceable to the National Bureau of Standards. Dead weight calibrations were conducted prior to each test run to verify repeatability of torque zeros and bridge linearity. In addition, extensive temperature calibrations were made to define torque zero and modulus changes over the operational temperature range, even though these effects are less than 0.25 percent.

TEST PROCEDURE

The turbine inlet conditions were set at 720° R and 45 psia, with the exception of the test points noted in the table below. These test points could not be set at the above conditions due to test facility and waterbrake limitations.

P_{T_1}/P_{S_3}	Percent Design Speed	P_{T_1}, psia	T_{T_o}, ° R
2.28	60	45	700
1.97	80	38	705
1.97	90	38	710
1.97	100,110,120	38	717
1.78	60,80,90,100,110,120	38	693

The performance mapping of the turbine was accomplished by selecting test points within the following range of variables:

- Speed - 60, 80, 90, 100, 110, 120 percent design speeds
- Total-to-total pressure ratio - from a maximum corresponding to 125% design work at design speed to a minimum equal to the pressure ratio that produces 60% design work at design speed.

Additional testing was done in the vicinity of the design point at 720° R and inlet pressures of 25, 38, and 50 psia to investigate effects of Reynolds number.

The following performance data were obtained at each test point:

- Turbine weight flow
- Rotative speed
- Torque
- Inlet total temperature
- Inlet total and static pressures
- Outlet absolute flow angles
- Outlet total and static pressures

- Outlet total temperatures
- Flowpath hub and tip interstage static pressures.

At each test point three complete sets of data were recorded and processed through the on-line computer which permitted an immediate evaluation of the reduced data.

Key performance parameters were continually monitored to insure accuracy and consistency of the test data. The design point was periodically reset throughout the testing to monitor the repeatability of the facility and the design point calculations.

One radial and three circumferential traverses were made at each test point to record the turbine exit total pressure, total temperature, and absolute flow angle. The circumferential traverses were taken at 10, 50, and 90 percent of the outlet turning vane height.

A detailed turbine exit survey was taken at the design speed and design pressure ratio. The survey included three radial traverses at 0, 50, and 100 percent of the circumferential traverse sector which was an arc of 11.32 degrees, and seven circumferential traverses at 10, 20, 30, 50, 70, 80, and 90 percent of the outlet turning vane height.

DATA REDUCTION PROCEDURE

<u>Turbine Overall Performance</u> - Two calculation schemes were used to reduce the overall performance data. The two methods differed in only one respect. The preliminary test cell data reduction program used measured exit total pressures for all performance calculations whereas the final data reduction was performed using calculated inlet and exit total pressures. This exit total pressure was calculated from continuity using outlet total temperature, outlet static pressure, measured weight flow, and outlet flow angle. The outlet total temperature was derived from the inlet total temperature, specific enthalpy drop obtained from the torque, speed and weight flow measurements. The outlet static pressure was calculated as the average of the measured exit hub and tip static pressures. The outlet flow angle was taken as an integrated average flow angle from the traverses. A more detailed description of all of the calculation procedures used in the data reduction may be found in Appendix A.

The following overall performance parameters were determined for each of the three readings taken at each test point:

1. Calculated inlet total to outlet total pressure ratio as obtained from indirect measurement.
2. Calculated inlet total to outlet static pressure ratio as obtained from indirect measurement.
3. Equivalent speed.
4. Equivalent weight flow.

5. Equivalent weight flow-speed parameter (product of equivalent speed and equivalent weight flow).

6. Equivalent torque.

7. Equivalent specific work.

8. Ideal equivalent specific work.

9. Efficiency based on calculated total-to-total pressure ratio.

10. Blade-jet speed ratio based on total-to-static pressure ratio.

These parameters are tabulated in Table I.

Outlet Turning Vane Exit Survey Calculations - The total pressure, total temperature, and absolute flow angle, which were recorded during the turbine exit surveys at the design point, were used in the construction of contour plots showing local efficiency. The local efficiencies were calculated from the following parameters:

- Measured inlet total temperature
- Calculated inlet total pressure based on continuity using measured inlet static pressure and measured airflow
- Local exit total temperature measured by the traverse probe
- Local exit total pressure measured by the traverse probe

Reynolds Number Calculations - The turbine Reynolds number was varied by operating the turbine over a range of inlet pressures (densities) while maintaining the design pressure ratio. A Reynolds number for each bladerow was calculated on the basis of leaving gas velocity, throat dimension and suction surface length of the particular blade as shown in the following expression which is derived in detail in Appendix B.

$$R_{N_i} = \left(\frac{12\, W\, \ell}{\mu\, n\, d_o\, h}\right)_i$$

where:

W = measured airflow (lbm/sec)
ℓ = suction surface length (inches)
μ = bladerow exit viscosity (lbm/sec-ft)
n = number of airfoils
h = height of blade at throat (inches)
d_o = blade throat dimension (inches)
i = ith stage

The turbine overall Reynolds number was obtained by energy weighting the individual bladerow Reynolds numbers as follows:

$$\bar{R}_N = \sum_{i=1}^{m} \Delta h_i R_{N_i} \Big/ \sum_{i=1}^{m} \Delta h_i$$

EXPERIMENTAL RESULTS AND DISCUSSION

Turbine Overall Performance - The reduced data and calculated parameters are presented in the following curves:

a. Equivalent torque versus calculated total-to-total pressure ratio.

b. Equivalent weight flow versus calculated total-to-total pressure ratio.

c. Equivalent specific work versus calculated total-to-total pressure ratio.

d. Total-to-total efficiency versus blade-jet speed ratio.

e. Total-to-total efficiency versus calculated total-to-total pressure ratio.

f. Equivalent specific work versus equivalent weight flow speed parameter with lines of constant calculated total-to-total pressure ratio, constant speed, and constant efficiency superimposed.

The above curves utilize constant values of percent equivalent design speed as a parameter and are presented in Figures 20 through 25.

Figures 26 through 29 show comparisons of the reduced data for equivalent torque, equivalent weight flow, equivalent specific work, and efficiency, respectively, to the pre-test predictions originally presented in Reference 1. The data show agreement with predicted trends but not with the predicted absolute levels. The disagreement in magnitude was primarily due to the selection of loss coefficients (such as bladerow efficiencies and rotor and stator total pressure recovery factors) which are considered as constants in the vector diagram performance calculations.

The lower predicted design point equivalent weight flow is considered to be a mismatch between the stage one stator physical throat area and the design intent.

Normalized interstage hub and tip static pressures versus axial station are presented in Figure 30 for the design speed at each turbine pressure ratio tested. These plots indicate that as turbine total-to-total pressure ratio increases the first stage hub reaction decreases from positive to negative. This downward trend was predicted but the absolute value of the

measured reactions was lower than the level predicted by the Turbine Computer Program.

Turbine Exit Survey - Figures 31 and 32 present the efficiency contours of the 4-1/2- and the 4-stage turbine configurations as a function of percent radial height and circumferential position. The local efficiencies were determined from the radial and circumferential total pressure and total temperature traverse surveys in the turbine exit plane. The 4-1/2-stage efficiency contour plot covers an arc of 2.1 outlet turning vane pitches and the 4-stage efficiency contour plot covers an arc of 1.56 fourth stage stator pitches. These plots illustrate the large radial efficiency gradients in the hub and tip regions of the flowpath. The 4-1/2-stage contours show the pronounced outlet turning vane wakes especially in the vicinity of the tip. The low efficiency regions at the hub are considered to be the strong secondary flow fields generated by the high turning stator and blade airfoils.

The reader is cautioned against drawing conclusions about the relative performance of the two configurations from these plots since their degree of accuracy is only sufficient to make qualitative but not quantitative judgment.

Figure 33 compares the turbine radial total pressure ratio distributions for the two configurations. Caution should be used when interpreting this plot since the two turbines were operating with slightly different equivalent energy extractions. This accounts for the exit total pressure for the 4-1/2-stage build being slightly greater than that for the 4-stage turbine.

A comparison of the radial exit swirl angle profiles for the two configurations are shown in Figure 34. The plot graphically shows the reduction in swirl achieved by the outlet turning vanes which turned the flow from positive 30 degrees at the inlet pitchline to minus one degree at the exit pitchline. These curves were drawn by averaging the radial swirl traverses made at three circumferential positions for the major design point of each configuration.

The design point radial total-to-total efficiency profile shown in Figure 35 for the 4-1/2-stage turbine was constructed by mass weighting the circumferential traverses of total pressure and total temperature at seven radial positions.

The high efficiency at the pitchline is a measure of the full potential of the turbine. The gradual fall-off in efficiency toward the tip and the steep decrease toward the hub are indications of the effects of strong secondary flow fields generated by the high turning bladerows. Additional improvements in the hub and tip regions are needed to enable the bladerows to fully utilize their potential.

Reynolds Number Effects - The turbine Reynolds number was varied for the 4-1/2-stage turbine by operating over a range of inlet pressures (thus changing the density level) while maintaining a constant turbine pressure ratio.

In Figure 36, a plot of total-to-total efficiency versus blade-jet speed ratio at constant total-to-static pressure ratio and with lines of constant inlet pressure is presented. The plot illustrates the effects of varying inlet pressure on turbine efficiency as the turbine operates through its speed range. The increase in efficiency becomes smaller with each increase in turbine inlet pressure (and corresponding increase in turbine Reynolds number) until at some point, no further efficiency increase will result. The curves show that the inlet pressure at which no efficiency increase occurs was attained in this test.

Radial efficiency profiles based on fixed rake data for two inlet pressures are presented in Figure 37. The profiles were constructed for inlet total pressures of 45 psi and 25 psi, corresponding to high and low Reynolds numbers, respectively. Figure 38 illustrates the change in efficiency between the low and high Reynolds number points. This figure indicates that the greatest change in efficiency due to Reynolds number effects occurs in the hub region.

Plots of total-to-total efficiency and equivalent weight flow versus turbine Reynolds number appear in Figures 39 and 40. Each point on the plots represents data obtained at or near the design operating point. Both turbine efficiency and equivalent weight flow increase with increase in Reynolds number up to a point where Reynolds number is approximately one million. Above this value, efficiency and equivalent weight flow level off at a constant value.

Outlet Turning Vane Performance - Figure 41 depicts the total pitchline turning done by the outlet turning vanes at the design and off-design operating points. This curve illustrates that the outlet turning vanes were highly successful in being able to turn the turbine exit flow to axial at all of the operating conditions investigated.

Figures 42 and 43 show the results of two independent methods used to determine the percent turbine performance loss attributed to the outlet turning vanes. It is assumed that this loss is reflected by the difference in efficiency between the 4- and 4-1/2-stage configurations at a given equivalent specific work extraction. Figure 42 was based on calculated exit total pressure and it indicates approximately 0.08 percent additional loss in overall efficiency at the turbine design point. Figure 43, however, was based on measured exit total-pressure and it shows the 4-1/2-stage design point efficiency to be approximately 0.5 percent below the 4-stage turbine. This level of loss appears to be more realistic when compared with compressor outlet guide vane performance.

Recommended Improvements - The analysis of the data acquired during the air turbine testing of the 4- and 4-1/2-stage configurations indicate specific areas of performance deficiencies in the 4-1/2-stage very highly loaded fan turbine. Several recommendations to improve the overall design and off design performance based on these test results are outlined below:

- Utilize leaned stators as reported in Reference 2. This will decrease the rotor hub inlet relative Mach numbers below their current levels which are approximately 0.7. Leaned stators will

also decrease the leakage loss across the rotor tip shrouds by decreasing the axial static pressure drop across the blade tip section.

- Use tandem stator airfoils in stages 2, 3 and 4. Reference 3 indicates the performance of a highly loaded two-stage turbine was increased 1.2 percent by installing a tandem stator in stage two. Tandem airfoils also increase the performance in the turbine hub region.

- Redesign the outlet turning vane and remove the design criteria that the diffusion factor equal 0.4. Parametric studies preceding the design of the outlet turning vane indicated higher performance could be achieved with diffusion factors higher than 0.4.

The design point measured radial efficiency profile indicates a significant loss in performance in the hub region of the turbine. It is suspected that this is the manifestation of the strong secondary flow fields generated by the high turning blade rows. In view of the experimental results it is highly desirable to test additional configurations to isolate the performance of the individual stages and to determine the nature of the low performance in the hub region.

MECHANICAL EVALUATION

The rotor blades were vibration tested under laboratory conditions to establish their fundamental and higher frequency modes. Fatigue tests were conducted to establish the endurance capability of the blades while operating in an air turbine environment. These tests substantiated the analytical effort reported in Reference 1.

LABORATORY TEST OF ROTOR BLADE AIRFOILS

Vibration Testing - A series of vibration tests were conducted to substantiate the predicted natural frequencies reported in Reference 1. The fundamental and higher frequency modes of vibration were determined for fixed- fixed (restrained at the hub and tip) end conditions.

The top tangs on the shrouds were machined off and a steel block was brazed to the top of the shrouds to allow for a tight clamping surface. The clamping was done across the pressure and suction sides of the blade's shroud region to simulate the "locking up" of the blade's shroud during air turbine operation. Due to the tight clamping necessary to get a good frequency response, the actual end condition imposed on the blades was a fixed end condition. The dovetail-shank region was clamped in the same manner. In the actual turbine, the blades will lock up in the tangential direction and should be free to move in the axial direction. To get a rigid clamp of the blade in the tangential direction at the shroud, and then allow an axial displacement to occur, is not feasible in a laboratory setup. This is due to the mass of the clamping setup and the lack of knowledge to the degree of displacement necessary to simulate actual turbine operation. The predicted blade analysis was done for each blade under fixed-fixed end conditions for comparison to the experimental results and is presented in Table III.

Campbell Diagrams incorporating the most probable modes of vibration are presented in Figures 44 through 47. The close agreement between the theoretical results and experimental data for the fixed-fixed end conditions provides the necessary credibility to the predicted axial modes.

Based on the theoretical analysis and the experimental results it was concluded that the blades would not experience any excessive vibrations during air turbine operation.

Fatigue Endurance Testing - Fatigue endurance testing was performed on test specimens from each blade row. The top portions of the blades were cut off which increased the first flex frequency response and shortened the fatigue testing time. The blades were clamped at the dovetail and fatigued in first flex to get an indication of the blade material endurance strength at an "A" ratio ($\sigma a/\sigma m$) of infinity. These stresses are shown on the Goodman diagram in Figure 48. The stress levels experienced by the test specimens were measured by strain gages located in the most likely regions of failure. First flex was used since it is usually the easiest to instrument. Runout for a particular

stress level was set at a million cycles before it was increased in increments of 10 KSIDA. Considering testing time and the cyclic endurance strength of the 410 stainless steel, a million cycles to failure would adequately indicate the level of the endurance strength. The stage one blade failed at 80 KSIDA in the trailing edge at 2.5% span. This is approximately 20 KSIDA less than average properties. The reason was due to a sharp trailing edge which caused a stress concentration in that region. Stages two and four failed in the trailing edge region at the stress level depicted on Figure 48. Stage three failed on the leading edge above the root fillet. Photographs of the blade failures are shown in Figure 49. The blades would have experienced failure at different points if they had been restrained at the tip, due to a different strain distribution. It isn't the failure location that is important in this particular test, but the level of stress at failure. The last three stages exhibited an endurance level above the curve on the Goodman Diagram. This curve is based on 10^7 cycles to failure and since a million cycles were used as a limit before increasing the stress, the test values would be above the curve.

Table IV illustrates the number of cycles run at the failure stress. Stage one, two and three were started at 50 KSIDA with 10 KSIDA incremental increases after 10^6 cycles until failure. Stage four was started at 70 KSIDA with incremental increases until failure.

The laboratory fatigue data compared favorably with the average fatigue characteristics for the 410 stainless steel. The material in a machined blade configuration suffered little or no fatigue strength deterioration relative to the polished barstock specimens established as the norm. It was concluded that the rotor blades had no inherently weak points and had sufficient fatigue endurance capability for successful air turbine operation.

SUMMARY OF RESULTS

A four and one-half stage turbine was tested in order to evaluate the performance of a very highly loaded fan turbine with outlet turning vanes. The most significant results of the testing and analysis are summarized below:

1. The four and one-half stage turbine achieved a total-to-total turbine efficiency of 0.853 at the design speed and pressure ratio ($N/\sqrt{\theta}_{cr}$ = 2171.2, P_{T1}/P_{T3}= 2.66).

2. The four stage configuration was tested to isolate the performance of the outlet turning vanes. The test results based on measured turbine exhaust total pressures indicated a 0.5 percent loss in four and one-half stage turbine efficiency can be attributed to the outlet turning vane performance. However, a difference of only 0.08 percent loss in performance was indicated when based on calculated exhaust total pressure.

3. The outlet turning vanes were successful in turning the turbine exit flow to axial at all of the operating conditons investigated.

4. High efficiencies in the pitchline region were indicated by the radial efficiency profiles. Efficiency drops were noticed toward the hub and tip with the effect more pronounced in the hub region.

5. Reynolds number testing showed that total-to-total efficiency and equivalent weight flow decrease with decreasing Reynolds number. Radial efficiency profiles indicated the greatest increase in loss with reduced Reynolds number occurs in the hub region.

APPENDIX A

OVERALL PERFORMANCE CALCULATION

Exit Flow Angle - In order to evaluate turbine performance on the basis of turbine exit total pressure calculated from continuity, an average turbine exit flow angle, $\bar{\Gamma}$, was determined. This angle is the absolute value of the deviation from axial direction, irrespective of sign. The turbine exit flowpath was divided into streamtubes, and measured values of swirl angles, total pressure, and total temperature were used to satisfy continuity within each streamtube. The turbine exit measured static pressure was assumed to vary linearly from hub to tip. The determination of the average turbine exit flow angle proceeded as follows:

$$(\rho\, V\, A_{ann} \cos \Gamma)_{avg} = \sum_{i=1}^{m} \rho_i\, V_i\, A_i \cos \Gamma_i$$

where: $$\rho_i\, V_i = P_{S_i} \sqrt{\frac{\gamma g}{R T_{T_i}}} \sqrt{\frac{2}{\gamma - 1} \left[\left(\frac{P_T}{P_S} \right)_i^{\left(\frac{\gamma-1}{\gamma}\right)} - 1 \right]} \Bigg/ \sqrt{\left(\frac{P_T}{P_S} \right)_i^{\frac{\gamma-1}{\gamma}}}$$

P_T = Measured total pressure at center of i-th streamtube.

P_S = Static pressure at center of i-th streamtube based on linear variation in measured static pressure from hub to tip

T_T = Measured total temperature at center of i-th streamtube

Γ = Swirl angle

ρ = Density

V = Absolute velocity

A = Area

m = Number of streamtubes

i = Subscript denoting streamtube value

ann = Subscript denoting value for total annulus

avg = Subscript denoting average value for total annulus

The average velocity representing the turbine exit flow field was calculated by conserving the axial and tangential components of momentum, such that

$$V_{avg} = \left(V^2_{u_{avg}} + V^2_{z_{avg}} \right)^{1/2}$$

where $$V_{u_{avg}} = \left(\sum_{i=1}^{m} W_i \, V_i \, |\sin \Gamma_i| \right) \Big/ \sum_{i=1}^{m} W_i$$

$$V_{z_{avg}} = \left(\sum_{i=1}^{m} W_i \, V_i \cos \Gamma_i \right) \Big/ \sum_{i=1}^{m} W_i$$

and $$V_i = \sqrt{2g \, Jc_p \, T_{T_i} \left[1 - \left(\frac{P_S}{P_T} \right)_i^{\frac{\gamma-1}{\gamma}} \right]}$$

V_u = Tangential component of absolute velocity

V_z = Axial component of absolute velocity

W_i = Weight flow through i-th streamtube

The average turbine exit total temperature was determined through an energy balance of the annular streamtubes.

$$T_{T_{avg}} = \left(\sum_{i=1}^{m} W_i \, T_{T_i} \right) \Big/ \sum_{i=1}^{m} W_i$$

The average density at the turbine exit was obtained from the equation of state.

$$\rho_{avg} = \frac{P_{S_{avg}}}{R \, T_{S_{avg}}}$$

where $$T_{S_{avg}} = T_{T_{avg}} - \frac{V^2_{avg}}{2g \, Jc_p}$$

Calculated Outlet Total Pressure - After obtaining the average turbine exit flow angle, the exit total pressure was calculated in the following manner:

$$P_{T_3} = P_{S_3} \left(1 + \frac{\gamma-1}{2} M_3^2\right)^{\gamma/\gamma-1}$$

Turbine exit Mach number, M_3, was determined from the following relationship:

$$\frac{W \sqrt{R\,T_{T_3}}}{P_S\,A_{ann} \cos \Gamma_{avg}} = \sqrt{\gamma g}\, M_3 \sqrt{1 + \frac{\gamma-1}{2} M_3^2}$$

Turbine exit total temperature, T_{T_3}, was determined as follows:

$$T_{T_3} = T_{T_o} - \frac{\Delta h}{c_p}$$

where $\Delta h = \frac{2\pi\ N\tau}{60\ JW}$

N = Turbine rotative speed

τ = Measured torque

T_{T_o} = Measured turbine inlet total temperature

W = Measured turbine weight flow

Inlet Total Pressure - Turbine inlet total pressure was calculated in the same manner as the turbine exit total pressure. The calculation used measured airflow, measured inlet total temperature, the average of measured hub and tip static pressures, and the assumption of zero inlet swirl angle.

Performance Parameters - The remaining parameters used in the overall performance calculation were obtained as follows:

$\delta = P_{T_1}/14.696$

$\theta_{cr} = T_{T_o}/518.688$

$\varepsilon = 1.0$ (for $\gamma = 1.4$)

Equivalent Speed, N EQV = $N/\sqrt{\theta_{cr}}$

Equivalent Weight Flow, WA EQV = $W\sqrt{\theta_{cr}}\ \varepsilon/\delta$

Weight Flow-Speed Parameter, WAN EQV = $WN\varepsilon/60\delta$

Equivalent Torque, TQ EQV = $\tau\varepsilon/\delta$

Equivalent Specific Work, DH EQV = $\dfrac{\Delta h}{\theta_{cr}} = \dfrac{2\pi\ N\tau}{60\ J\ \theta_{cr}}$

Ideal Equivalent Specific Work, DHI EQV =

$$\left(\frac{\Delta h}{\theta_{cr}}\right)_{ideal} = c_p\ T_{T_o}\left[1-\left(\frac{P_{T_3}}{P_{T_1}}\right)^{\frac{\gamma-1}{\gamma}}\right]\Bigg/\theta_{cr}$$

Total-to-total Efficiency, ETA TT =

$$\eta_{TT} = \left(\frac{\Delta h}{\theta_{cr}}\right)\Bigg/\left(\frac{\Delta h}{\theta_{cr}}\right)_{ideal}$$

Blade-Jet Speed Ratio, U/CO =

$$\nu = \left\{\frac{U_m^2}{c_p\ T_{T_o}\left[1-\left(\frac{P_{S_3}}{P_{T_1}}\right)^{\frac{\gamma-1}{\gamma}}\right]}\right\}^{1/2}$$

APPENDIX B

REYNOLDS NUMBER CALCULATION

The turbine Reynolds numbers were based on the energy weighted Reynolds numbers of each blade row as defined below:

$$\bar{R}_N = \left(\sum_{i=1}^{m} \Delta h_i \, R_{N_i} \right) \Big/ \sum_{i=1}^{m} \Delta h_i$$

where

$$R_{N_i} = \left(\frac{12 \, W \, \ell}{\mu \, n d_o \, h} \right)_i$$

and Δh_i = Equivalent fractional energy extraction of i-th bladerow.

The viscosities μ were obtained from Reference 5.

The equivalent fractional energy extraction of each bladerow is derived as follows. The velocity diagram energy for each stage can be divided into two constituents associated with the stator and rotor leaving energies. This division of the total stage energy is illustrated on the following enthalpy-entropy diagram:

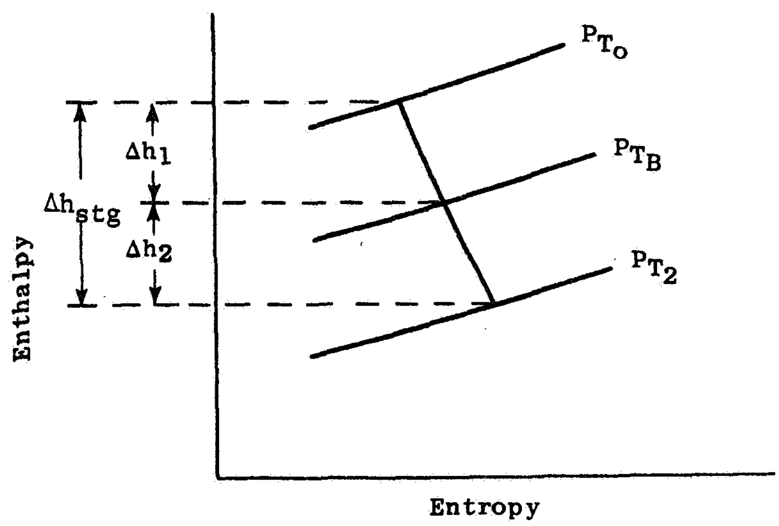

The energies Δh_1 and Δh_2 can be expressed in terms of the stage velocity diagram parameters as shown below:

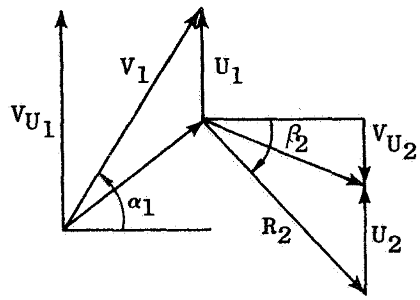

From the sketches,

$$\Delta h_{stg} = \frac{1}{gJ} \left(U_1 V_{u_1} + U_2 V_{u_2}\right)$$

$$\Delta h_{stg} = \frac{1}{gJ} \left(U_1 V_1 \sin \alpha_1 + U_2 R_2 \sin \beta_2 - U_2^{2}\right)$$

With the appropriate combination of terms and algebraic manipulations the above expressions can be simply expressed as:

$$\Delta h_{stg} = \Delta h_1 + \Delta h_2 + \frac{U_1^{2} - U_2^{2}}{2gJ}$$

where

$$\Delta h_1 = \frac{V_1^{2}}{2gJ} \left[\left(\frac{U_1}{V_1}\right)\left(2 \sin \alpha_1 - \frac{U_1}{V_1}\right)\right]$$

and

$$\Delta h_2 = \frac{R_2^{2}}{2gJ} \left[\left(\frac{U_2}{R_2}\right)\left(2 \sin \beta_2 - \frac{U_2}{R_2}\right)\right]$$

The terms $\frac{V_1^{\ 2}}{2gJ}$ and $\frac{R_2^{\ 2}}{2gJ}$ are the energy equivalents of velocity leaving the stator and rotor respectively.

The terms $\left[\left(\frac{U_1}{V_1}\right)\left(2 \sin \alpha_1 - \frac{U_1}{V_1}\right)\right]$ and $\left[\left(\frac{U_2}{R_2}\right)\left(2 \sin \beta_2 - \frac{U_2}{R_2}\right)\right]$ are properties of the velocity diagrams at the stator and rotor exit planes.

The velocity diagram parameters used in this analysis for each blade row were calculated using the Turbine Computer Program described in Reference 6.

APPENDIX C

LIST OF SYMBOLS

A	Area (in.^{2}, cm^2)
c_p	Specific heat at constatnt pressure (ft^2/sec^2 °R, m^2/sec^2 °K)
D	Diameter (in., cm)
d_o	Throat dimension (in., cm)
Δh	Turbine energy extraction (Btu/lbm, joules/kg)
Δh_{stg}	Stage energy extraction (Btu/lbm, joules/kg)
h	Height at bladerow throat (in., cm)
ℓ	Blade or vane suction surface length (in., cm)
M	Mach number
m	Number of bladerows, streamtubes, or stages
N	Rotational speed (rev/min)
n	Number of vanes or blades
P_s	Static pressure (psia, newtons/cm^2)
P_{S_3}	Turbine exit static pressure (psia, newtons/cm^2)
P_T	Total pressure (psia, newtons/cm^2)
P_{T_1}	Turbine inlet total pressure, station 1 (psia, newtons/cm^2)
P_{T_3}	Turbine exit total pressure, station 2 (psia, newtons/cm^2)
R	Gas constant (ft^2/sec^2 °R, m^2/sec^2 °K)
R_2	Rotor exit relative gas velocity (ft/sec, m/sec)
R_N	Reynolds number
$\overline{R_N}$	Energy weighted overall Reynolds number
T_S	Static temperature (°R, °K)
T_T	Total temperature (°R, °K)
T_{T_o}	Turbine inlet total temperature, station 0 and station 1 (°R, °K)

T_{T_3}	Turbine exit total temperature, station 2 (°R, °K)
t	Spacing (in., cm)
U	Wheel speed (ft/sec, m/sec)
V	Absolute velocity (ft/sec, m/sec)
W	Mass flow rate (lbm/sec, kg/sec)
$\Delta h/\theta_{cr}$	Equivalent specific work (Btu/lbm, joules/kg)
$W\sqrt{\theta_{cr}}\ \varepsilon/\delta$	Equivalent weight flow (lbm/sec, kg/sec)
$N/\sqrt{\theta_{cr}}$	Equvalent rotative speed (rev/min)
$WN\varepsilon/60\delta$	Weight flow - speed parameter (lbm/sec^2, kg/sec^2)
$gJ\Delta h/2U^2$	Loading factor
α_o	Vane inlet absolute flow angle (degrees)
α_1	Vane exit absolute flow angle (degrees)
β_1	Blade inlet relative flow angle (degrees)
β_2	Blade exit relative flow angle (degrees)
Γ	Stage leaving swirl angle (degrees)
$\bar{\Gamma}$	Turbine out flow angle (defined in Appendix A)
γ	Specific heat ratio
δ	Ratio of turbine pressure to pressure at standard sea level conditions
ε	Function of γ defined as $\frac{\gamma_{SL}}{\gamma}\left\{\left[\frac{\gamma+1}{2}\right]^{\gamma/(\gamma-1)}\Big/\left[\frac{\gamma_{SL}+1}{2}\right]^{\gamma_{SL}/(\gamma_{SL}-1)}\right\}$
η_{TT}	Total-to-total efficiency
θ_{cr}	Squared ratio of critical velocity at turbine inlet temperature to critical velocity at standard sea level temperature
μ	Viscosity (lbm/sec-ft, kg/sec-m)
ν	Blade-jet speed ratio
ρ	Density (in., cm)

σ_a	Alternating stress (ksi, newtons/cm^2)
σ_m	Mean stress (ksi, newtons/cm^2)
τ	Torque (ft-lbf, m-newtons)
τ_{eq}	Equivalent torque, $\tau_{eq} = \tau\varepsilon/\delta$ (ft-lbf, m-newtons)

Subscripts

a	Alternating
B	Relative to rotor blade
h	Hub
i	Current axial station, stage, or streamtube, or ideal
m	Mean
p	Pitch
R	Relative
r	Radial component
t	Tip
u	Tangential component
z	Axial component

REFERENCES

1. Evans, D.C. and Hill, J.M., "Experimental Investigation of a $4\frac{1}{2}$ - Stage Turbine with Very High Stage Loading Factor. I - Turbine Design," NASA CR-2140, 1973.

2. Evans, D.C. and Wolfmeyer, G.W., "Highly Loaded Multi-Stage Fan Drive Turbine - Leaned Stator Configuration Design," NASA CR-2096, July 1972.

3. Wolfmeyer, G.W., and Thomas, W.W., "Highly Loaded Multi-Stage Fan Drive Turbine - Test and Performance Report," General Electric R73AEG154, March 1973.

4. General Electric Company, Materials Property Data Handbook - Vol. 3.

5. Keenan, J.H. and Kay, E., Gas Tables, John Wiley and Sons, Inc., New York, 1948.

6. Flagg, E.E., "Analytical Procedure and Computer Program for Determining the Off-Design Performance of Axial-Flow Turbines, "NASA CR-710, March 1966.

Table I. Reduced Test Data and Calculated Performance Parameters, 4-1/2-Stage Configuration.

RDG	PCT NDES	PTO	PTO/PT3	PTO/PS3	N EQV	WA EQV	WAN EQV	TQ EQV	DH EQV	DHI EQV	ETA TT	U/CO	FLOWANG
98	100	45.06	2.694	2.958	2170.16	25.446	920.36	2283.15	26.204	30.702	0.8535	0.1396	2.94
99	100	45.07	2.697	2.960	2169.83	25.440	920.00	2283.26	26.208	30.722	0.8530	0.1396	2.94
100	100	45.09	2.697	2.961	2169.44	25.438	919.77	2283.69	26.210	30.725	0.8531	0.1395	2.94
101	63	45.07	2.664	2.970	1362.28	26.639	604.82	3135.38	21.578	30.400	0.7098	0.0875	1.95
102	63	45.08	2.660	2.965	1362.68	26.643	605.11	3134.46	21.574	30.361	0.7106	0.0876	1.95
103	63	45.07	2.660	2.964	1362.26	26.645	604.95	3134.81	21.568	30.352	0.7106	0.0876	1.95
104	80	45.20	2.676	2.965	1730.39	26.278	757.87	2747.30	24.345	30.522	0.7976	0.1112	2.62
105	80	45.16	2.674	2.962	1730.28	26.282	757.91	2746.04	24.329	30.502	0.7976	0.1113	2.62
106	80	45.19	2.678	2.966	1730.16	26.271	757.56	2745.68	24.334	30.537	0.7969	0.1112	2.62
107	90	45.02	2.680	2.954	1950.86	25.886	841.67	2504.09	25.396	30.559	0.8311	0.1256	1.78
108	90	45.02	2.679	2.952	1950.88	25.884	841.61	2502.82	25.386	30.549	0.8310	0.1256	1.78
109	90	45.03	2.680	2.953	1950.93	25.897	842.07	2504.03	25.385	30.554	0.8308	0.1256	1.78
110	100	45.15	2.695	2.958	2168.37	25.423	918.76	2282.86	26.203	30.703	0.8534	0.1395	1.62
111	100	45.14	2.694	2.957	2169.25	25.419	918.99	2282.14	26.209	30.698	0.8538	0.1396	1.62
112	100	45.13	2.693	2.956	2167.58	25.443	919.16	2281.66	26.159	30.684	0.8525	0.1395	1.62
113	110	45.13	2.706	2.958	2383.43	24.903	989.26	2076.80	26.748	30.819	0.8679	0.1533	1.05
114	110	45.12	2.707	2.960	2383.74	24.915	989.84	2075.92	26.728	30.826	0.8671	0.1533	1.05
115	110	45.13	2.707	2.959	2383.42	24.909	989.49	2075.64	26.727	30.824	0.8671	0.1533	1.05
116	120	45.11	2.712	2.951	2600.89	24.319	1054.19	1869.01	26.900	30.875	0.8712	0.1675	1.14
117	120	45.11	2.713	2.952	2603.50	24.294	1054.17	1866.68	26.921	30.890	0.8715	0.1676	1.14
118	120	45.10	2.714	2.954	2603.21	24.316	1055.02	1870.28	26.945	30.896	0.8721	0.1676	1.14
119	120	45.11	2.477	2.651	2599.81	23.880	1034.71	1683.57	24.666	28.422	0.8679	0.1751	1.21
120	120	45.12	2.478	2.652	2600.08	23.890	1035.27	1682.20	24.638	28.427	0.8667	0.1751	1.21
121	120	45.12	2.477	2.650	2599.62	23.875	1034.43	1681.73	24.642	28.417	0.8672	0.1751	1.21
122	110	45.12	2.471	2.655	2384.61	24.542	975.39	1883.18	24.624	28.357	0.8684	0.1605	0.76
123	110	45.10	2.469	2.652	2385.74	24.543	975.88	1883.71	24.642	28.330	0.8698	0.1607	0.76
124	110	45.12	2.471	2.655	2385.29	24.544	975.73	1884.05	24.641	28.356	0.8690	0.1606	0.76
125	100	45.07	2.461	2.653	2168.59	25.134	908.43	2088.67	24.252	28.237	0.8589	0.1460	0.95
126	100	45.08	2.460	2.653	2168.80	25.121	908.05	2087.52	24.253	28.236	0.8589	0.1460	0.95
127	100	45.07	2.460	2.652	2169.14	25.127	908.41	2088.32	24.260	28.234	0.8593	0.1461	0.95
129	90	45.05	2.441	2.639	1953.11	25.641	834.67	2289.81	23.472	28.013	0.8379	0.1318	2.21
130	90	45.04	2.438	2.636	1953.20	25.641	834.69	2288.81	23.463	27.985	0.8384	0.1319	2.21
131	80	45.12	2.440	2.650	1735.49	26.113	755.33	2530.64	22.633	28.004	0.8082	0.1169	1.89
132	80	45.11	2.439	2.649	1735.29	26.115	755.28	2530.20	22.625	27.998	0.8081	0.1169	1.89
133	80	45.09	2.438	2.648	1735.21	26.118	755.34	2530.03	22.620	27.988	0.8082	0.1169	1.89
134	61	45.10	2.428	2.652	1323.25	26.612	586.91	2966.45	19.850	27.869	0.7123	0.0891	1.17
135	61	45.10	2.427	2.651	1323.22	26.623	587.13	2966.88	19.845	27.856	0.7124	0.0891	1.17
136	61	45.09	2.427	2.651	1323.19	26.621	587.09	2965.87	19.838	27.854	0.7122	0.0891	1.17
137	100	45.09	2.693	2.955	2166.30	25.416	917.64	2282.51	26.181	30.689	0.8531	0.1394	1.25
138	100	45.09	2.692	2.953	2167.17	25.422	918.22	2282.91	26.190	30.674	0.8538	0.1395	1.25
139	100	45.08	2.692	2.955	2167.06	25.425	918.29	2284.26	26.201	30.682	0.8539	0.1395	1.25
140	61	45.14	2.136	2.284	1318.68	26.495	582.31	2654.63	17.780	24.265	0.7327	0.0955	0.94
141	61	45.14	2.137	2.285	1318.94	26.494	582.41	2654.43	17.783	24.278	0.7325	0.0955	0.94
142	61	45.14	2.137	2.285	1318.08	26.494	582.03	2656.04	17.782	24.281	0.7324	0.0955	0.94
143	80	45.11	2.143	2.277	1731.21	25.684	741.08	2205.78	20.008	24.358	0.8214	0.1256	0.95
144	80	45.10	2.144	2.278	1731.48	25.682	741.14	2205.20	20.008	24.368	0.8211	0.1256	0.95
145	80	45.09	2.141	2.275	1732.36	25.680	741.46	2202.76	19.997	24.328	0.8220	0.1258	0.95
146	90	45.06	2.149	2.276	1948.90	25.066	814.19	1979.64	20.713	24.441	0.8475	0.1414	0.6
147	90	45.06	2.150	2.277	1948.48	25.060	813.60	1979.23	20.710	24.452	0.8470	0.1414	0.63
148	90	45.05	2.149	2.276	1948.77	25.063	814.03	1978.75	20.705	24.445	0.8470	0.1414	0.63

Table I. Reduced Test Data and Calculated Performance Parameters, 4-1/2-Stage Configuration (Continued).

RDG	PCT NDES	PTO	PTO/PT3	PTO/PS3	N EQV	WA EQV	WAN EQV	TQ EQV	DH EQV	DHI EQV	ETA TT	U/CO	FLOWANG
149	100	45.03	2.154	2.274	2167.10	24.404	881.43	1771.21	21.166	24.507	0.8637	0.1573	0.82
150	100	45.03	2.153	2.273	2165.79	24.414	881.26	1771.95	21.154	24.495	0.8636	0.1573	0.82
151	100	45.03	2.155	2.275	2166.33	24.407	881.24	1771.80	21.163	24.516	0.8632	0.1573	0.82
152	110	45.00	2.161	2.274	2380.51	23.731	941.54	1577.82	21.299	24.595	0.8660	0.1726	0.84
153	110	45.01	2.161	2.275	2381.46	23.709	941.04	1575.99	21.303	24.600	0.8660	0.1729	0.84
154	110	45.00	2.161	2.275	2382.27	23.720	941.79	1577.63	21.323	24.600	0.8668	0.1729	0.84
155	120	44.99	2.169	2.275	2598.95	22.895	991.73	1373.67	20.984	24.700	0.8496	0.1886	0.65
156	120	44.99	2.170	2.276	2600.88	22.887	992.09	1372.40	20.988	24.715	0.8492	0.1887	0.65
157	120	45.00	2.170	2.277	2597.18	22.901	991.32	1375.04	20.985	24.717	0.8490	0.1885	0.65
158	81	37.99	1.881	1.964	1753.02	24.659	720.48	1801.17	17.231	20.557	0.8382	0.1590	0.67
159	81	37.98	1.881	1.963	1753.71	24.655	720.64	1800.31	17.233	20.553	0.8385	0.1591	0.67
160	81	38.00	1.881	1.964	1753.14	24.657	720.46	1800.68	17.229	20.557	0.8381	0.1590	0.67
161	91	37.99	1.886	1.964	1969.70	23.889	784.22	1595.35	17.702	20.644	0.8575	0.1562	0.74
162	91	37.98	1.886	1.964	1968.54	23.902	784.21	1596.22	17.691	20.644	0.8570	0.1561	0.74
163	91	37.99	1.887	1.965	1968.07	23.898	783.69	1595.54	17.682	20.652	0.8562	0.1560	0.74
164	100	37.96	1.892	1.965	2174.38	23.128	838.16	1410.31	17.843	20.731	0.8607	0.1724	0.74
165	100	37.95	1.891	1.964	2173.54	23.133	838.01	1410.84	17.839	20.720	0.8609	0.1724	0.74
166	100	37.95	1.890	1.963	2172.99	23.136	837.91	1410.25	17.825	20.709	0.8607	0.1724	0.74
167	110	37.97	1.896	1.964	2390.51	22.194	884.26	1208.62	17.519	20.800	0.8423	0.1896	1.27
168	110	37.95	1.896	1.963	2390.54	22.200	884.50	1208.72	17.516	20.790	0.8425	0.1896	1.27
169	110	37.95	1.896	1.963	2390.07	22.206	884.57	1209.59	17.520	20.794	0.8426	0.1896	1.27
170	120	37.97	1.901	1.963	2610.60	21.216	923.11	1016.71	16.836	20.872	0.8066	0.2071	0.92
171	120	37.98	1.901	1.964	2608.65	21.218	922.49	1017.94	16.842	20.880	0.8066	0.2069	0.92
172	120	37.97	1.902	1.964	2610.08	21.215	922.90	1018.34	16.860	20.685	0.8073	0.2070	0.92
173	100	44.95	2.696	2.960	2164.86	25.455	918.43	2288.26	26.189	30.716	0.8526	0.1592	1.37
174	100	44.97	2.697	2.961	2164.20	25.459	918.30	2289.04	26.186	30.724	0.8523	0.1592	1.37
175	100	44.96	2.699	2.964	2164.38	25.453	918.15	2289.40	26.190	30.746	0.8521	0.1591	1.37
176	100	44.99	2.691	2.954	2166.64	25.456	919.24	2282.22	26.140	30.668	0.8524	0.1595	1.58
177	100	44.99	2.692	2.955	2166.61	25.441	918.67	2281.46	26.147	30.678	0.8523	0.1595	1.58
178	100	45.00	2.694	2.956	2166.37	25.414	917.59	2279.12	26.145	30.695	0.8518	0.1594	1.58
179	61	37.98	1.712	1.780	1325.07	25.289	558.48	1963.92	13.848	17.734	0.7809	0.1129	1.28
180	61	37.96	1.712	1.779	1325.60	25.286	558.64	1963.46	13.852	17.718	0.7818	0.1130	1.28
181	61	37.95	1.711	1.779	1325.01	25.283	558.33	1962.60	13.842	17.714	0.7814	0.1130	1.28
182	81	37.95	1.719	1.776	1768.41	23.520	693.21	1498.55	15.163	17.847	0.8496	0.1509	2.33
183	81	37.94	1.719	1.777	1768.35	23.515	693.05	1499.27	15.173	17.856	0.8497	0.1509	2.33
184	81	37.94	1.720	1.778	1768.63	23.521	693.32	1499.37	15.173	17.869	0.8491	0.1509	2.33
185	92	37.98	1.720	1.773	1990.24	22.585	749.14	1292.44	15.327	17.876	0.8574	0.1701	1.07
186	92	37.97	1.721	1.774	1990.64	22.582	749.21	1292.93	15.338	17.884	0.8577	0.1701	1.07
187	92	37.95	1.720	1.773	1991.04	22.594	749.76	1294.12	15.347	17.875	0.8585	0.1702	1.07
188	102	37.97	1.731	1.780	2210.24	21.646	797.38	1105.94	15.197	18.057	0.8416	0.1884	1.22
189	102	38.00	1.731	1.781	2210.26	21.648	797.47	1106.02	15.197	18.071	0.8410	0.1883	1.22
190	102	37.99	1.731	1.780	2210.26	21.644	797.33	1106.16	15.201	18.067	0.8414	0.1883	1.22
191	112	37.94	1.735	1.780	2434.06	20.590	835.27	916.87	14.586	18.126	0.8047	0.2074	1.22
192	112	37.94	1.735	1.780	2434.13	20.588	835.22	916.53	14.583	18.136	0.8041	0.2074	1.22
193	112	37.93	1.735	1.780	2433.58	20.588	835.03	916.82	14.584	18.125	0.8047	0.2074	1.22
194	122	37.96	1.736	1.776	2652.67	19.676	869.69	760.24	13.793	18.156	0.7597	0.2262	1.80
195	122	37.64	1.730	1.772	2652.83	19.666	869.51	756.91	13.740	18.046	0.7614	0.2269	1.80
196	122	37.60	1.733	1.774	2652.63	19.602	866.61	750.91	13.675	18.099	0.7556	0.2266	1.80
197	100	37.94	2.695	2.959	2167.47	25.419	918.24	2276.88	26.128	30.709	0.8508	0.1594	1.81
198	100	37.93	2.694	2.958	2168.07	25.436	919.13	2276.84	26.116	30.701	0.8507	0.1595	1.81

Table I. Reduced Test Data and Calculated Performance Parameters, 4-1/2-Stage Configuration (Continued).

RDG	PCT NDES	PTO	PTO/PT3	PTO/PS3	N EQV	WA EQV	WAN EQV	TQ EQV	DH EQV	DHI EQV	ETA IT	U/CO	FLOWANG
199	100	37.92	2.694	2.958	2167.52	25.432	918.76	2277.35	26.119	30.700	0.8508	0.1095	1.81
200	100	45.09	2.695	2.959	2172.15	25.435	920.80	2279.01	26.192	30.706	0.8530	0.1097	2.04
201	100	45.07	2.694	2.958	2172.39	25.447	921.35	2278.96	26.182	30.698	0.8529	0.1096	2.04
202	100	45.08	2.694	2.958	2172.23	25.446	921.24	2281.16	26.206	30.701	0.8536	0.1098	2.04
203	80	49.94	2.667	2.953	1734.96	26.320	761.07	2741.51	24.319	30.430	0.7992	0.1117	2.62
204	80	49.97	2.670	2.957	1734.90	26.320	761.05	2741.70	24.320	30.461	0.7984	0.1116	2.62
205	80	50.06	2.671	2.956	1735.15	26.310	760.86	2741.64	24.333	30.470	0.7986	0.1116	2.62
206	100	50.08	2.693	2.956	2168.74	25.456	920.14	2284.44	26.191	30.686	0.8535	0.1096	1.72
207	100	50.07	2.695	2.959	2168.76	25.466	920.50	2285.51	26.193	30.702	0.8531	0.1095	1.72
208	100	50.08	2.694	2.957	2168.80	25.460	920.30	2284.23	26.186	30.693	0.8532	0.1096	1.72
209	110	50.09	2.708	2.961	2383.27	24.951	991.08	2081.40	26.755	30.833	0.8677	0.1033	1.07
210	110	50.08	2.710	2.965	2383.32	24.941	990.69	2081.11	26.763	30.860	0.8672	0.1032	1.07
211	110	50.04	2.708	2.962	2383.34	24.967	991.75	2082.77	26.756	30.832	0.8678	0.1033	1.07
212	80	38.06	2.670	2.956	1738.79	26.261	761.04	2727.21	24.300	30.460	0.7978	0.1119	2.62
213	80	38.06	2.673	2.959	1738.39	26.271	761.15	2731.55	24.324	30.484	0.7979	0.1116	2.62
214	80	38.03	2.670	2.956	1738.70	26.280	761.55	2729.32	24.300	30.460	0.7978	0.1119	2.62
215	110	38.12	2.703	2.954	2388.24	24.883	990.45	2062.24	26.636	30.785	0.8652	0.1037	1.07
216	110	38.27	2.706	2.958	2388.96	24.894	991.17	2067.38	26.690	30.821	0.8663	0.1037	1.07
217	110	38.28	2.706	2.958	2388.86	24.894	991.16	2066.21	26.682	30.820	0.8658	0.1037	1.07
218	110	25.04	2.709	2.960	2390.23	24.781	987.22	2042.67	26.514	30.843	0.8597	0.1037	1.07
219	110	25.06	2.720	2.974	2391.26	24.760	986.80	2044.90	26.577	30.956	0.8585	0.1035	1.07
220	110	25.06	2.712	2.963	2390.59	24.736	985.54	2036.42	26.485	30.879	0.8577	0.1037	1.07
221	100	25.04	2.698	2.960	2172.99	25.314	916.80	2253.67	26.034	30.734	0.8471	0.1098	1.72
222	100	25.04	2.695	2.957	2173.53	25.313	916.99	2251.53	26.017	30.711	0.8472	0.1099	1.72
223	100	25.04	2.697	2.958	2174.17	25.311	917.17	2251.51	26.027	30.723	0.8472	0.1099	1.72
224	80	25.03	2.673	2.959	1739.14	26.217	759.90	2707.18	24.168	30.488	0.7927	0.1119	2.62
225	80	25.04	2.671	2.955	1738.81	26.207	759.49	2704.45	24.147	30.467	0.7926	0.1119	2.62
226	80	24.99	2.664	2.940	1738.88	26.238	760.42	2703.15	24.108	30.396	0.7931	0.1121	2.62
227	80	45.02	2.927	3.317	1736.72	26.353	762.80	2924.46	25.936	32.897	0.7884	0.1071	1.42
228	80	45.02	2.924	3.313	1736.31	26.363	762.91	2924.57	25.921	32.870	0.7886	0.1071	1.42
229	80	45.02	2.926	3.315	1736.71	26.355	762.84	2923.71	25.928	32.882	0.7885	0.1071	1.42
230	90	45.03	2.937	3.311	1950.97	26.037	846.64	2693.07	27.156	32.981	0.8234	0.1204	1.20
231	90	45.02	2.939	3.315	1950.97	26.037	846.63	2692.33	27.148	33.003	0.8226	0.1203	1.20
232	90	45.02	2.938	3.313	1950.60	26.041	846.58	2693.60	27.152	32.989	0.8231	0.1203	1.20
233	100	45.04	2.950	3.310	2170.69	25.624	927.04	2462.33	28.071	33.099	0.8481	0.1040	1.26
234	100	44.99	2.950	3.310	2170.62	25.626	927.08	2463.96	28.086	33.101	0.8485	0.1039	1.26
235	100	45.00	2.953	3.314	2170.69	25.628	927.19	2463.96	28.085	33.125	0.8478	0.1039	1.26
236	110	45.08	2.960	3.305	2382.73	25.176	999.81	2251.41	28.675	33.186	0.8641	0.1471	2.12
237	110	45.07	2.959	3.304	2382.56	25.165	999.29	2250.48	28.673	33.178	0.8642	0.1471	2.12
238	110	45.06	2.962	3.306	2382.76	25.177	999.85	2250.54	28.663	33.200	0.8633	0.1471	2.12
239	120	45.06	2.981	3.315	2606.36	24.633	1070.06	2043.51	29.097	33.373	0.8719	0.1008	2.57
240	120	45.05	2.981	3.315	2606.45	24.638	1070.28	2043.09	29.087	33.374	0.8715	0.1008	2.57
241	120	45.06	2.982	3.316	2606.81	24.636	1070.35	2043.78	29.103	33.382	0.8718	0.1008	2.57
242	100	45.02	2.687	2.949	2166.47	25.461	919.34	2290.70	26.231	30.627	0.8564	0.1096	1.44
243	100	45.03	2.701	2.967	2166.05	25.467	919.38	2290.10	26.212	30.767	0.8520	0.1092	1.44
244	100	45.02	2.698	2.964	2166.45	25.475	919.85	2289.65	26.204	30.741	0.8524	0.1093	1.44
245	100	45.03	3.193	3.670	2166.82	25.740	929.58	2618.34	29.662	35.143	0.8440	0.1292	1.11
246	100	45.04	3.199	3.679	2166.49	25.738	929.34	2619.08	29.669	35.193	0.8430	0.1291	1.11
247	100	45.04	3.191	3.665	2166.52	25.737	929.32	2616.35	29.639	35.123	0.8439	0.1292	1.11
248	100	45.04	3.193	3.669	2166.83	25.737	929.45	2617.59	29.658	35.140	0.8440	0.1292	1.11

Table I. Reduced Test Data and Calculated Performance Parameters, 4-1/2-Stage Configuration (Concluded).

RDG	PCT DES	PTO	PTO/PT3	PTO/PS3	N EQV	WA EQV	WAN EQV	TQ EQV	DH EQV	DHI EQV	ETA IT	U/C0	FLOWANG
249	90	45.02	3.162	3.640	1949.01	26.106	848.02	2841.11	28.544	34.890	0.8181	0.1164	1.58
250	90	45.02	3.166	3.655	1948.90	26.102	847.04	2841.20	28.548	34.928	0.8173	0.1163	1.58
251	90	45.04	3.169	3.650	1949.23	26.101	847.93	2840.77	28.550	34.949	0.8169	0.1163	1.58
252	80	45.02	3.151	3.650	1731.94	26.382	761.53	3074.19	27.150	34.806	0.7803	0.1034	1.19
253	80	45.03	3.153	3.660	1731.90	26.382	761.53	3074.35	27.160	34.822	0.7800	0.1033	1.19
254	80	45.04	3.149	3.654	1731.94	26.386	761.64	3071.95	27.135	34.786	0.7801	0.1034	1.19
255	109	45.11	3.214	3.674	2379.30	25.296	1003.12	2401.19	30.393	35.311	0.8607	0.1418	1.50
256	109	45.08	3.215	3.677	2378.96	25.325	1004.12	2405.98	30.415	35.316	0.8612	0.1418	1.50
257	109	45.10	3.218	3.680	2379.21	25.312	1003.73	2404.82	30.410	35.340	0.8607	0.1417	1.50
258	120	45.08	3.231	3.674	2604.09	24.820	1077.20	2187.70	30.880	35.446	0.8714	0.1552	2.06
259	120	45.09	3.233	3.677	2604.37	24.807	1076.79	2187.49	30.905	35.463	0.8715	0.1552	2.06
260	120	45.07	3.232	3.675	2605.02	24.816	1077.46	2187.89	30.907	35.450	0.8718	0.1552	2.06
261	100	45.07	3.856	4.830	2169.64	25.776	932.08	2831.51	32.074	39.831	0.8053	0.1197	2.59
262	100	45.07	3.863	4.851	2169.33	25.779	932.07	2832.87	32.080	39.874	0.8045	0.1196	2.59
263	100	45.07	3.864	4.853	2169.29	25.775	931.89	2832.83	32.085	39.883	0.8045	0.1195	2.59
264	80	45.10	3.776	4.812	1734.01	26.390	762.67	3222.56	28.496	39.320	0.7247	0.0958	1.60
265	80	45.10	3.776	4.810	1733.99	26.380	762.38	3222.17	28.502	39.321	0.7248	0.0958	1.60
266	80	45.10	3.774	4.800	1734.02	26.387	762.59	3222.32	28.496	39.307	0.7250	0.0958	1.60
267	110	45.09	3.881	4.818	2384.80	25.405	1009.77	2644.94	33.412	39.985	0.8356	0.1317	1.72
268	110	45.11	3.887	4.829	2385.49	25.401	1009.89	2643.83	33.414	40.022	0.8349	0.1316	1.72
269	110	45.08	3.888	4.830	2386.84	25.385	1009.85	2642.35	33.434	40.032	0.8352	0.1317	1.72
270	120	45.09	3.917	4.821	2601.51	24.971	1082.68	2454.55	34.414	40.208	0.8559	0.1436	2.00
271	120	45.06	3.917	4.823	2600.89	24.986	1083.08	2456.28	34.400	40.207	0.8558	0.1435	2.00
272	120	45.06	3.915	4.819	2601.43	24.983	1083.20	2456.75	34.426	40.197	0.8564	0.1436	2.00
273	60	45.10	3.125	3.668	1298.22	26.686	577.40	3492.39	22.864	34.592	0.6610	0.0774	1.47
274	60	45.09	3.120	3.660	1298.74	26.692	577.77	3490.56	22.856	34.552	0.6615	0.0775	1.47
275	60	45.09	3.119	3.658	1299.47	26.685	577.94	3489.58	22.868	34.542	0.6620	0.0776	1.47
276	60	45.07	2.893	3.304	1298.67	26.688	577.64	3364.12	22.030	32.588	0.6760	0.0602	1.84
277	60	45.07	2.895	3.307	1298.53	26.680	577.42	3363.64	22.031	32.610	0.6756	0.0602	1.84
278	60	45.07	2.894	3.305	1298.15	26.701	577.70	3364.56	22.013	32.594	0.6754	0.0601	1.84
279	60	45.04	2.650	2.953	1299.24	26.682	577.77	3188.70	20.895	30.252	0.6907	0.0637	1.36
280	60	45.06	2.650	2.952	1299.34	26.675	577.67	3189.71	20.908	30.252	0.6911	0.0637	1.36
281	60	45.04	2.652	2.956	1299.70	26.686	578.06	3191.45	20.917	30.278	0.6908	0.0636	1.36
282	100	45.06	2.696	2.961	2166.38	25.460	919.27	2289.94	26.222	30.722	0.8535	0.1393	1.72
283	100	45.07	2.695	2.960	2166.51	25.449	918.94	2288.61	26.219	30.711	0.8537	0.1394	1.72
284	100	45.03	2.694	2.958	2165.97	25.458	919.03	2289.81	26.217	30.694	0.8541	0.1394	1.72

Table II. Reduced Test Data and Calculated Performance Parameters, 4-Stage Configuration.

RDG	PCT NDES	PTO	PTO/PT3	PTO/PS3	N EQV	WA EQV	WAN EQV	TQ EQV	DH EQV	DHI EQV	ETA TT	U/CO	FLOWANG
1	100	45.05	2.709	3.078	2172.93	25.433	921.08	2286.05	26.284	30.843	0.8522	0.1377	28.67
2	100	44.99	2.706	3.074	2171.83	25.442	920.95	2284.72	26.246	30.820	0.8516	0.1377	28.64
3	100	44.99	2.706	3.074	2172.32	25.441	921.09	2286.63	26.275	30.817	0.8526	0.1377	28.68
7	80	45.08	2.640	3.084	1733.89	26.263	758.96	2713.78	24.110	30.154	0.7996	0.1098	34.20
8	80	45.07	2.638	3.081	1733.38	26.263	758.74	2712.83	24.088	30.137	0.7993	0.1098	34.17
9	80	45.09	2.640	3.083	1733.94	26.262	758.95	2712.64	24.102	30.153	0.7993	0.1098	34.16
10	90	45.03	2.670	3.082	1952.02	25.884	842.11	2494.32	25.314	30.453	0.8312	0.1236	32.38
11	90	45.14	2.676	3.089	1952.52	25.824	840.38	2486.73	25.302	30.513	0.8292	0.1236	32.38
12	90	45.06	2.669	3.081	1952.98	25.885	842.54	2495.16	25.335	30.447	0.8321	0.1237	32.39
13	100	45.36	2.731	3.104	2167.35	25.276	913.03	2273.68	26.237	31.066	0.8446	0.1369	28.47
14	100	45.28	2.727	3.097	2166.98	25.279	912.99	2276.19	26.258	31.021	0.8465	0.1370	28.48
15	100	45.21	2.723	3.094	2166.63	25.348	915.32	2284.07	26.273	30.984	0.8480	0.1370	28.47
16	110	45.02	2.758	3.068	2384.58	24.975	992.60	2100.49	26.989	31.329	0.8615	0.1513	19.58
17	110	44.94	2.753	3.062	2384.56	25.027	994.65	2102.28	26.955	31.277	0.8618	0.1514	19.58
18	110	46.29	2.838	3.157	2385.32	24.304	966.19	2043.53	26.991	32.082	0.8413	0.1497	19.58
19	120	45.19	2.772	3.083	2601.11	24.337	1055.03	1905.82	27.412	31.459	0.8713	0.1647	22.93
20	120	45.07	2.766	3.076	2601.76	24.363	1056.46	1908.74	27.430	31.406	0.8734	0.1649	22.94
21	120	45.28	2.778	3.088	2600.74	24.276	1052.27	1900.07	27.393	31.512	0.8693	0.1646	22.92
22	100	45.11	2.703	3.071	2167.36	25.430	918.59	2288.65	26.250	30.791	0.8525	0.1374	28.77
23	100	45.11	2.704	3.071	2167.58	25.429	918.64	2286.24	26.226	30.792	0.8517	0.1375	28.77
24	100	45.38	2.719	3.089	2167.59	25.275	913.11	2271.78	26.218	30.949	0.8471	0.1372	28.77
25	100	45.12	2.455	2.699	2167.19	25.120	907.33	2081.80	24.170	28.175	0.8578	0.1448	26.05
26	100	45.14	2.457	2.701	2168.02	25.078	906.17	2075.99	24.152	28.200	0.8564	0.1448	26.04
27	100	45.12	2.455	2.699	2167.97	25.117	907.53	2081.38	24.177	28.178	0.8580	0.1449	26.05
28	110	45.16	2.480	2.703	2381.85	24.544	974.33	1893.17	24.724	28.454	0.8689	0.1591	22.85
29	110	45.02	2.472	2.694	2381.36	24.623	977.28	1901.67	24.750	28.364	0.8726	0.1593	22.86
30	110	45.04	2.475	2.697	2382.14	24.581	975.93	1894.59	24.708	28.393	0.8702	0.1592	22.86
31	120	45.18	2.507	2.710	2598.45	23.887	1034.47	1704.30	24.950	28.748	0.8679	0.1733	18.92
32	120	45.26	2.512	2.716	2604.11	23.864	1035.75	1702.70	25.004	28.804	0.8681	0.1736	18.91
33	120	45.27	2.512	2.715	2604.28	23.853	1035.33	1700.92	24.991	28.801	0.8677	0.1736	18.91
34	60	45.35	2.377	2.712	1312.06	26.460	578.62	2881.80	19.230	27.278	0.7050	0.0875	35.08
35	60	45.14	2.364	2.697	1314.16	26.601	582.63	2898.31	19.269	27.127	0.7103	0.0878	35.09
36	60	45.04	2.360	2.693	1314.00	26.650	583.63	2902.70	19.260	27.080	0.7112	0.0879	35.08
37	100	45.24	2.708	3.074	2165.16	25.329	914.01	2275.27	26.174	30.839	0.8487	0.1372	28.75
38	100	45.24	2.713	3.083	2164.50	25.383	915.70	2284.10	26.211	30.883	0.8487	0.1371	28.77
39	100	45.21	2.707	3.078	2165.61	25.490	920.01	2301.58	26.315	30.824	0.8537	0.1372	28.79
40	100	48.83	2.928	3.325	2171.16	23.460	848.91	2106.02	26.230	32.902	0.7972	0.1338	28.80
41	100	45.36	2.721	3.091	2171.10	25.261	914.08	2266.52	26.215	30.962	0.8467	0.1374	28.79
42	100	50.84	3.051	3.466	2171.86	22.528	815.45	2022.67	26.242	33.974	0.7724	0.1319	28.79
43	80	44.90	2.121	2.298	1730.76	25.656	740.07	2178.24	19.775	24.058	0.8220	0.1250	29.71
44	80	44.91	2.121	2.299	1730.71	25.641	739.62	2177.54	19.780	24.069	0.8218	0.1249	29.71
46	100	44.97	2.158	2.302	2168.17	24.478	884.53	1784.13	21.267	24.564	0.8658	0.1564	22.63
47	100	45.14	2.168	2.312	2168.55	24.380	881.16	1777.10	21.272	24.686	0.8617	0.1561	22.63
48	100	44.98	2.161	2.305	2168.27	24.465	884.13	1783.63	21.273	24.594	0.8650	0.1563	22.63
49	120	44.92	2.176	2.291	2601.52	23.051	999.44	1403.13	21.311	24.798	0.8594	0.1881	13.76
50	120	44.92	2.176	2.291	2601.71	23.047	999.37	1402.76	21.310	24.797	0.8594	0.1882	13.70
51	120	45.01	2.181	2.296	2601.09	22.979	996.19	1398.82	21.308	24.868	0.8568	0.1879	13.71
52	122	44.74	1.738	1.784	2653.03	20.111	889.25	814.75	14.464	18.182	0.7955	0.2257	15.69
53	122	44.70	1.739	1.784	2653.31	20.103	889.00	814.54	14.468	18.196	0.7951	0.2257	15.51
54	122	44.58	1.736	1.782	2653.61	20.141	890.79	815.75	14.463	18.146	0.7971	0.2260	15.48

Table II. Reduced Test Data and Calculated Performance Parameters, 4-Stage Configuration (Concluded).

RDG	PCT NDES	PTO	PTO/PT3	PTO/PS3	N EQV	WA EQV	WAN EQV	TQ EQV	DH EQV	DHI EQV	ETA TT	U/CO	FLOWANG
55	102	44.69	1.708	1.757	2207.88	21.820	802.93	1117.12	15.212	17.654	0.8617	0.1902	9.49
56	102	44.85	1.716	1.765	2207.76	21.742	800.01	1113.93	15.222	17.791	0.8556	0.1894	9.57
57	102	44.54	1.708	1.758	2207.29	21.929	806.72	1127.79	15.277	17.655	0.8653	0.1900	10.65
58	102	44.60	1.721	1.772	2207.52	21.976	808.55	1143.33	15.455	17.887	0.8641	0.1888	9.53
60	81	44.94	1.710	1.770	1765.86	23.516	692.11	1490.41	15.061	17.694	0.8512	0.1508	22.02
61	81	44.91	1.709	1.775	1766.31	23.527	692.59	1490.77	15.062	17.676	0.8521	0.1509	22.02
63	61	43.90	1.652	1.737	1326.84	25.798	570.50	1967.69	13.619	16.634	0.8188	0.1154	29.05
64	61	45.15	1.709	1.787	1327.01	25.072	554.52	1912.45	13.622	17.510	0.7779	0.1127	29.93
65	61	42.22	1.962	2.163	1327.00	28.268	625.20	2770.15	17.500	21.805	0.8026	0.0991	34.53
66	61	42.87	1.991	2.195	1327.03	27.840	615.75	2727.84	17.498	22.239	0.7868	0.0982	34.54
67	61	45.16	2.098	2.313	1326.98	26.440	584.75	2591.06	17.500	23.749	0.7369	0.0955	34.53
68	100	45.25	2.707	3.076	2168.23	25.443	919.42	2287.58	26.235	30.822	0.8512	0.1374	28.79
69	100	45.29	2.708	3.079	2167.14	25.483	920.41	2291.68	26.227	30.832	0.8507	0.1373	28.78
70	100	45.25	2.708	3.079	2165.87	25.451	918.72	2290.79	26.235	30.837	0.8507	0.1372	28.80
71	100	44.97	2.698	3.067	2170.72	25.488	922.13	2295.43	26.308	30.732	0.8560	0.1377	29.15
72	100	44.77	2.686	3.054	2170.52	25.598	926.01	2305.14	26.304	30.618	0.8591	0.1379	29.14
73	100	45.83	2.749	3.126	2170.76	25.011	904.90	2252.73	26.311	31.240	0.8422	0.1367	29.14
77	80	44.99	2.852	3.486	1735.71	26.333	761.77	2882.48	25.569	32.216	0.7937	0.1052	35.79
78	80	44.95	2.852	3.485	1735.33	26.344	761.93	2884.12	25.567	32.208	0.7938	0.1052	35.79
79	80	44.78	2.847	3.483	1733.86	26.428	763.71	2894.60	25.556	32.169	0.7944	0.1051	35.78
80	100	45.02	2.961	3.503	2166.47	25.600	924.55	2470.30	28.133	33.192	0.8476	0.1311	30.70
81	100	44.75	2.944	3.483	2167.10	25.754	930.18	2486.46	28.157	33.041	0.8522	0.1314	30.69
82	100	43.99	2.897	3.431	2166.42	26.214	946.52	2531.38	28.153	32.627	0.8629	0.1320	30.66
83	120	44.98	3.033	3.500	2598.93	24.674	1068.77	2085.98	29.568	33.824	0.8742	0.1573	26.37
84	120	44.97	3.034	3.502	2599.61	24.683	1069.44	2086.68	29.575	33.830	0.8742	0.1574	26.36
85	120	44.98	3.037	3.505	2599.43	24.671	1068.84	2086.69	29.588	33.853	0.8740	0.1573	26.36
86	100	45.03	3.546	5.192	2168.96	25.754	930.99	2792.44	31.648	37.780	0.8377	0.1176	37.00
87	100	45.06	3.549	5.200	2168.92	25.758	931.13	2795.43	31.676	37.797	0.8380	0.1175	36.98
88	100	45.05	3.546	5.191	2169.06	25.765	931.42	2798.96	31.710	37.777	0.8394	0.1176	37.00
89	120	45.05	3.742	5.199	2601.43	24.959	1082.14	2418.51	33.923	39.099	0.8676	0.1410	33.55
90	120	45.06	3.744	5.205	2600.46	24.952	1081.46	2418.95	33.925	39.116	0.8673	0.1409	33.55
91	120	45.05	3.736	5.180	2601.73	24.949	1081.85	2416.38	33.910	39.065	0.8680	0.1411	33.55
92	80	45.08	3.363	4.987	1732.89	26.374	761.72	3182.56	28.141	36.454	0.7719	0.0949	38.28
93	80	45.07	3.361	4.978	1732.98	26.369	761.61	3181.91	28.142	36.443	0.7722	0.0949	38.29
94	80	45.07	3.361	4.976	1733.11	26.371	761.72	3180.98	28.134	36.438	0.7721	0.0949	38.28
95	100	45.10	2.708	3.077	2168.50	25.434	919.24	2297.28	26.358	30.835	0.8548	0.1374	28.79
96	100	45.09	2.707	3.076	2168.12	25.451	919.67	2298.33	26.349	30.826	0.8548	0.1374	28.79
97	99	45.11	2.706	3.077	2143.45	25.486	910.47	2317.91	26.234	30.818	0.8513	0.1358	28.80

Table III. Comparison of Predicted and Experimentally Observed Blade Natural Frequencies with Fixed-Fixed End Conditions.

Stage	First Flex		Second Flex		First Torsion	
	Predicted	Experimental	Predicted	Experimental	Predicted	Experimental
1	*	*	*	*	4103	4590
2	*	*	*	*	3308	3522
3	3913	3594	*	*	2443	2380
4	2034	2078	4992	5008	2118	2314

*Above region of frequency search.

Table IV. Fatigue Endurance Test Results.

Stage	Cycles to Failure At Failure Stress	Failure Stress KSIDA
1	750000	80
2	436000	110
3	434000	110
4	275000	130

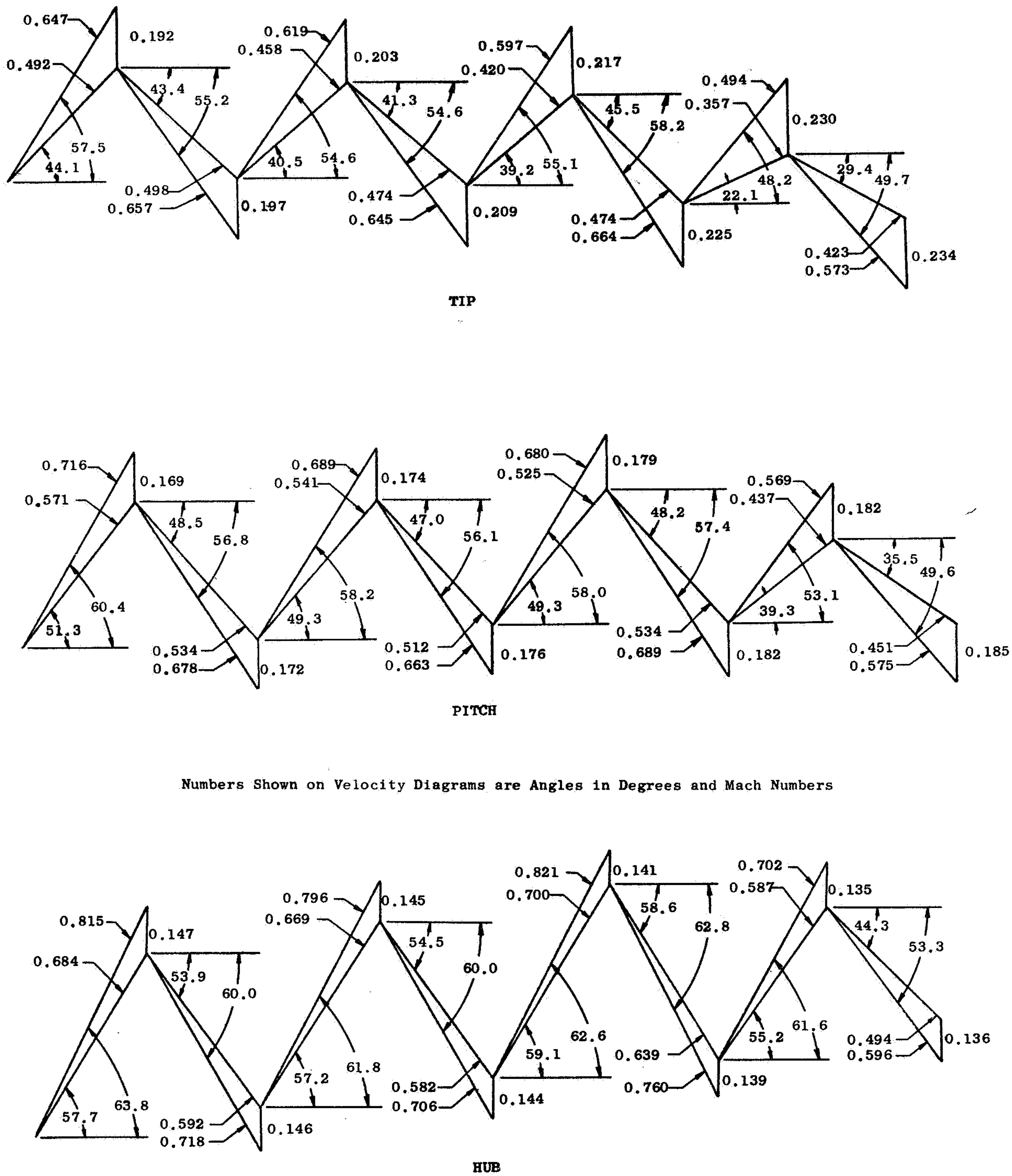

Figure 1. Turbine Design Velocity Diagrams.

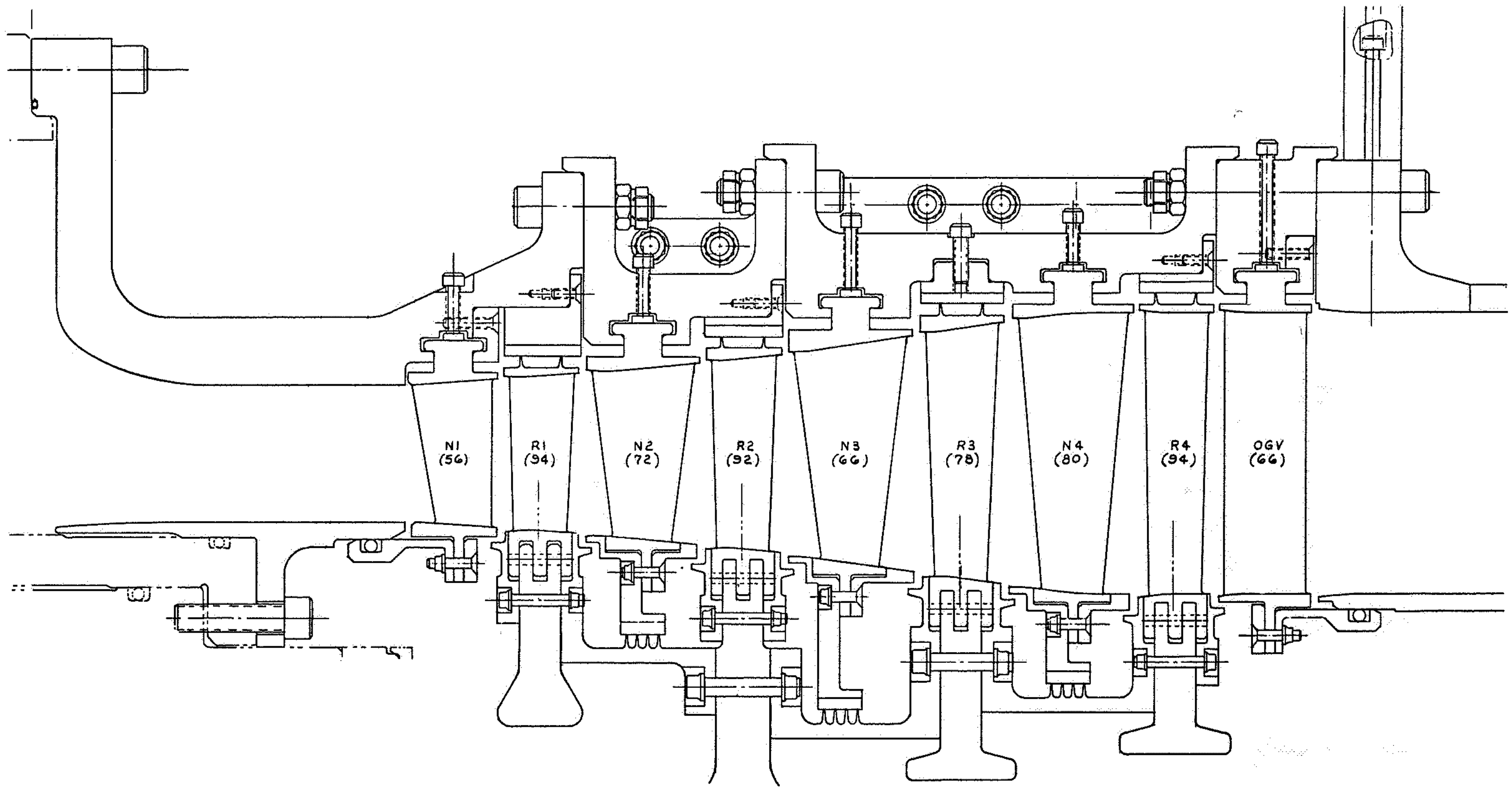

Figure 2. Four and One-Half-Stage Turbine Flowpath.

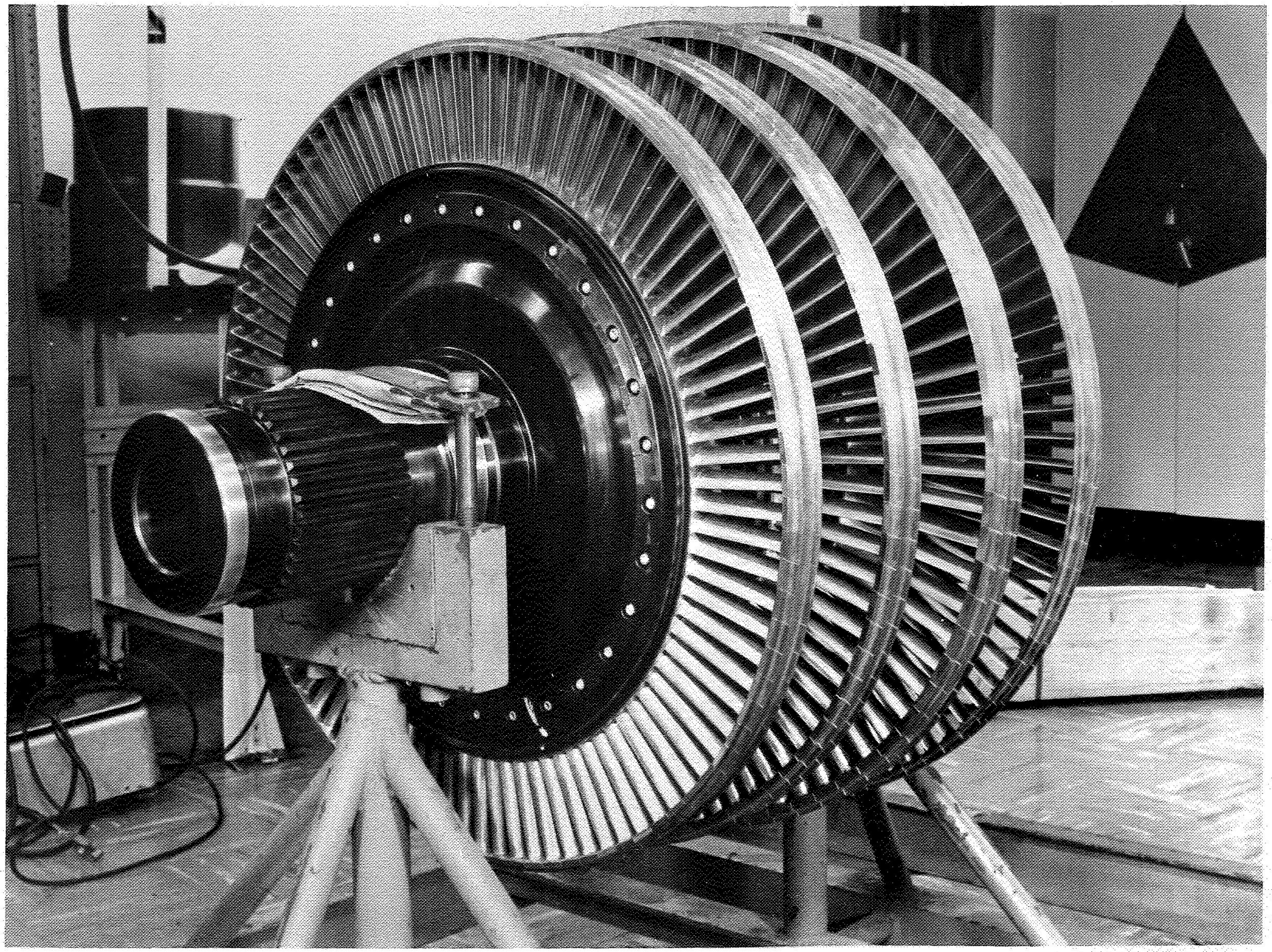

Figure 3. Four Stage Turbine Rotor Assembled.

Figure 4. Stage One Rotor Assembled.

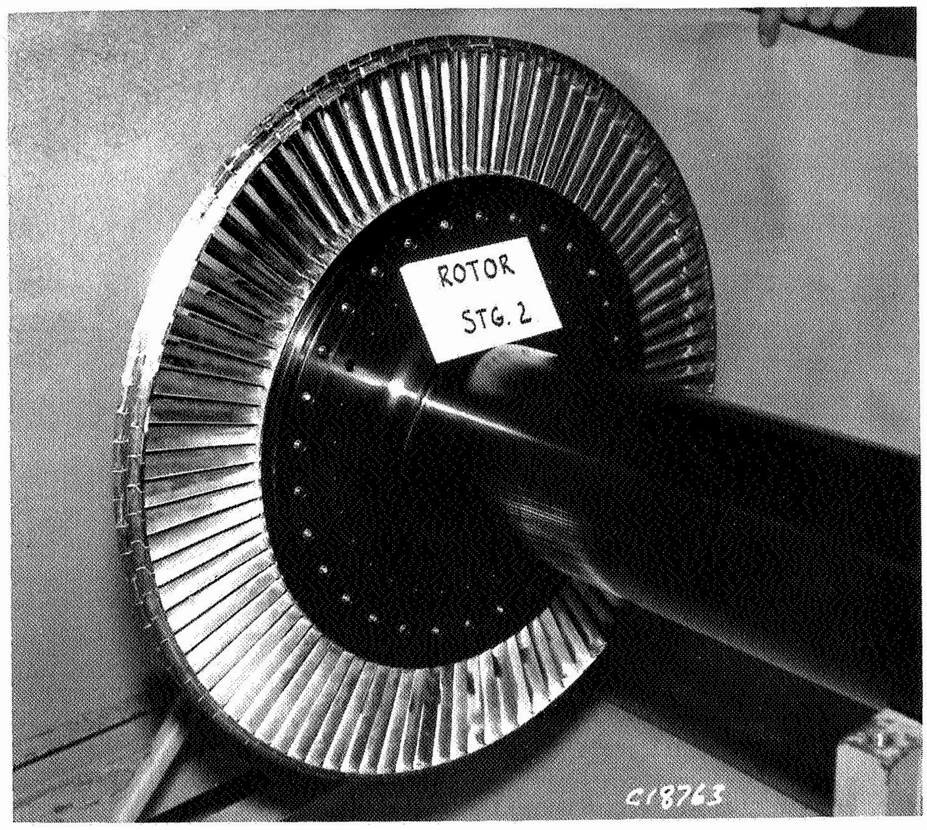

Figure 5. Stage Two Rotor Assembled.

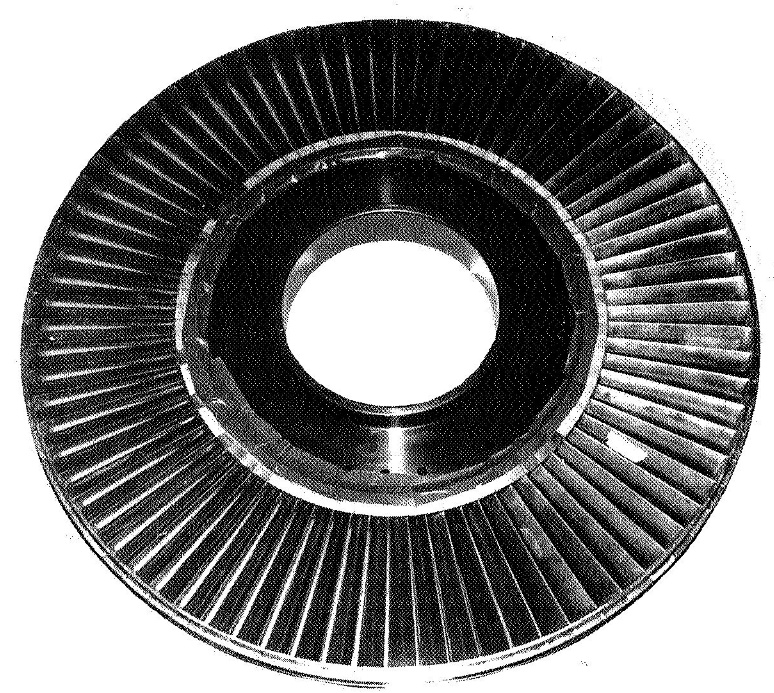

Figure 6. Stage Three Rotor Assembled.

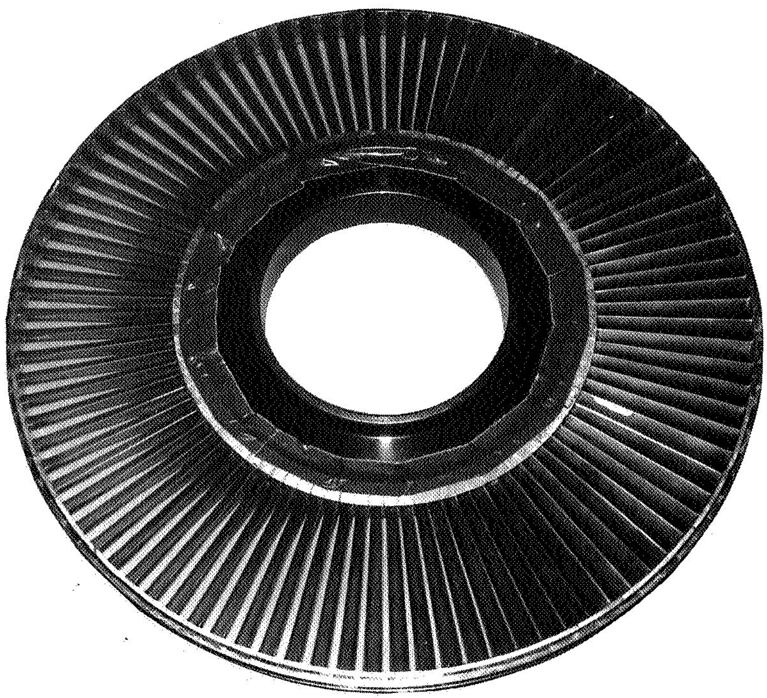

Figure 7. Stage Four Rotor Assembled.

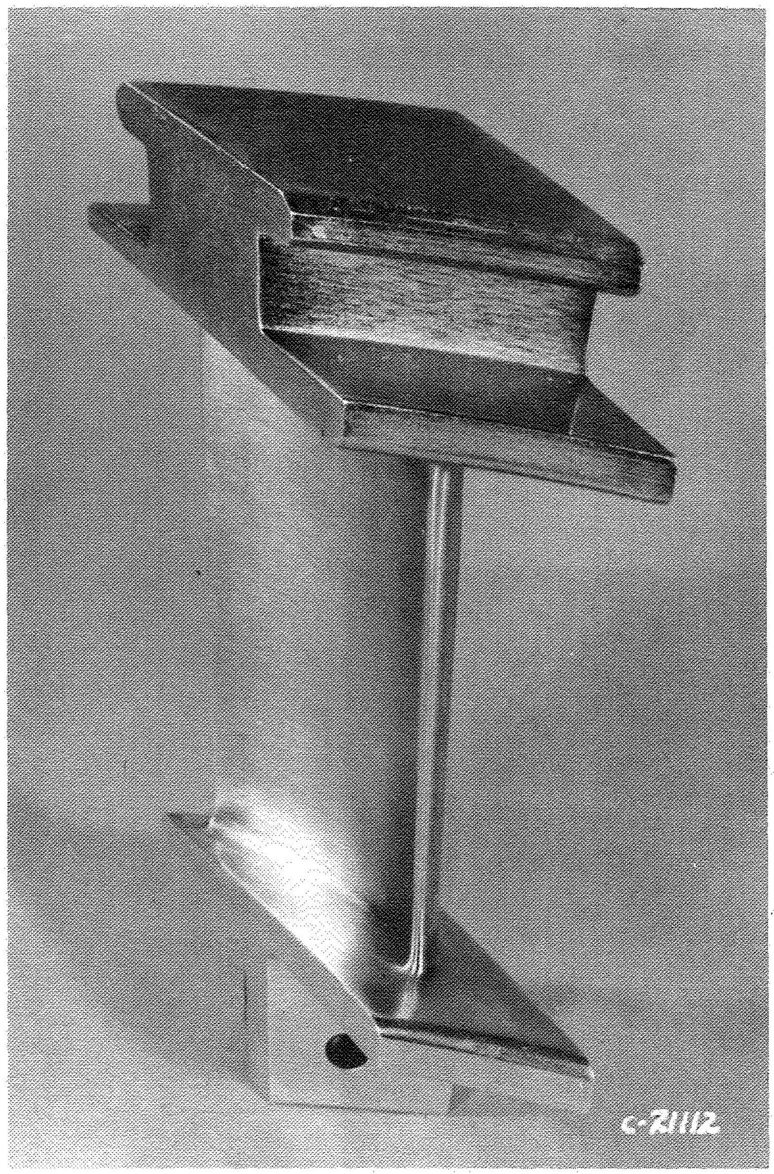

Figure 8. Stage One Stator.

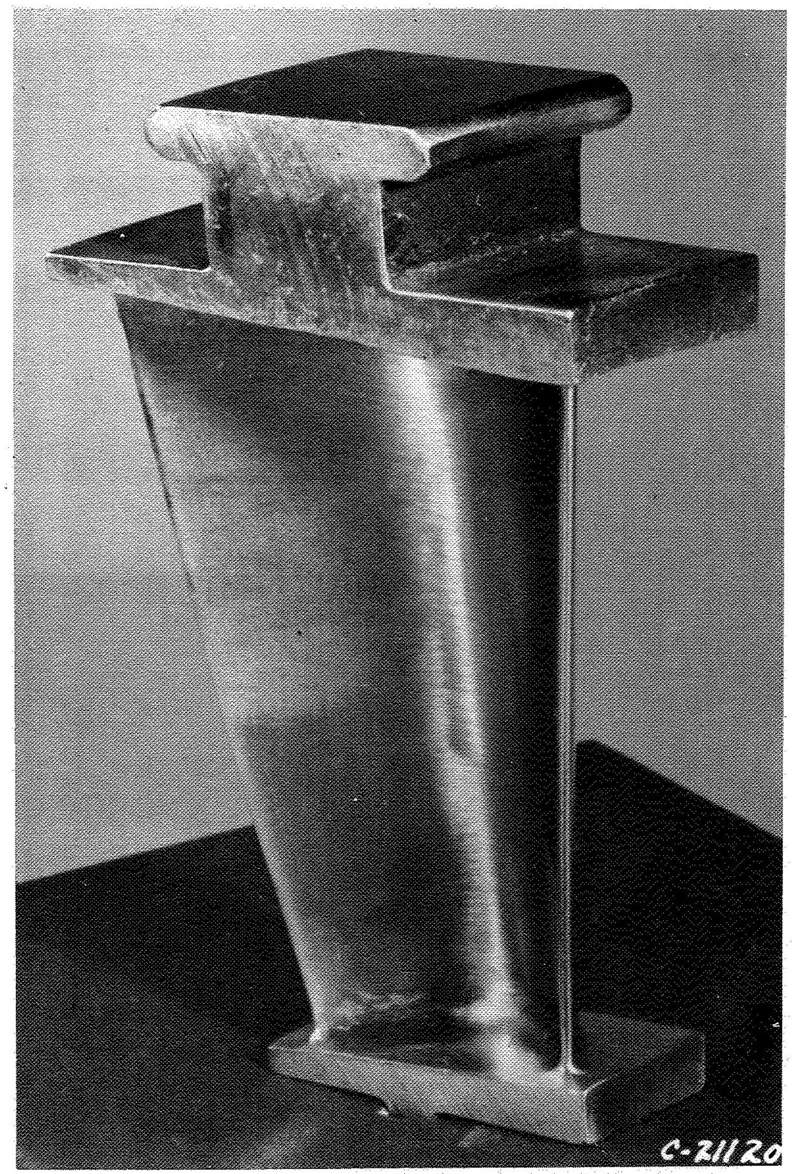

Figure 9. Stage Two Stator.

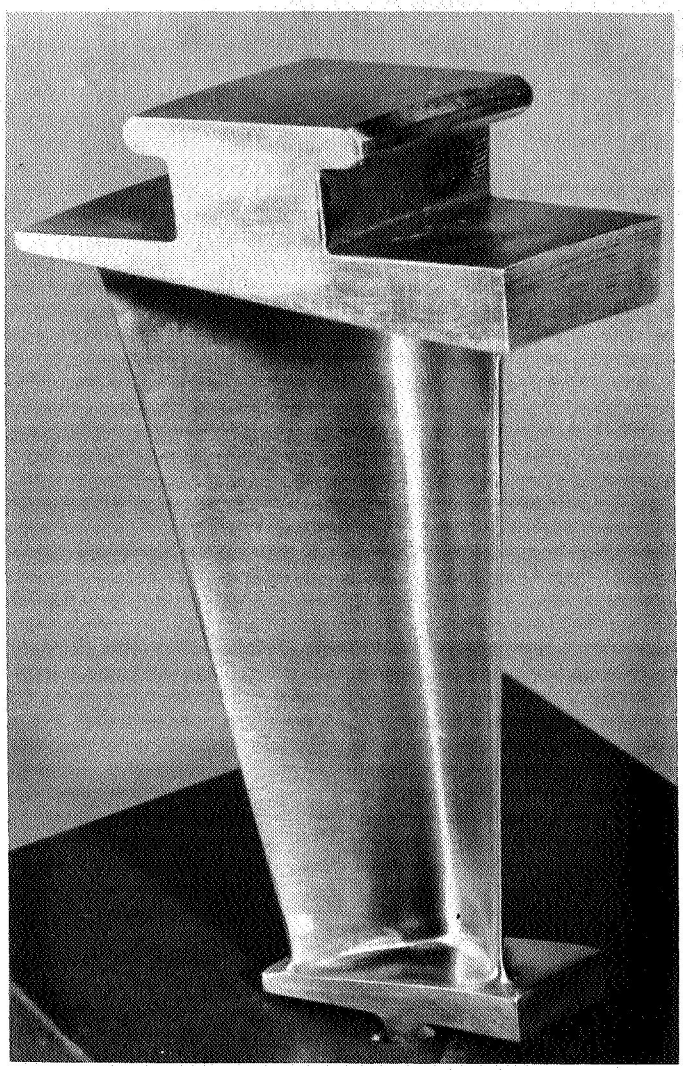

Figure 10. Stage Three Stator.

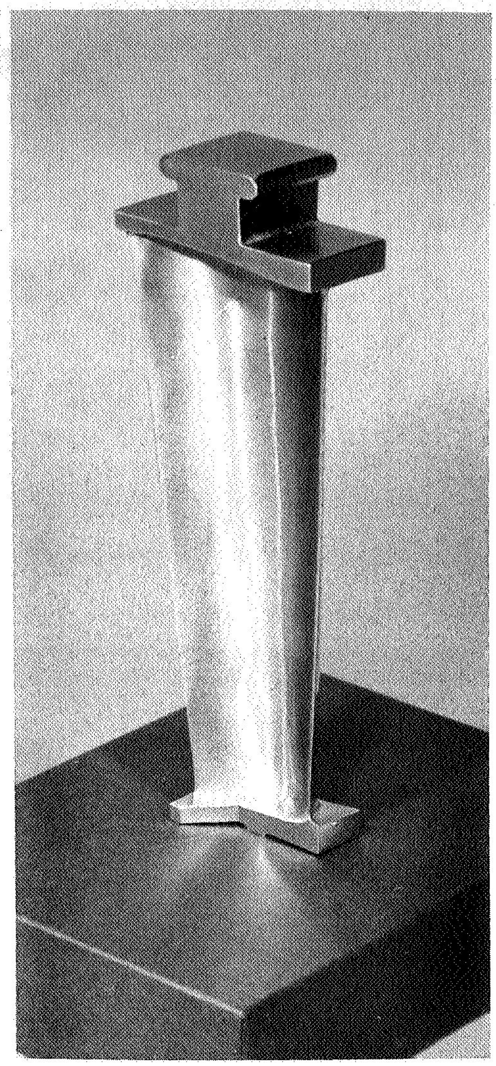

Figure 11. Stage Four Stator.

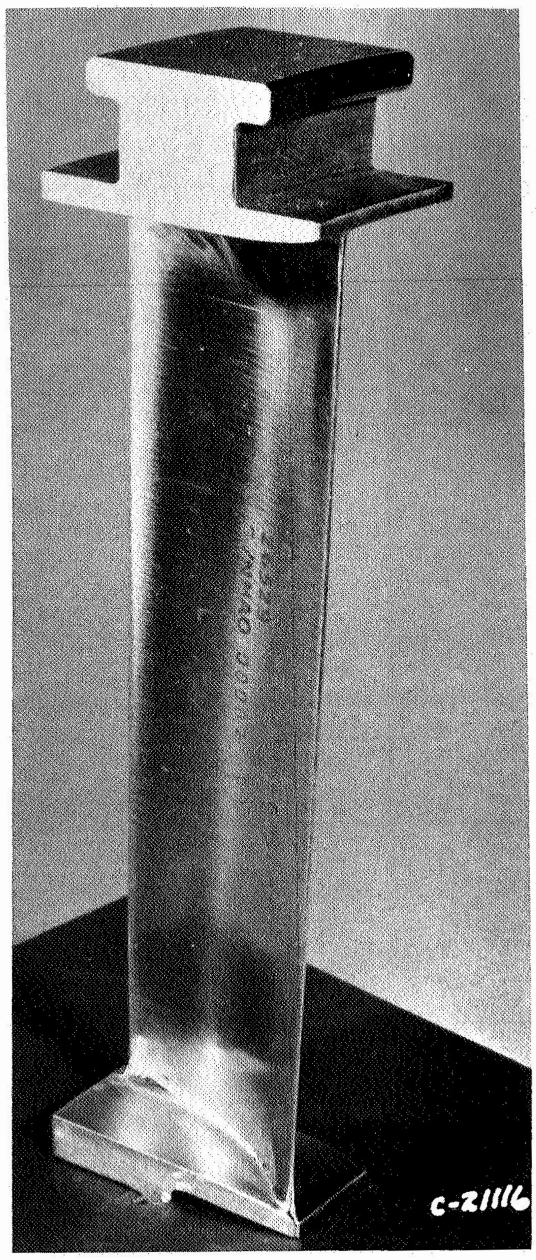

Figure 12. Outlet Turning Vane.

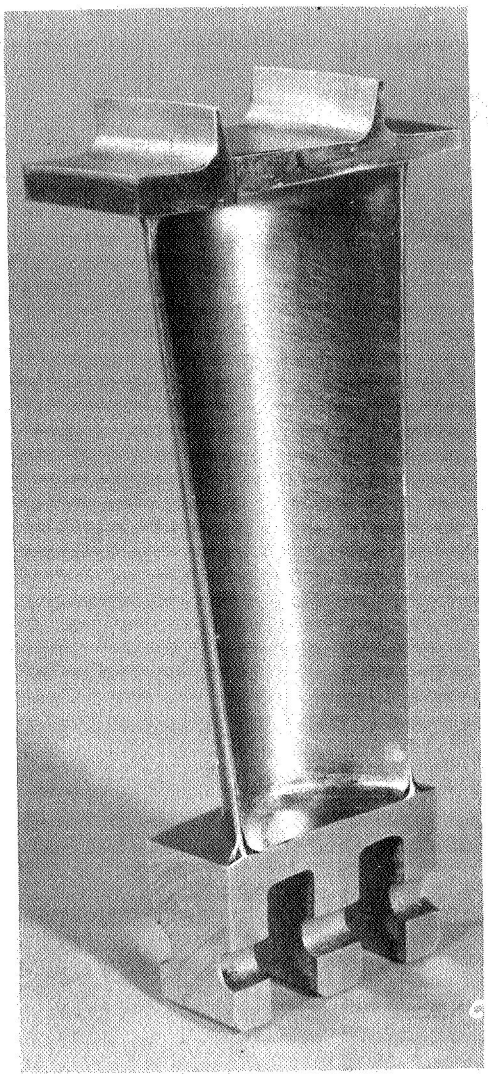

Figure 13. Stage One Rotor.

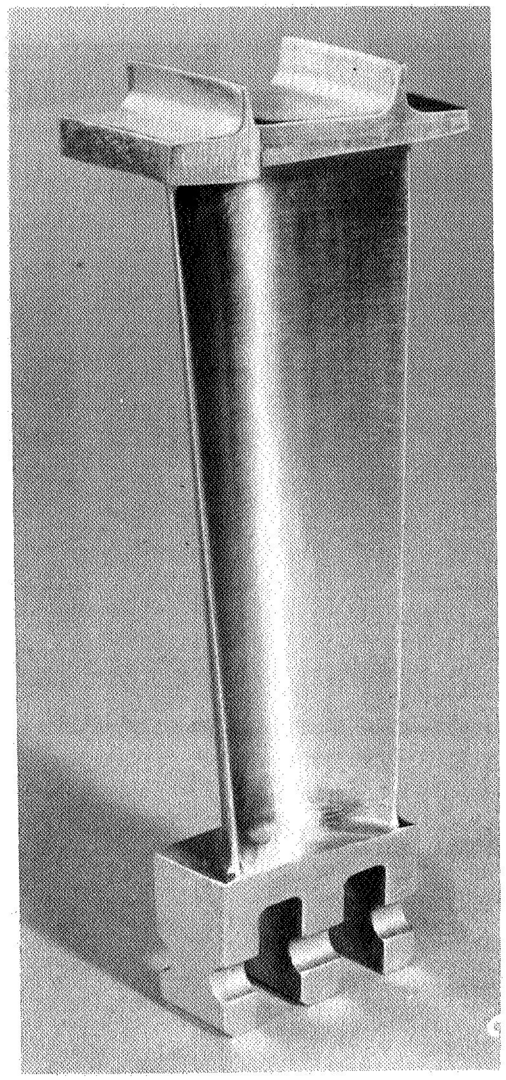

Figure 14. Stage Two Rotor.

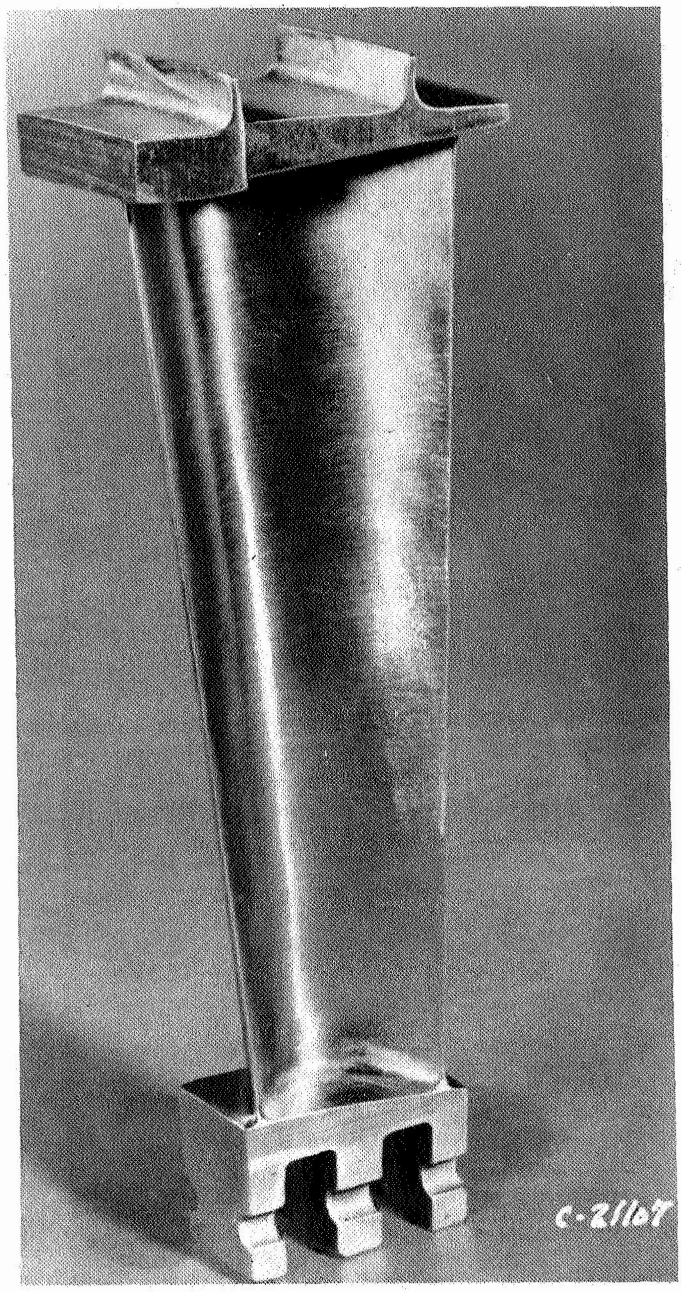

Figure 15. Stage Three Rotor.

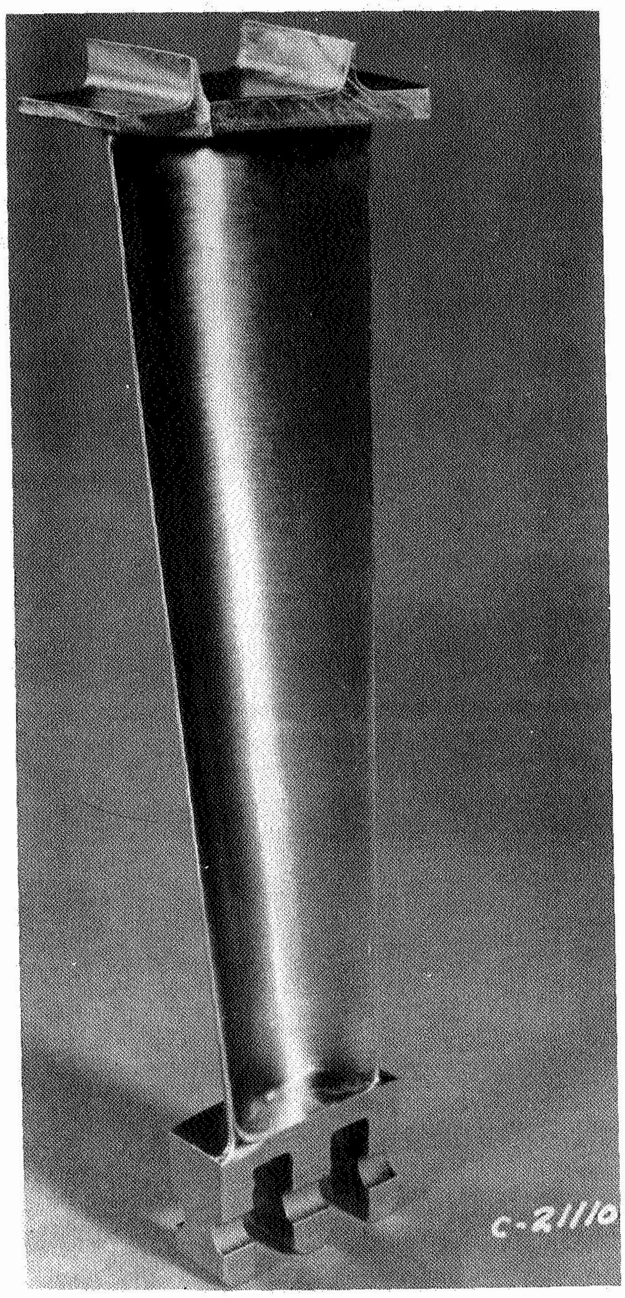

Figure 16. Stage Four Rotor.

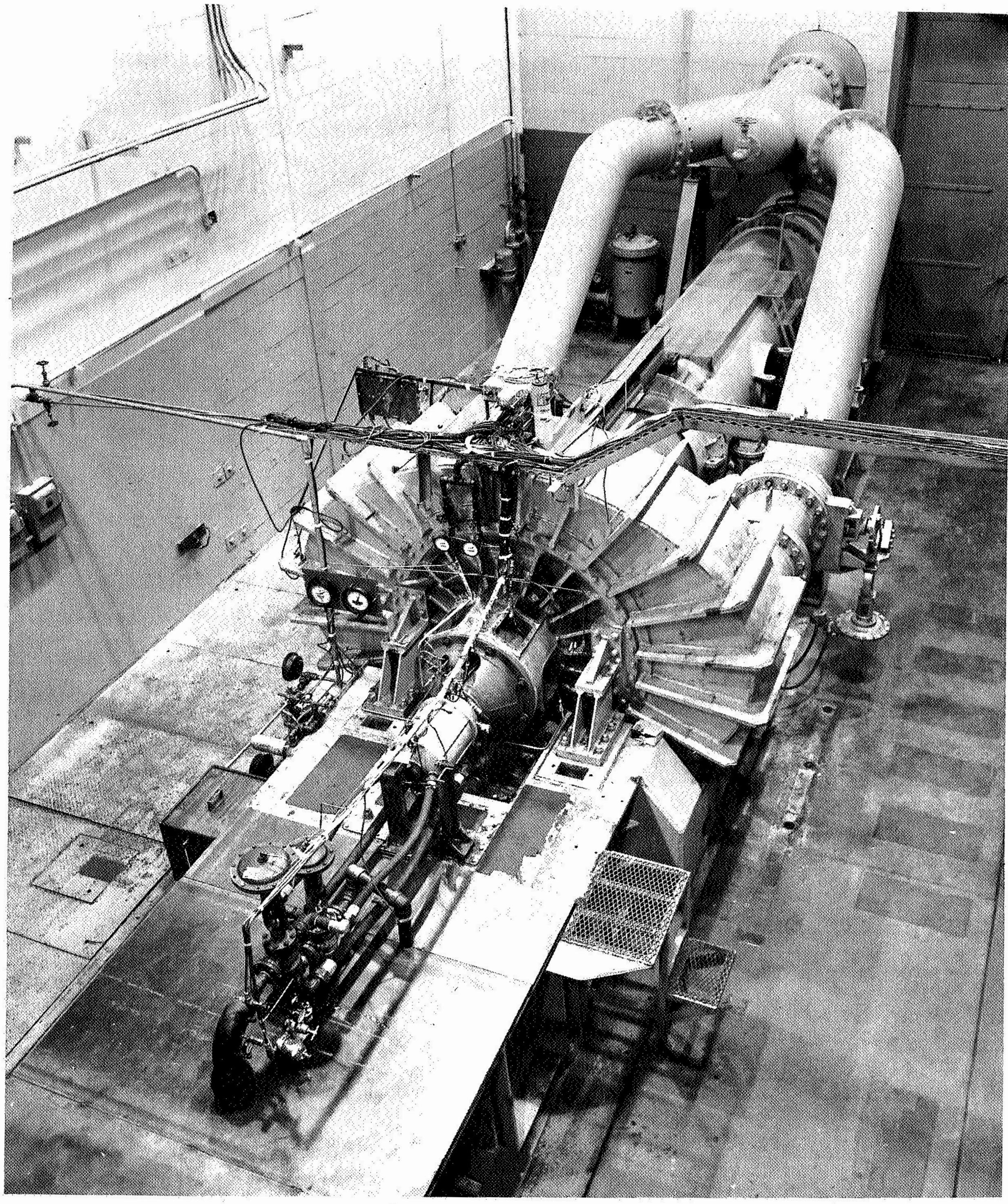

Figure 17. Typical General Electric, Evendale, Air Turbine Test Facility Configuration.

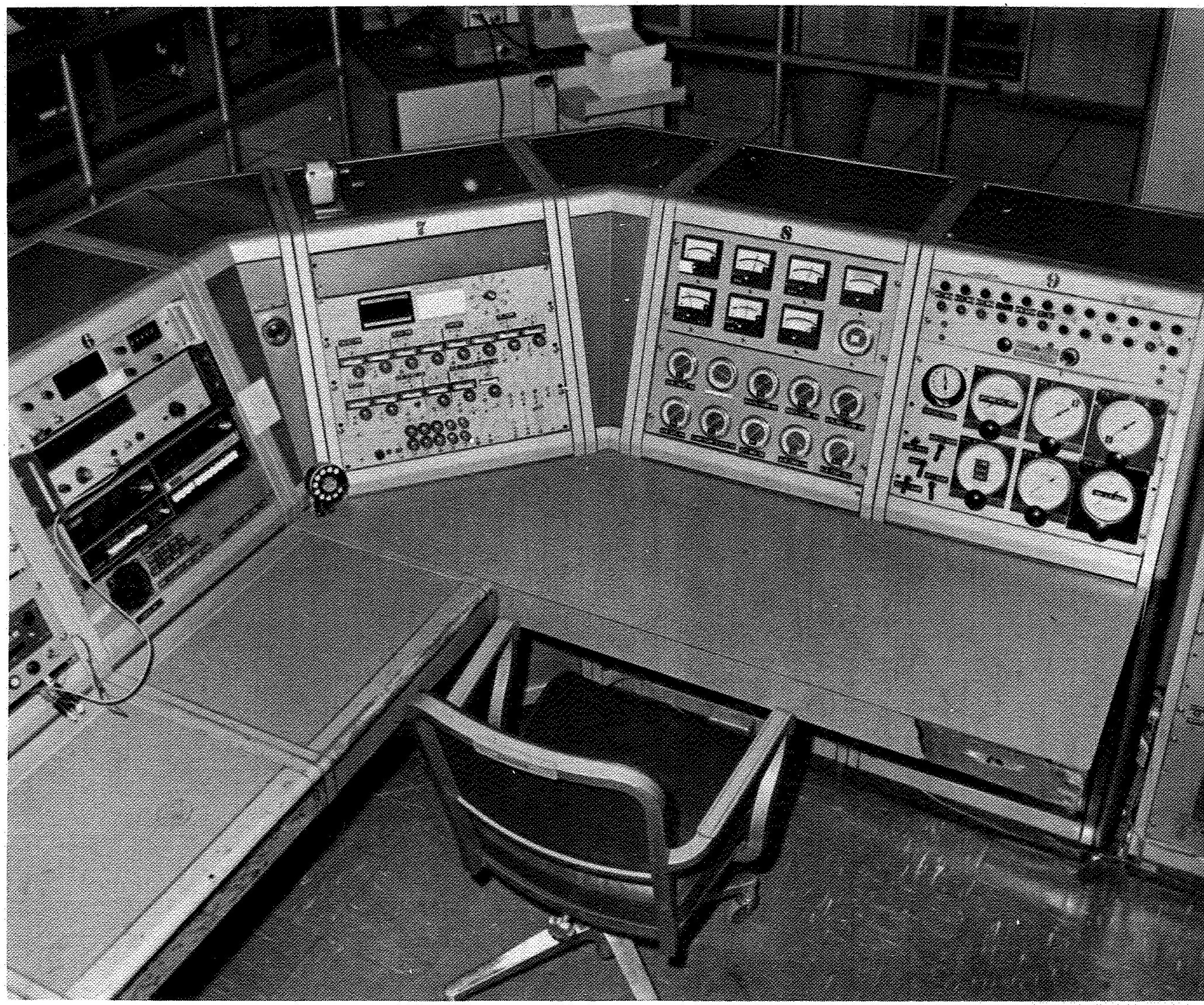

Figure 18. Turbine Facility Control Console.

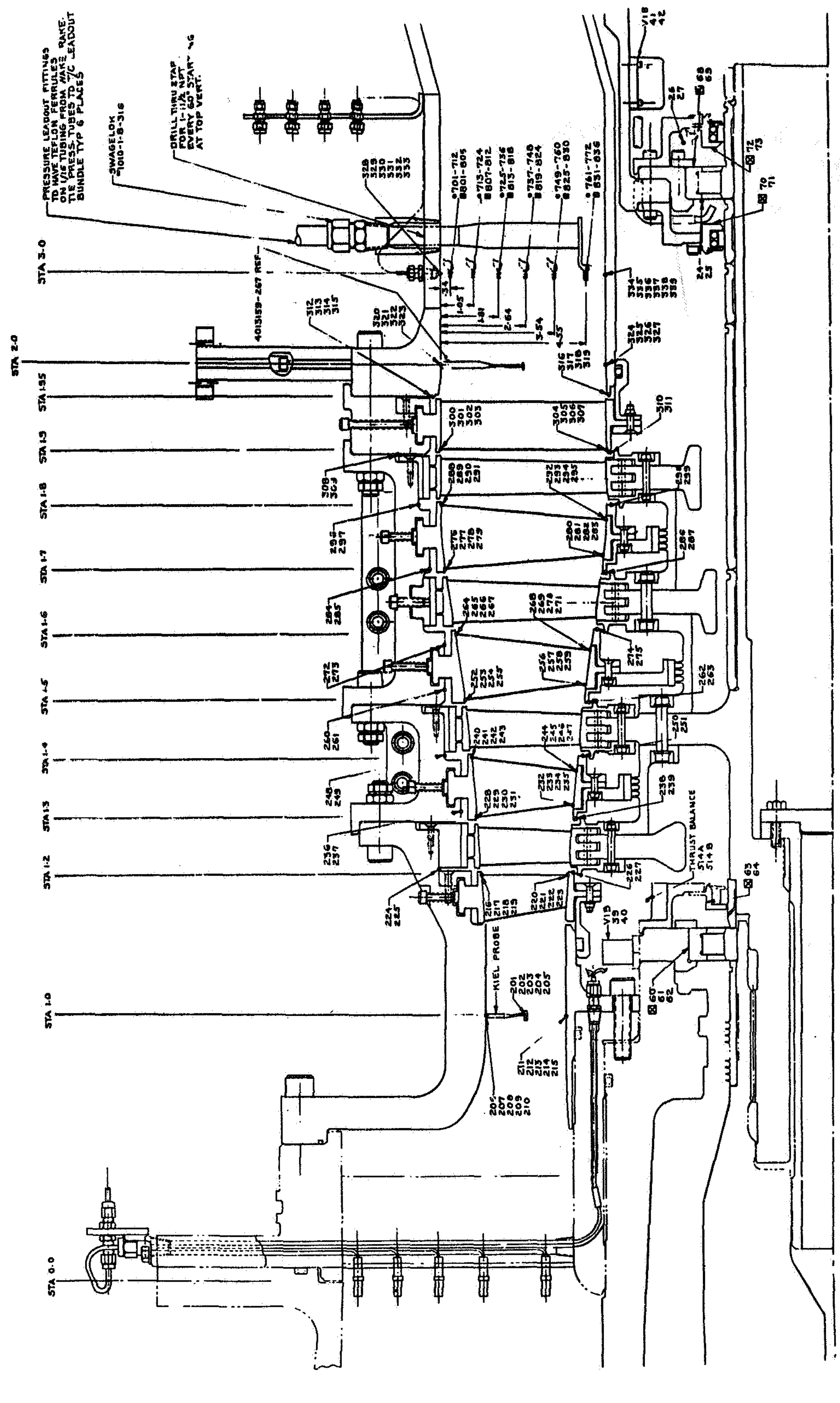

Figure 19. Air Turbine Test Instrumentation.

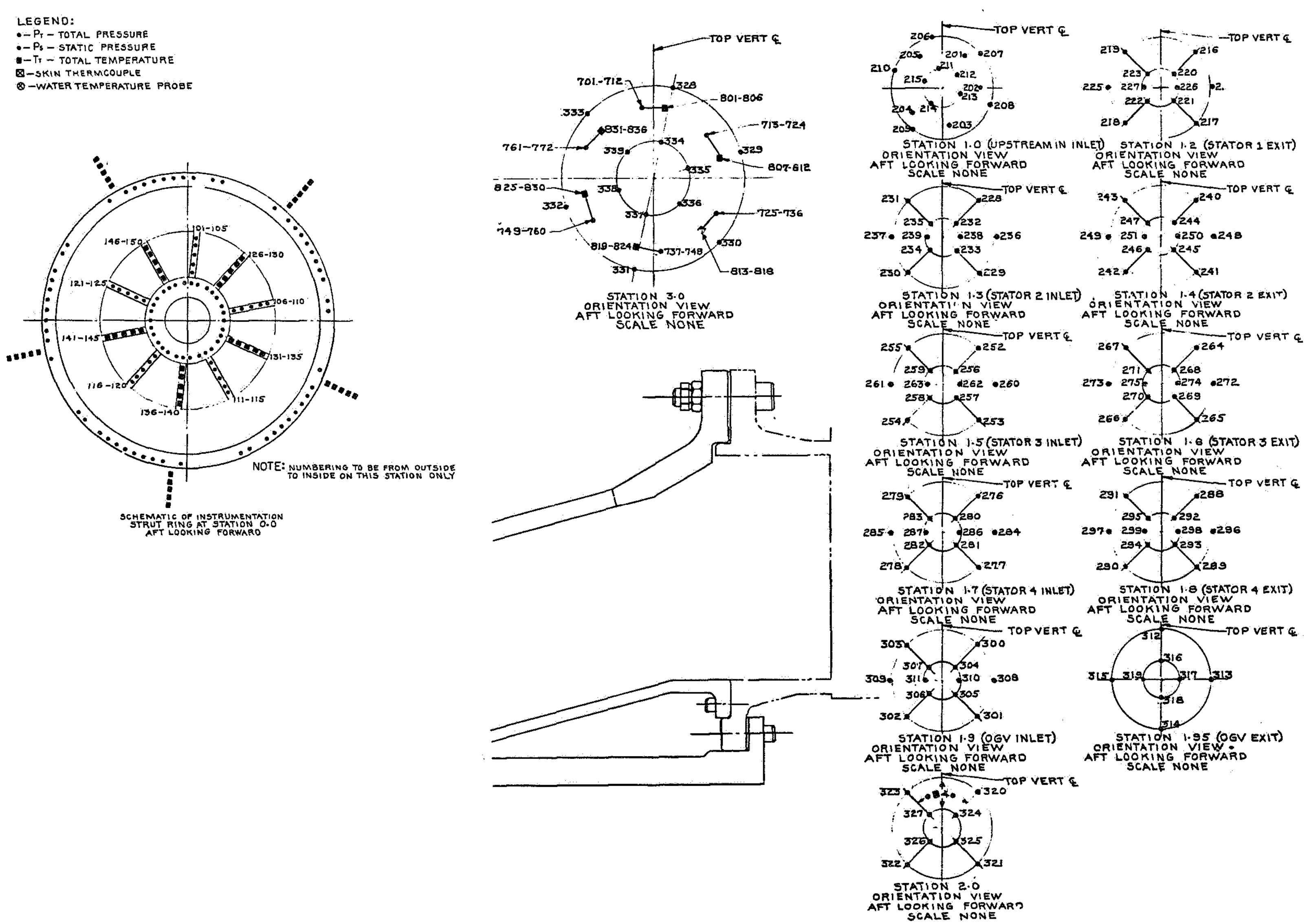

Figure 19. Air Turbine Test Instrumentation (Concluded).

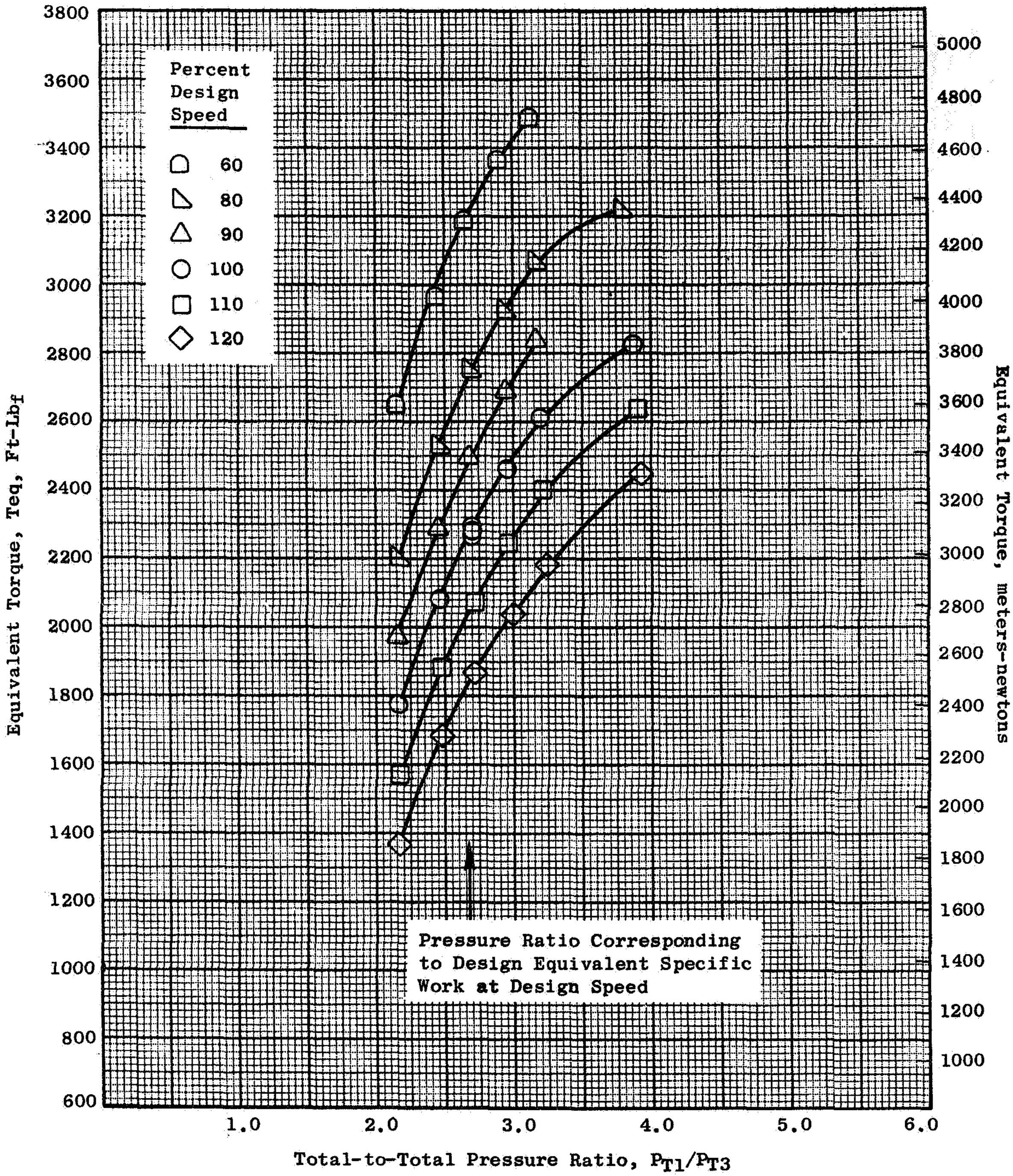

Figure 20. Equivalent Torque Vs. Total-to-Total Pressure Ratio.

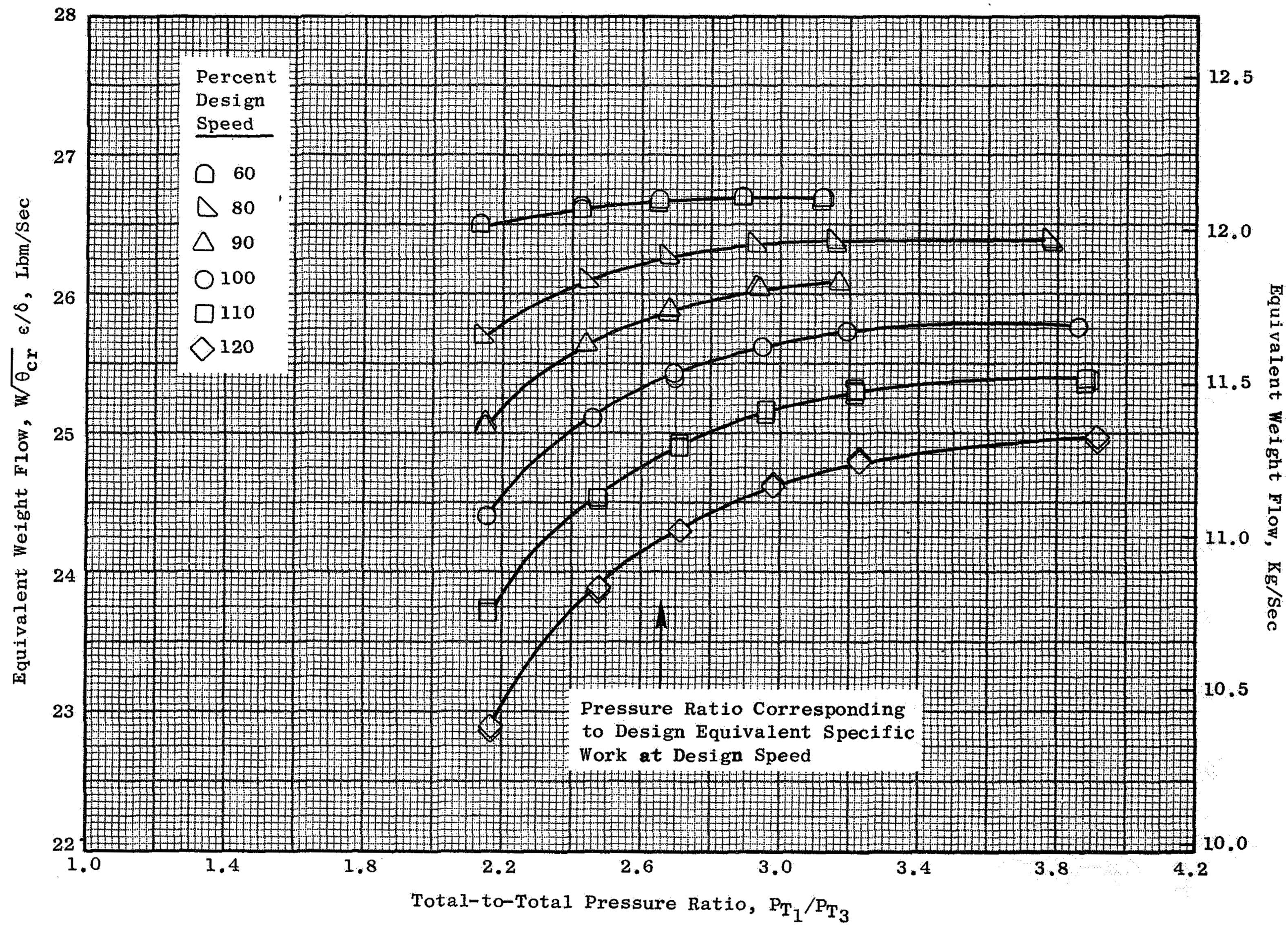

Figure 21. Equivalent Weight Flow Vs. Total-to-Total Pressure Ratio.

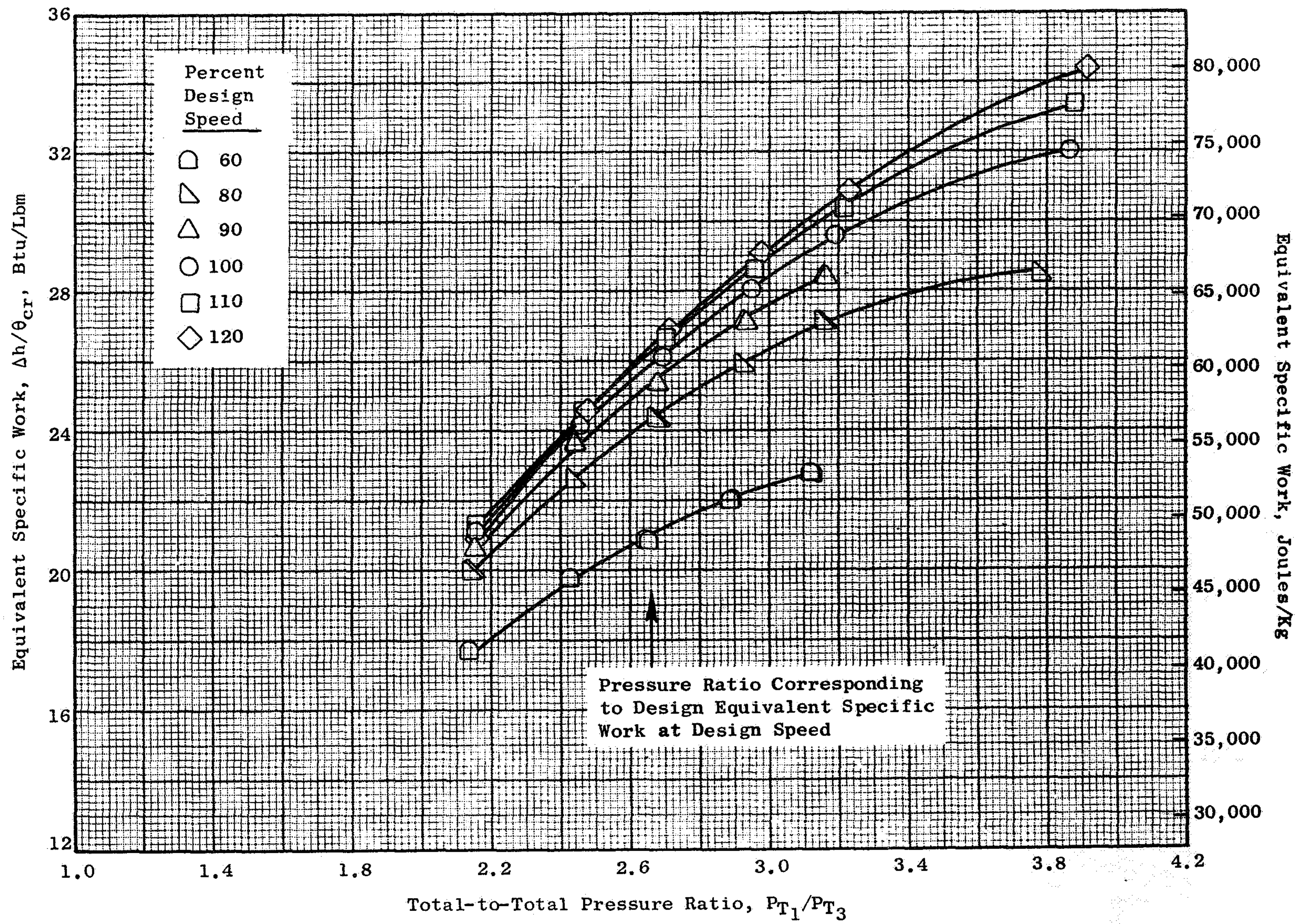

Figure 22. Equivalent Specific Work Vs. Total-to-Total Pressure Ratio.

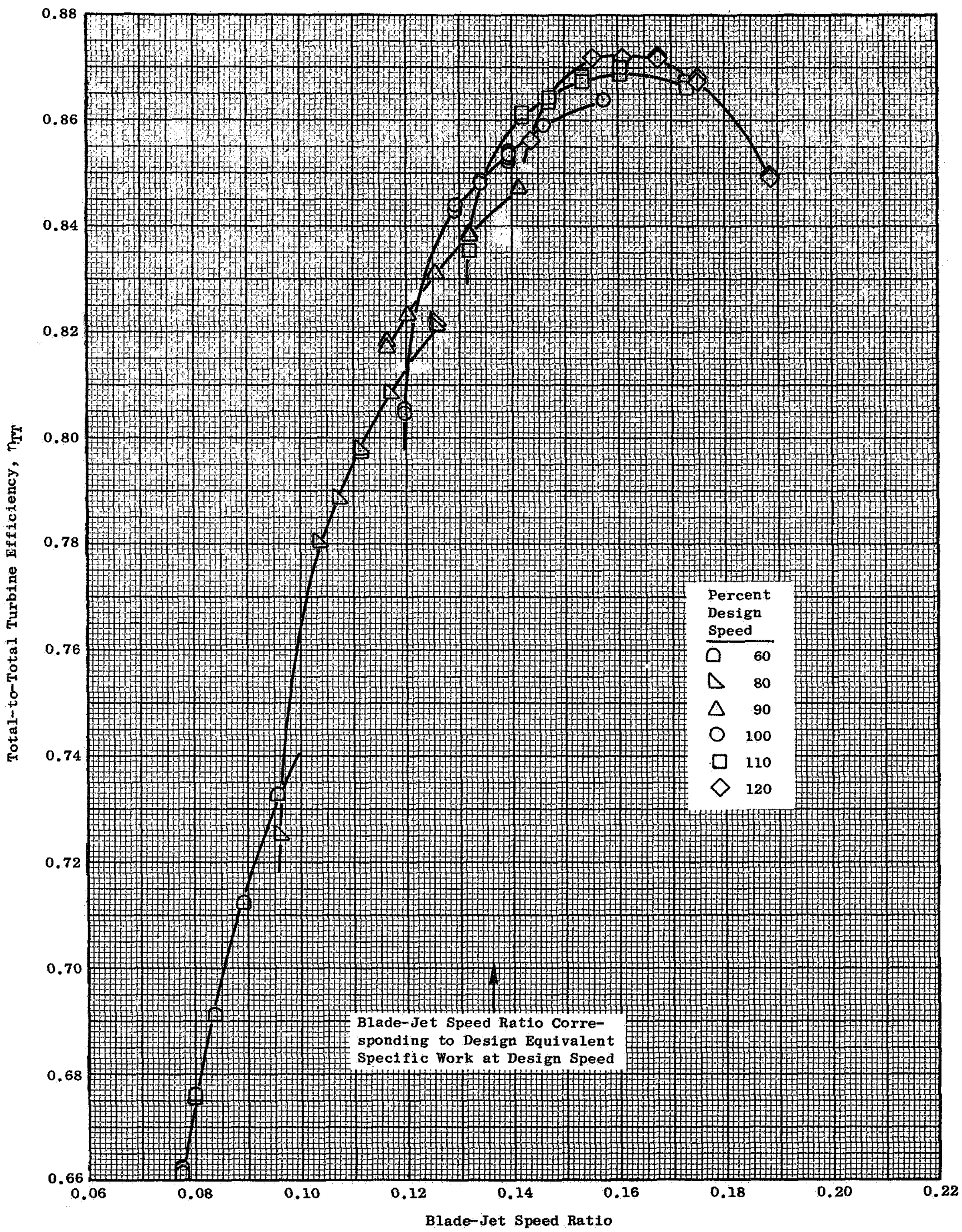

Figure 23. Total-to-Total Efficiency Vs. Blade - Jet Speed Ratio.

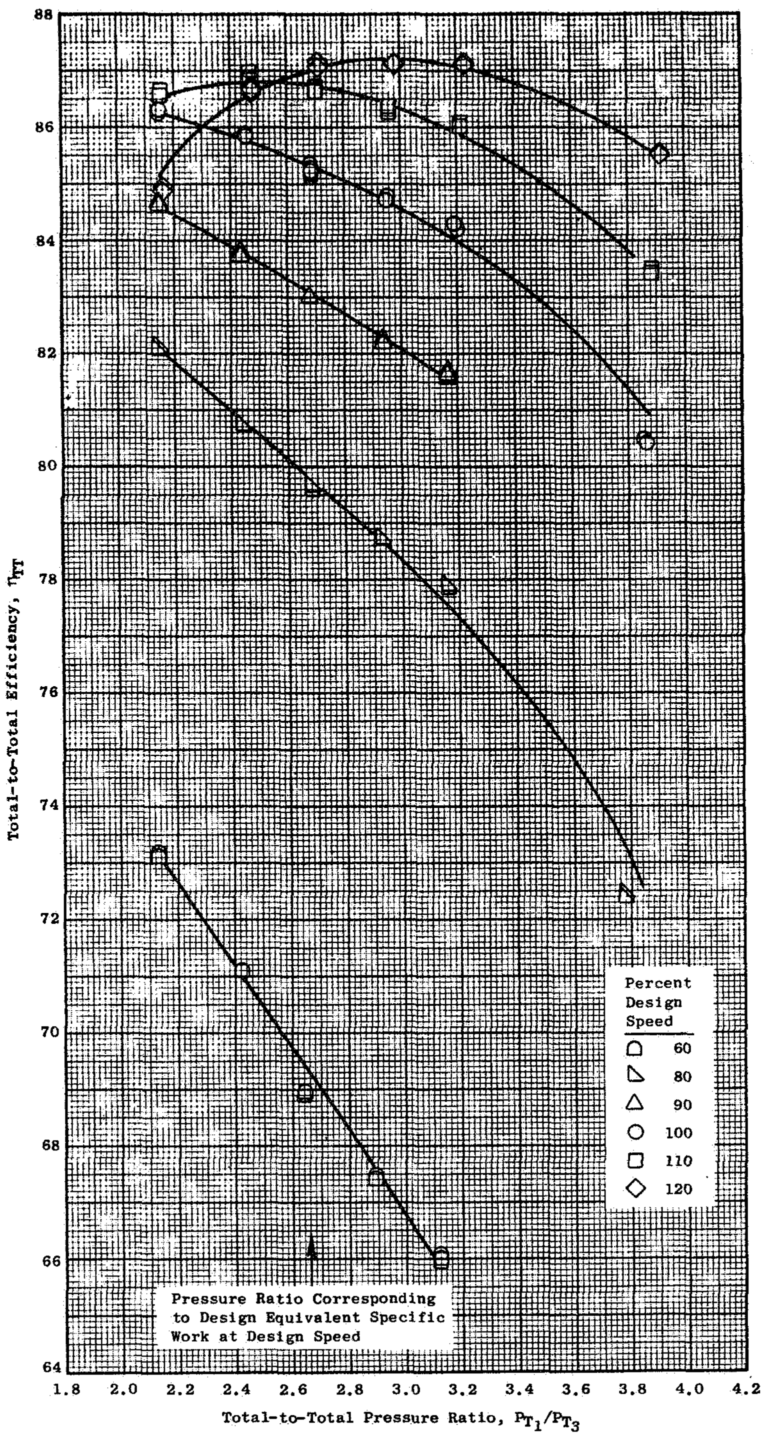

Figure 24. Total-to-Total Efficiency Vs. Total-to-Total Pressure Ratio.

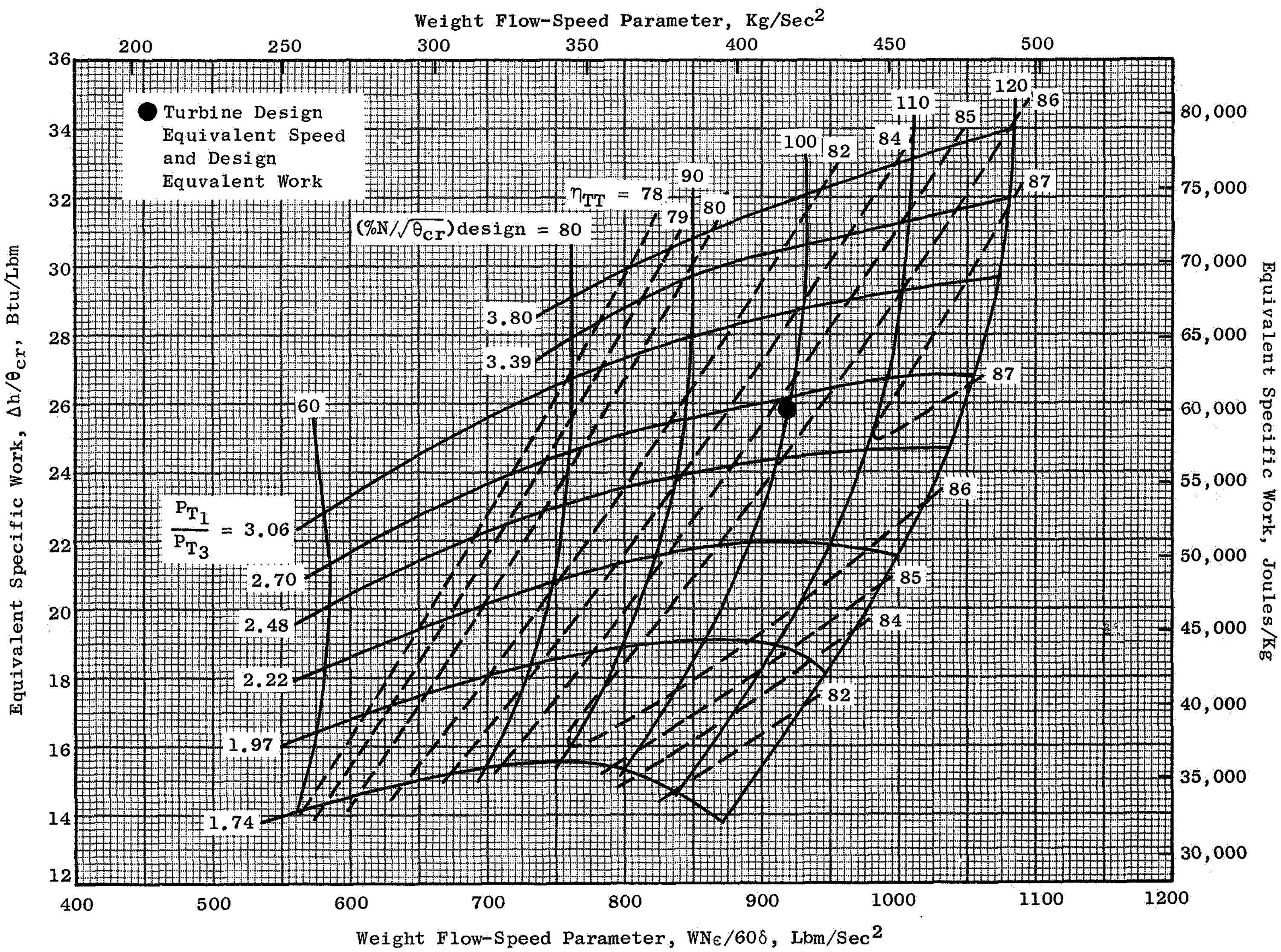

Figure 25. Equivalent Specific Work Vs. Weight Flow-Speed Parameter.

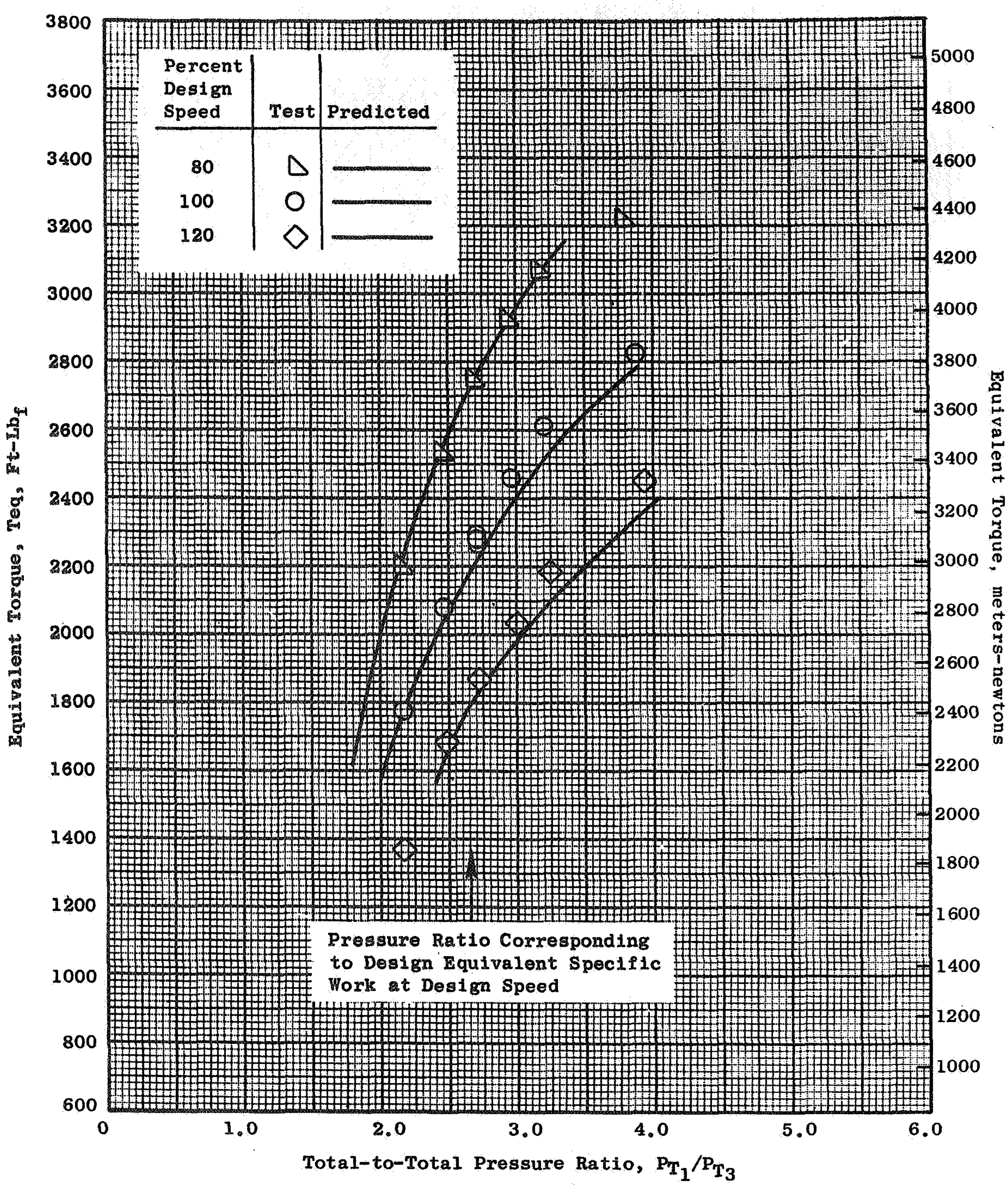

Figure 26. Predicted and Actual Equivalent Torque Vs. Total-to-Total Pressure Ratio.

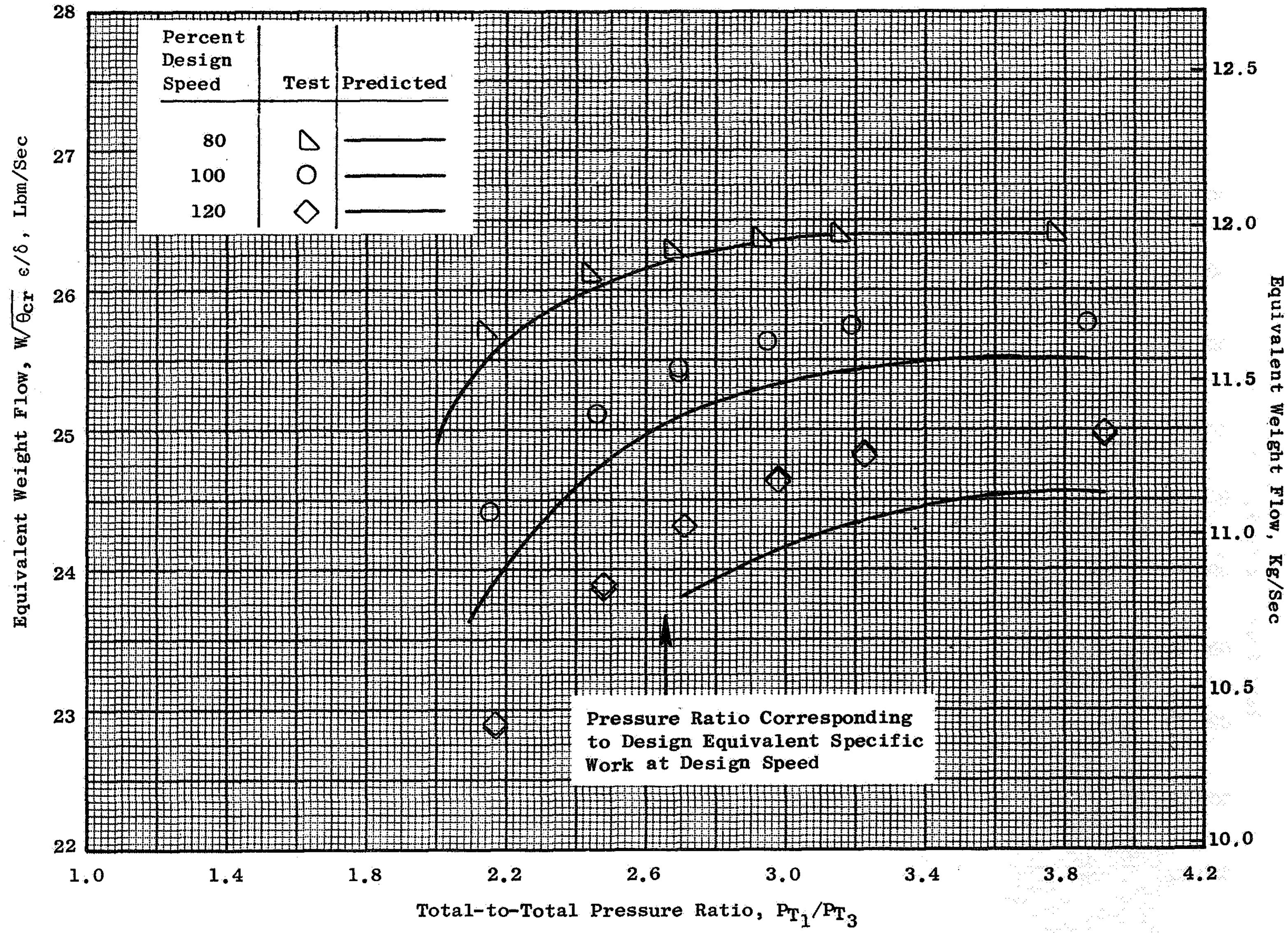

Figure 27. Predicted and Actual Equivalent Weight Flow Vs. Total-to-Total Pressure Ratio.

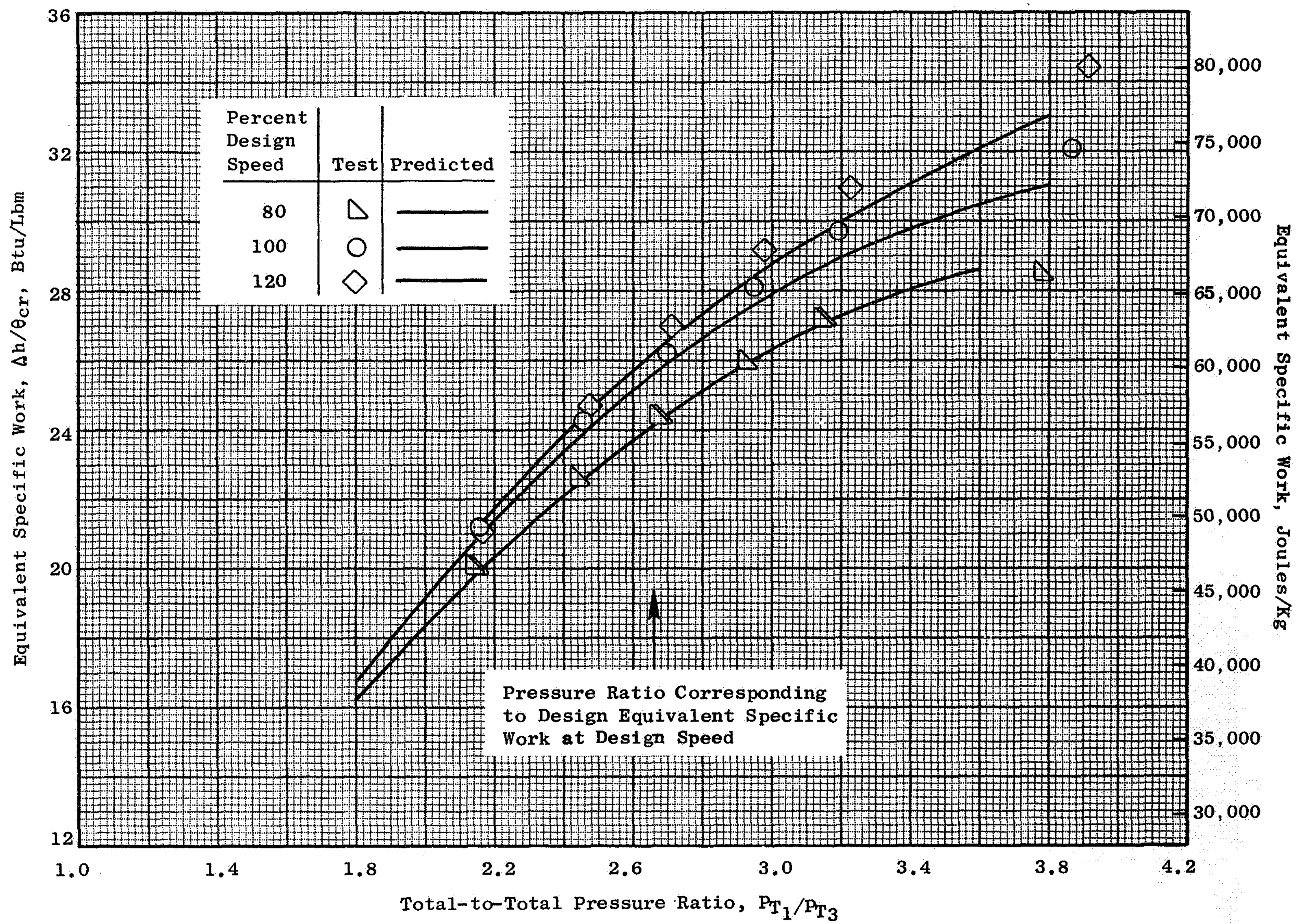

Figure 28. Predicted and Actual Equivalent Specific Work Vs. Total-to-Total Pressure Ratio.

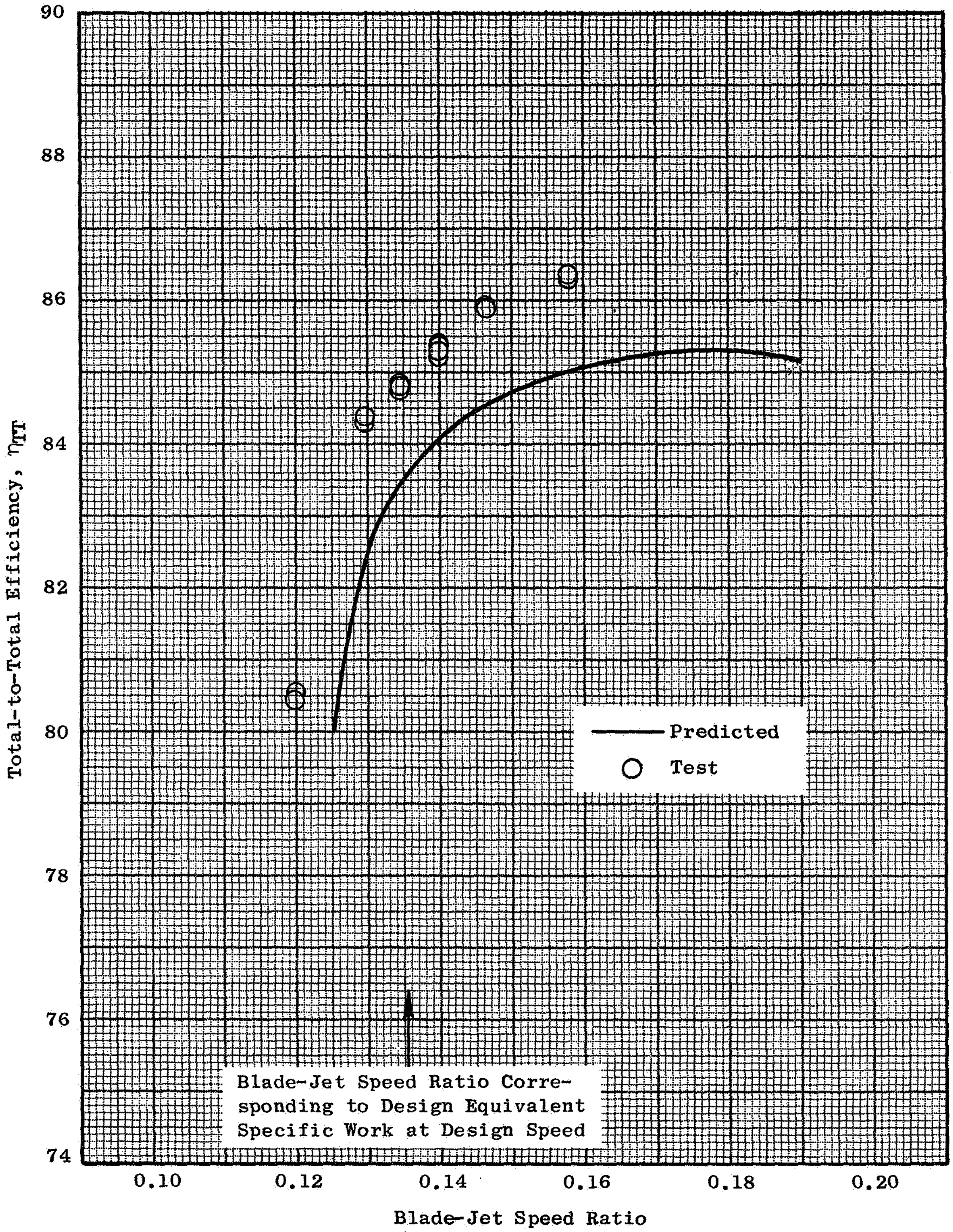

Figure 29. Predicted and Actual Total-to-Total Efficiency Vs. Blade - Jet Speed Ratio, at Design Speed.

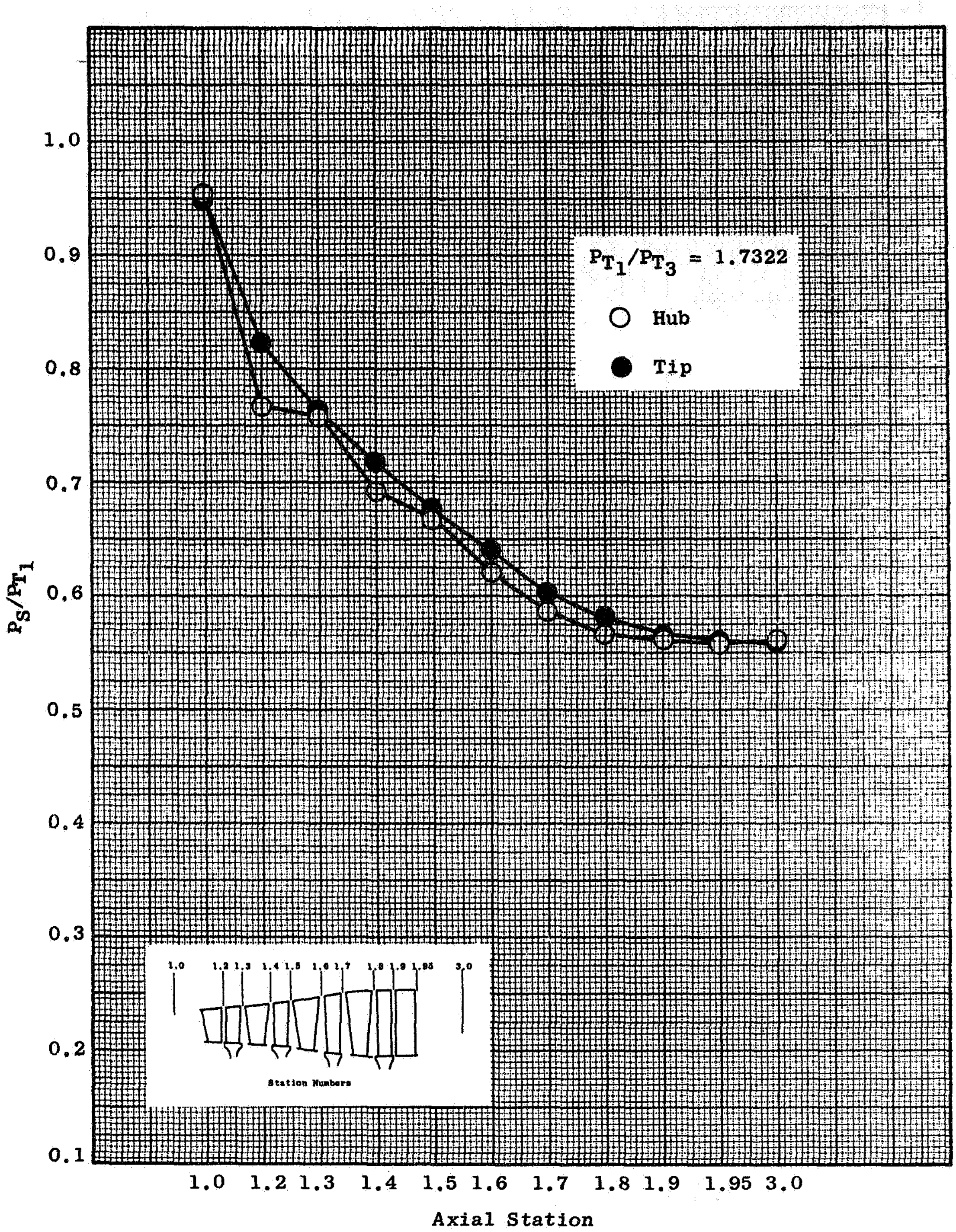

Figure 30. Normalized Static Pressure Vs. Axial Station, at Design Speed.

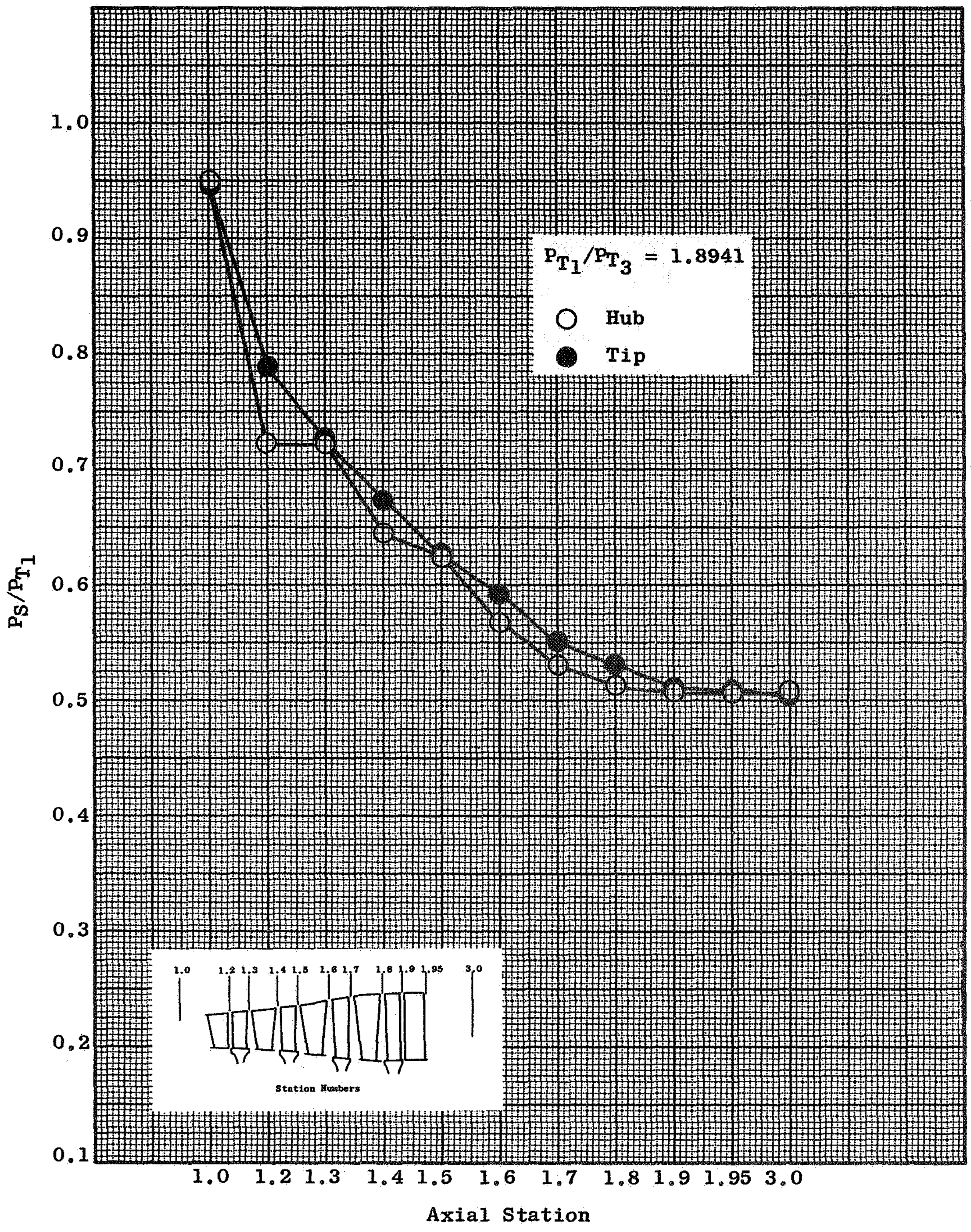

Figure 30. Normalized Static Pressure Vs. Axial Station, at Design Speed (Continued).

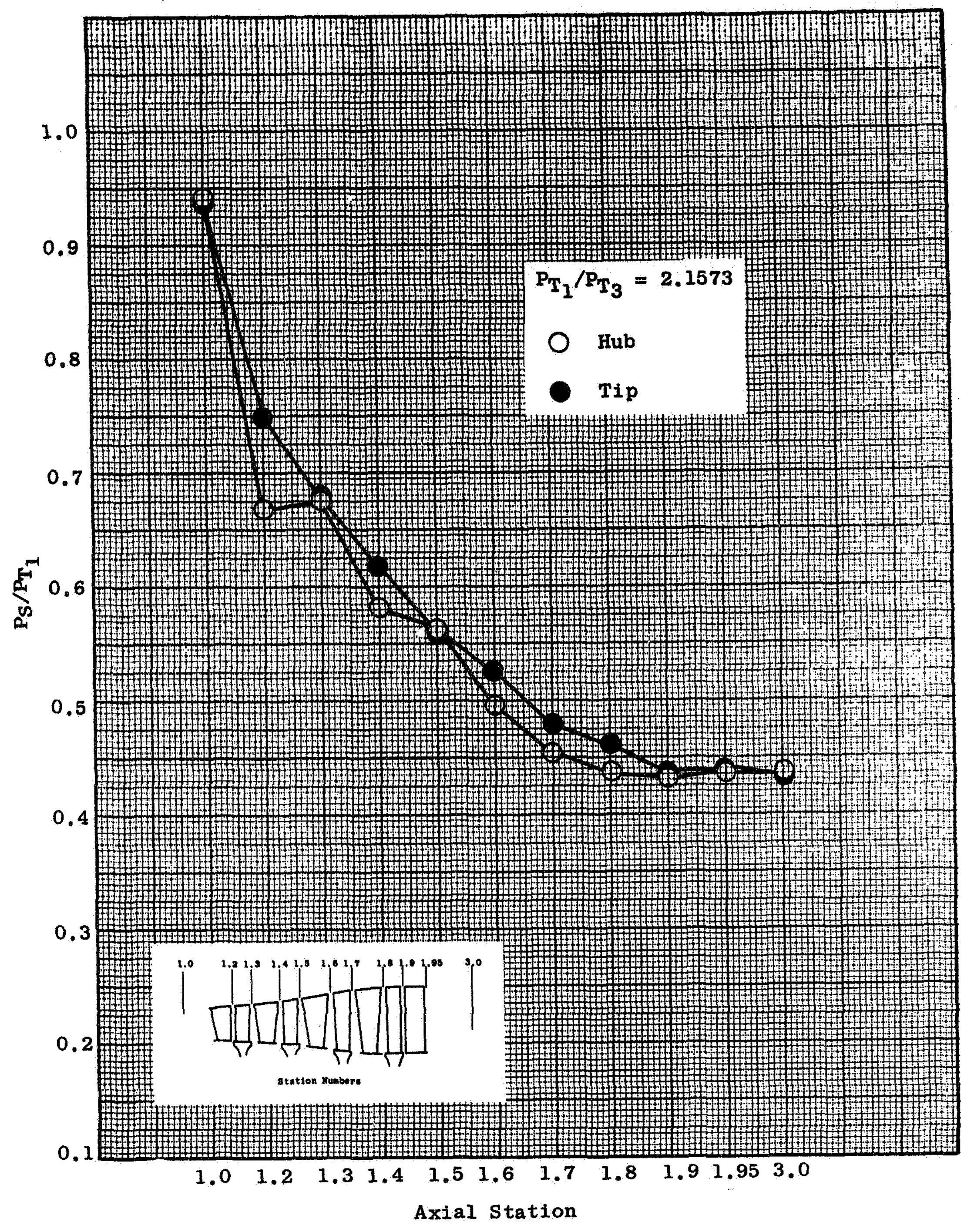

Figure 30. Normalized Static Pressure Vs. Axial Station, at Design Speed (Continued).

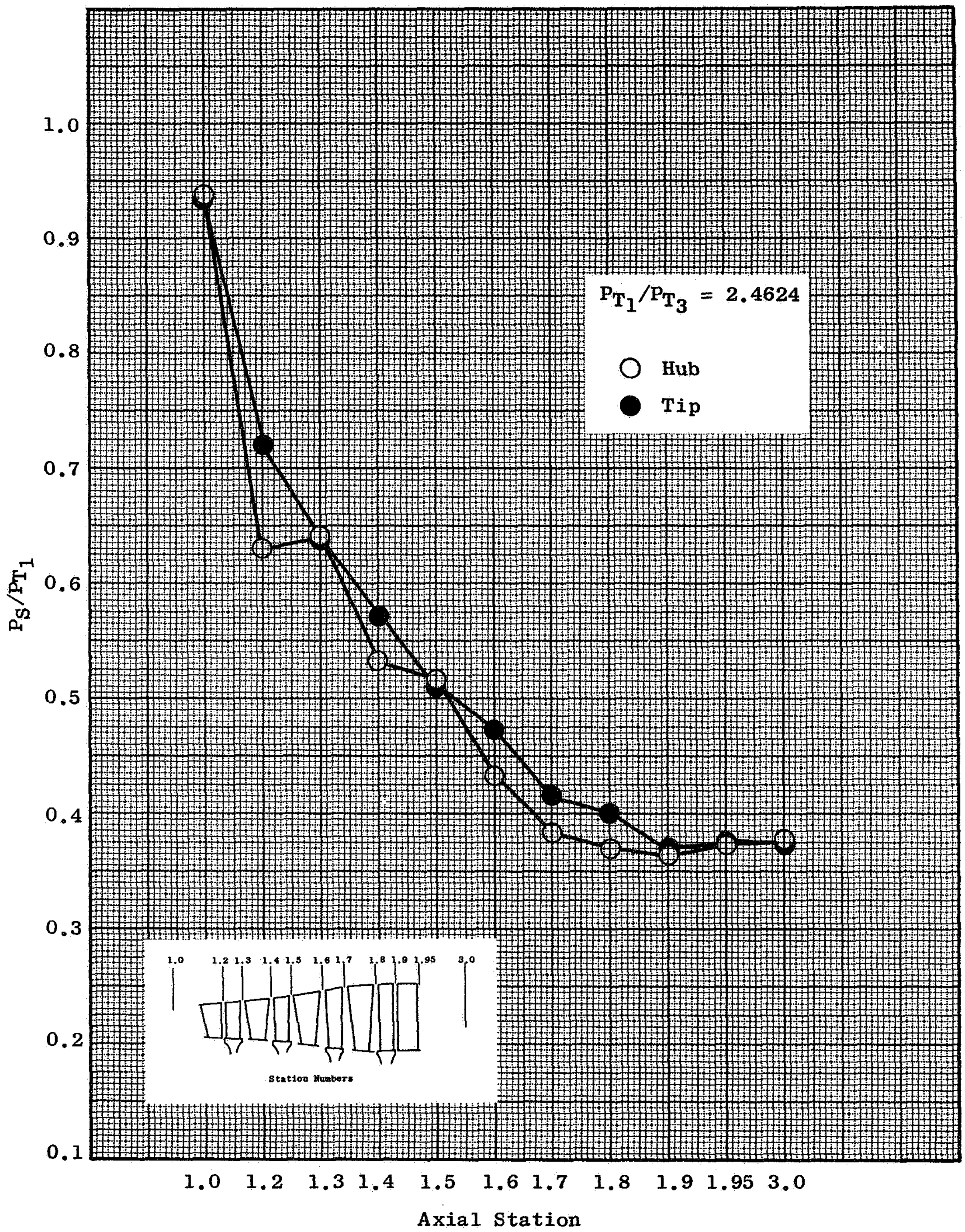

Figure 30. Normalized Static Pressure Vs. Axial Station, at Design Speed (Continued).

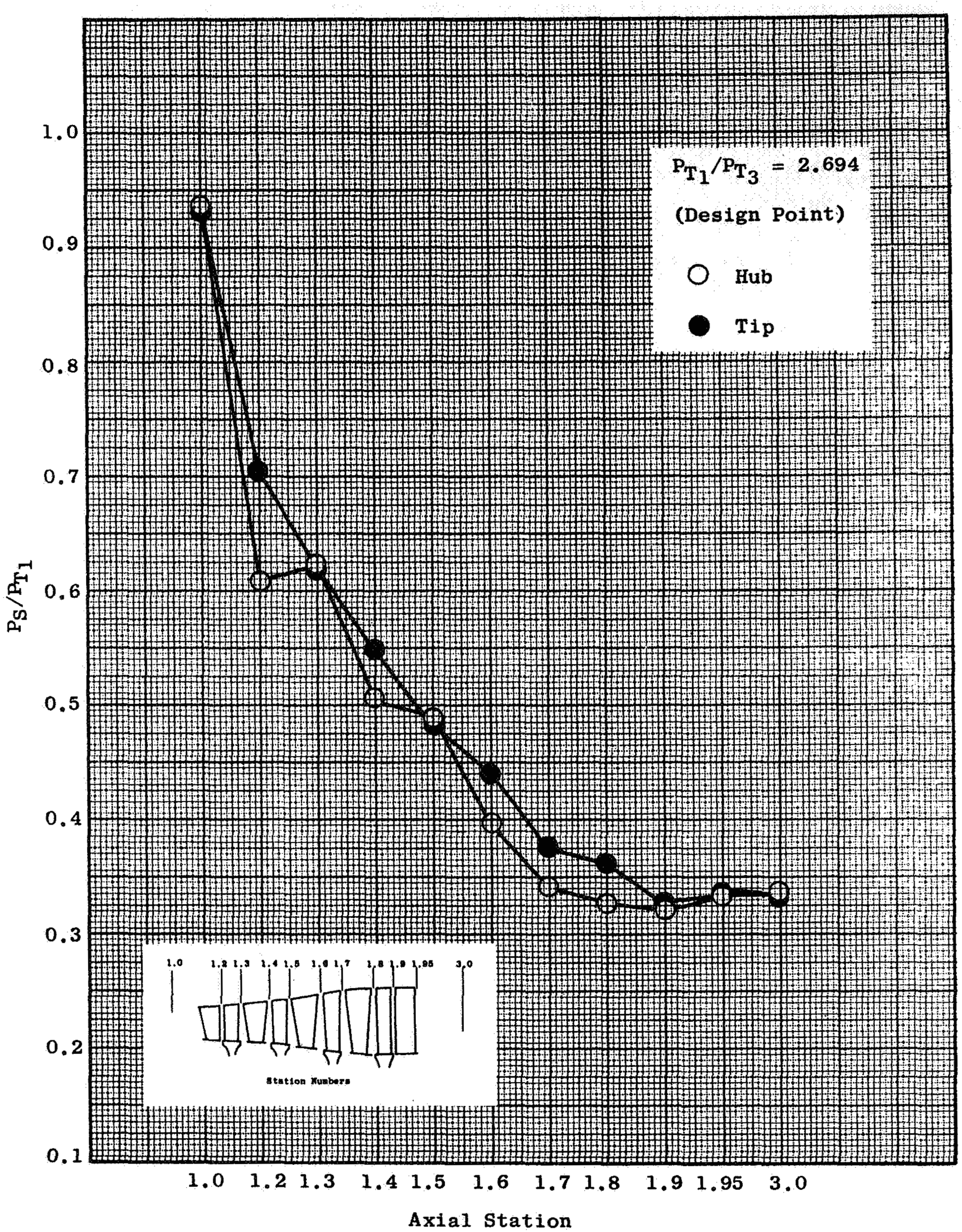

Figure 30. Normalized Static Pressure Vs. Axial Station, at Design Speed (Continued).

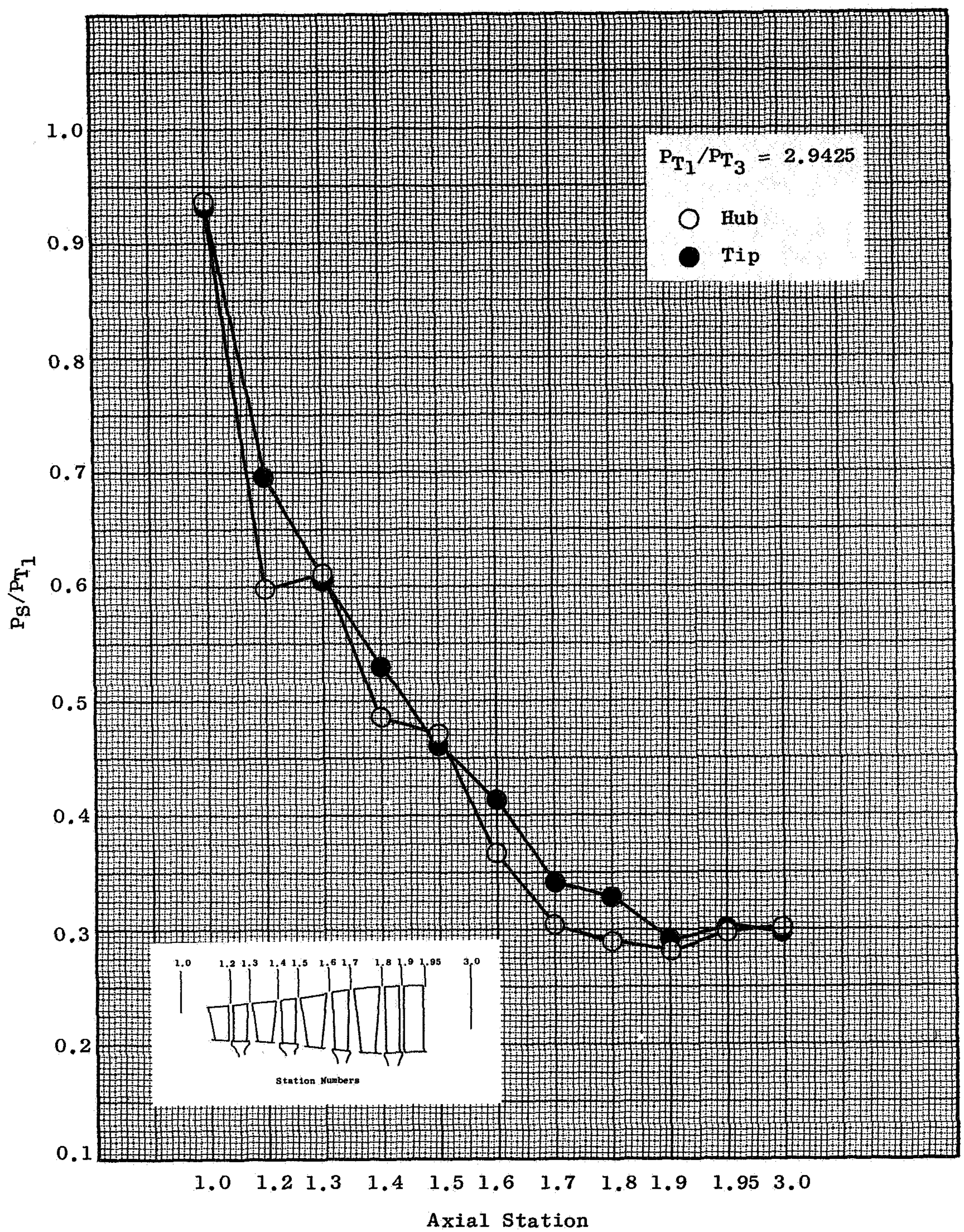

Figure 30. Normalized Static Pressure Vs. Axial Station, at Design Speed (Continued).

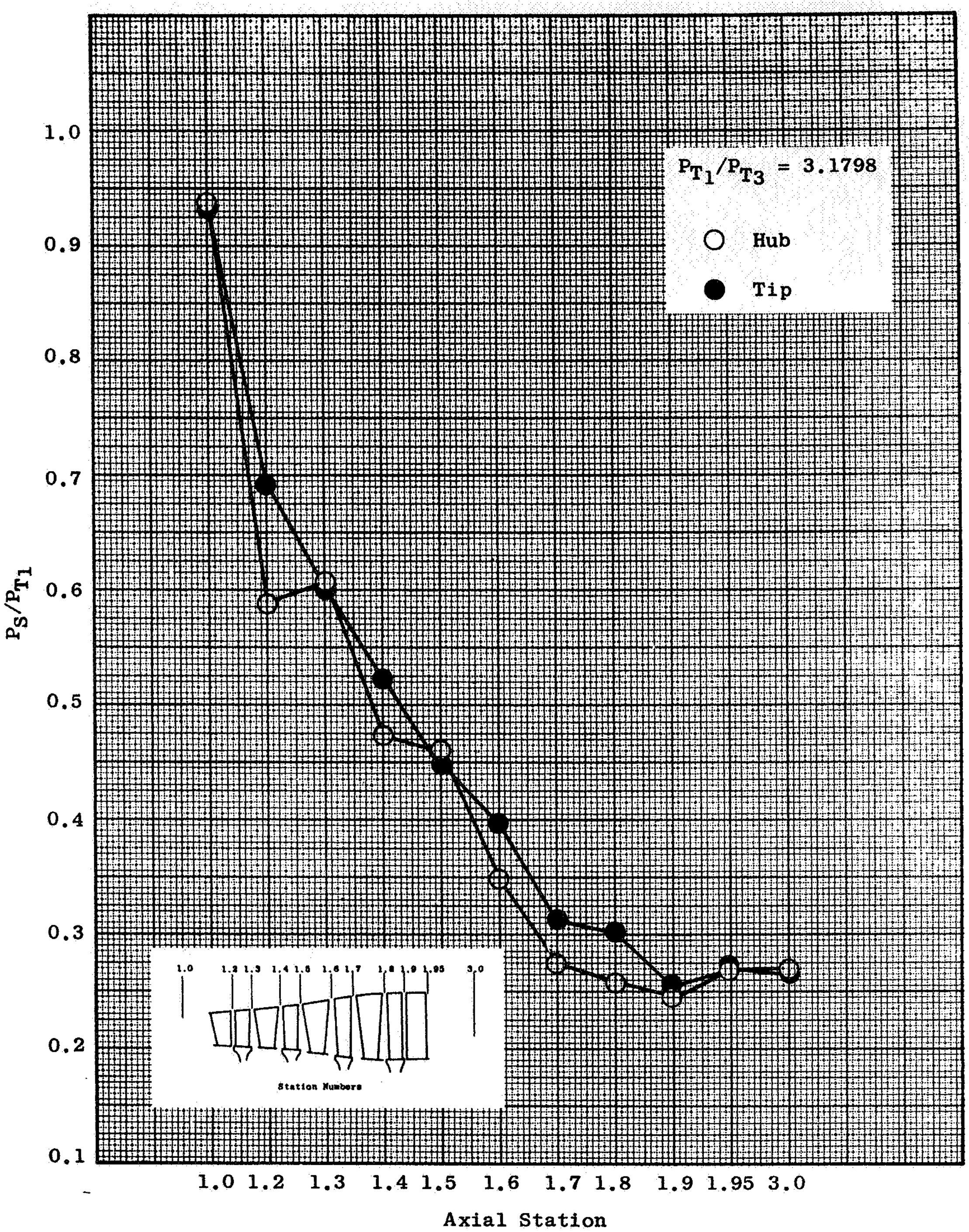

Figure 30. Normalized Static Pressure Vs. Axial Station, at Design Speed (Continued).

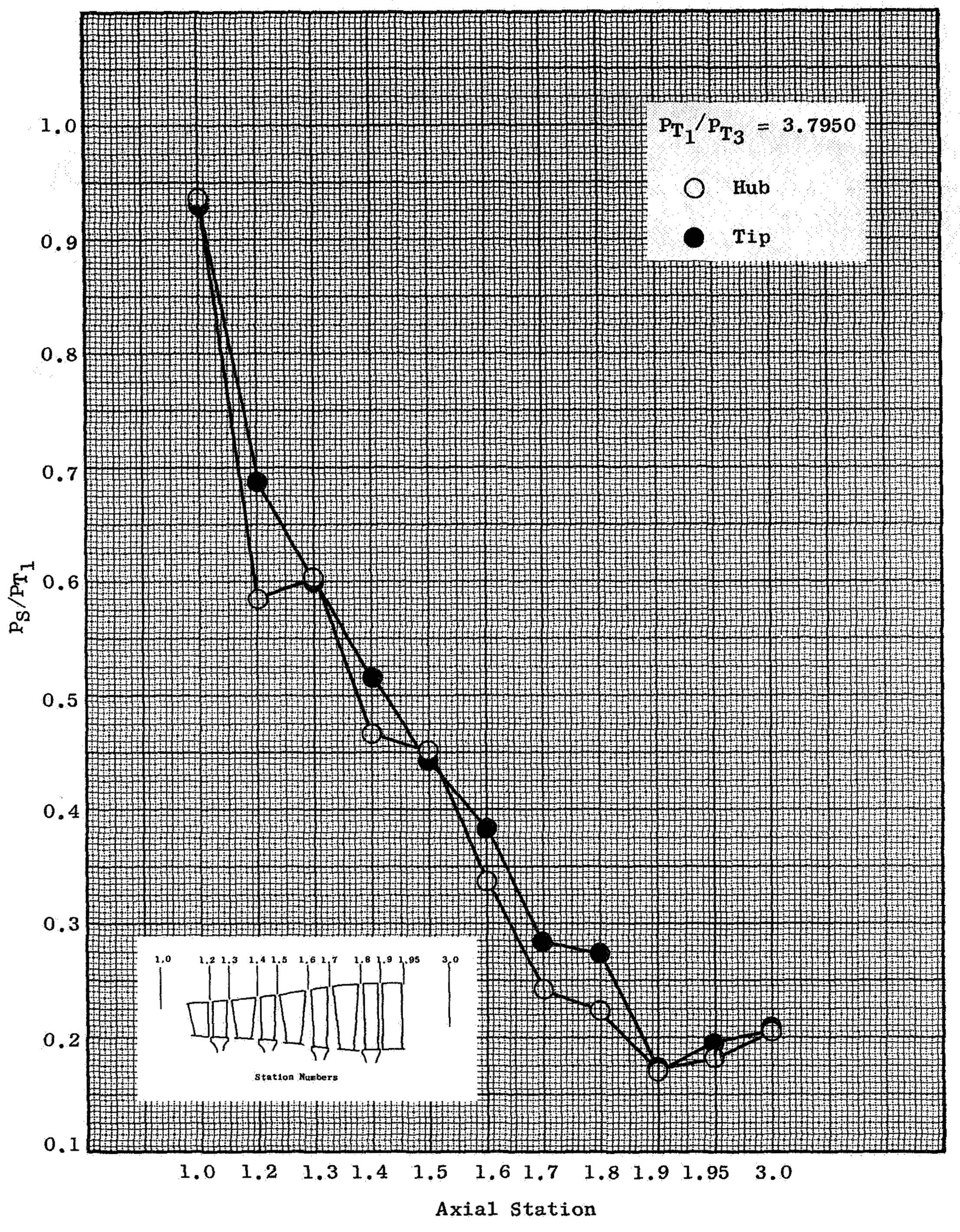

Figure 30. Normalized Static Pressure Vs. Axial Station, at Design Speed (Concluded).

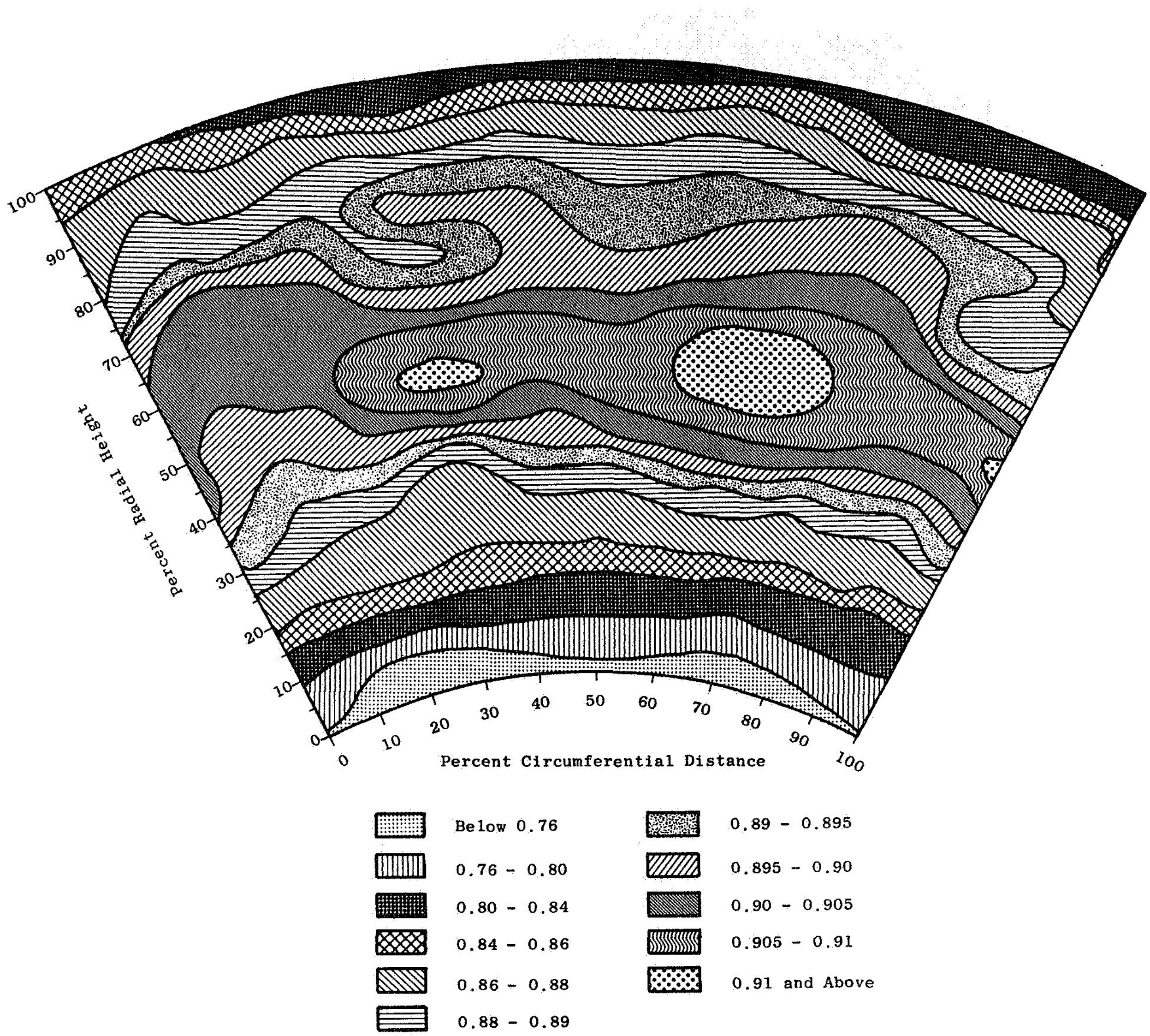

Figure 31. Turbine Efficiency Contour Plot, 4-1/2-Stage.

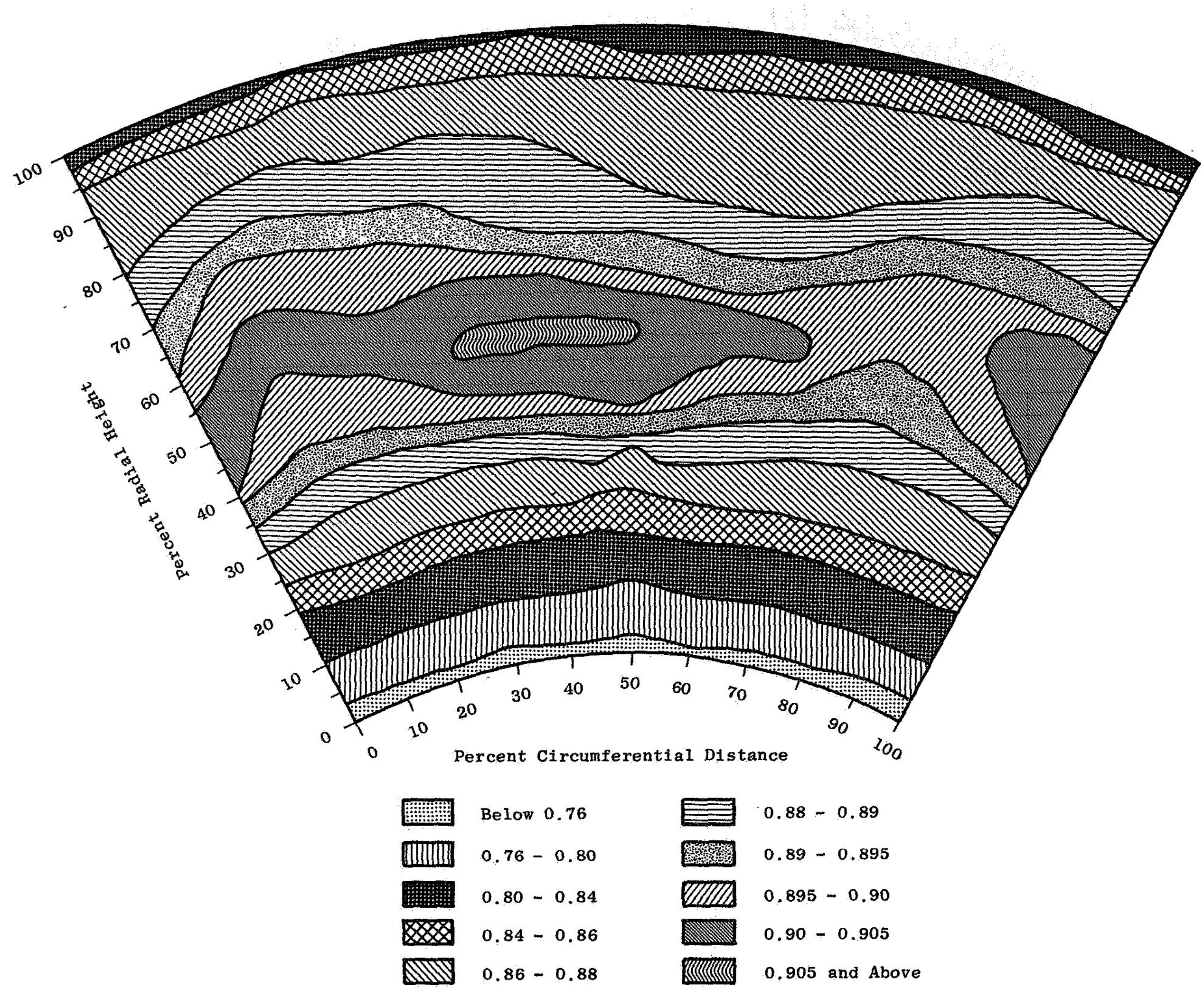

Figure 32. Turbine Efficiency Contour Plot, 4-Stage.

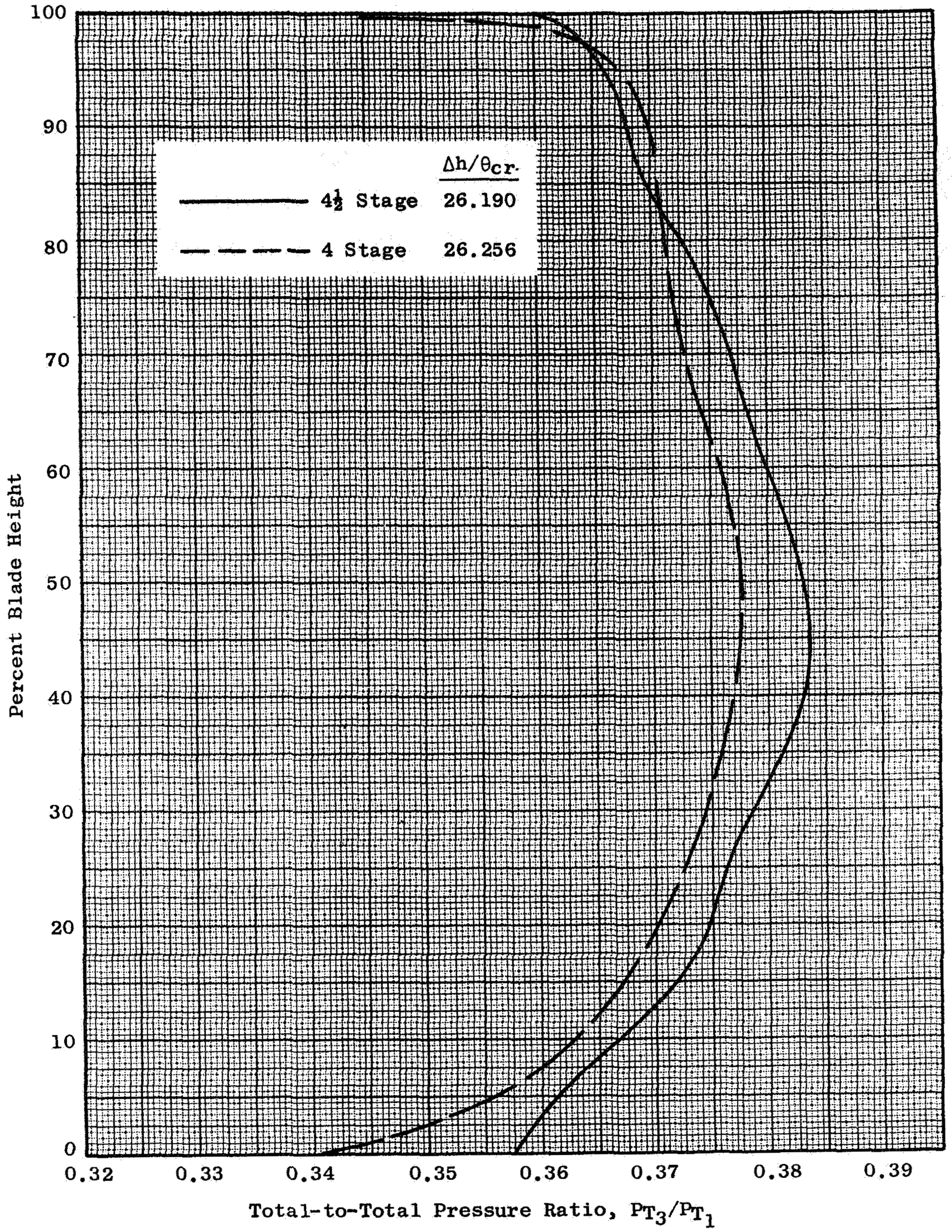

Figure 33. Normalized Exit Radial Total Pressure Profile.

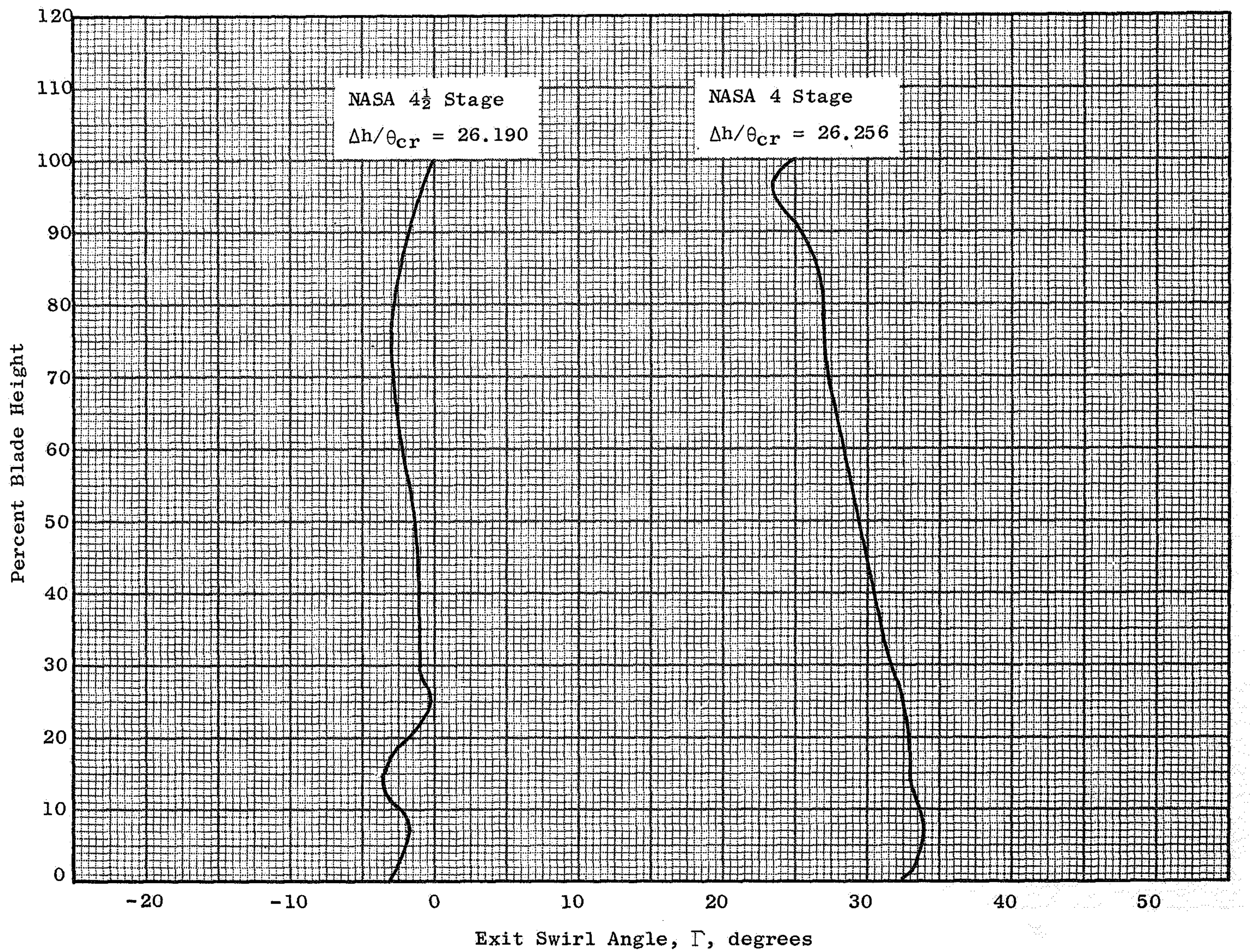

Figure 34. Radial Exit Swirl Profile.

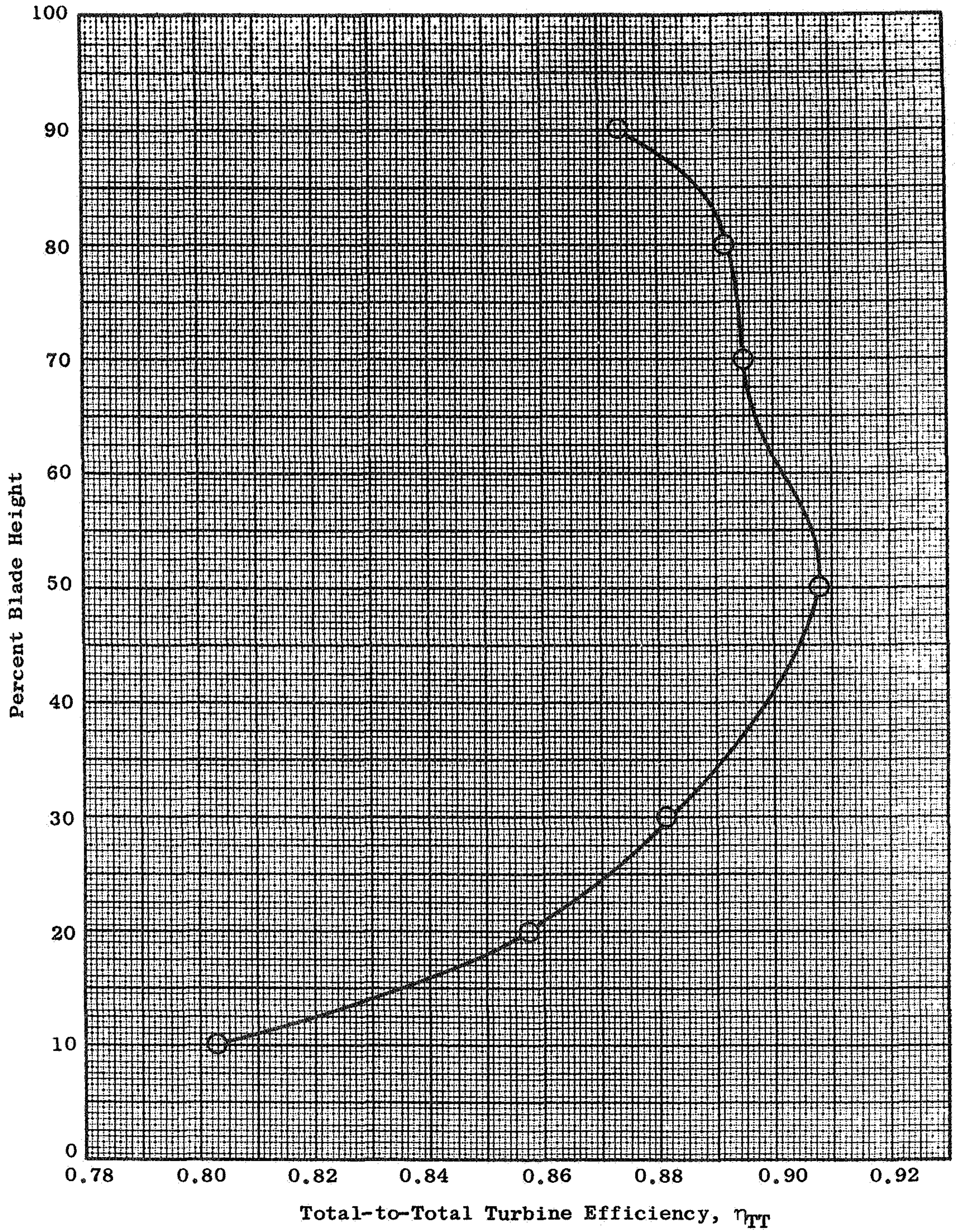

Figure 35. Radial Total-to-Total Efficiency Profile for 4-1/2-Stage Configuration.

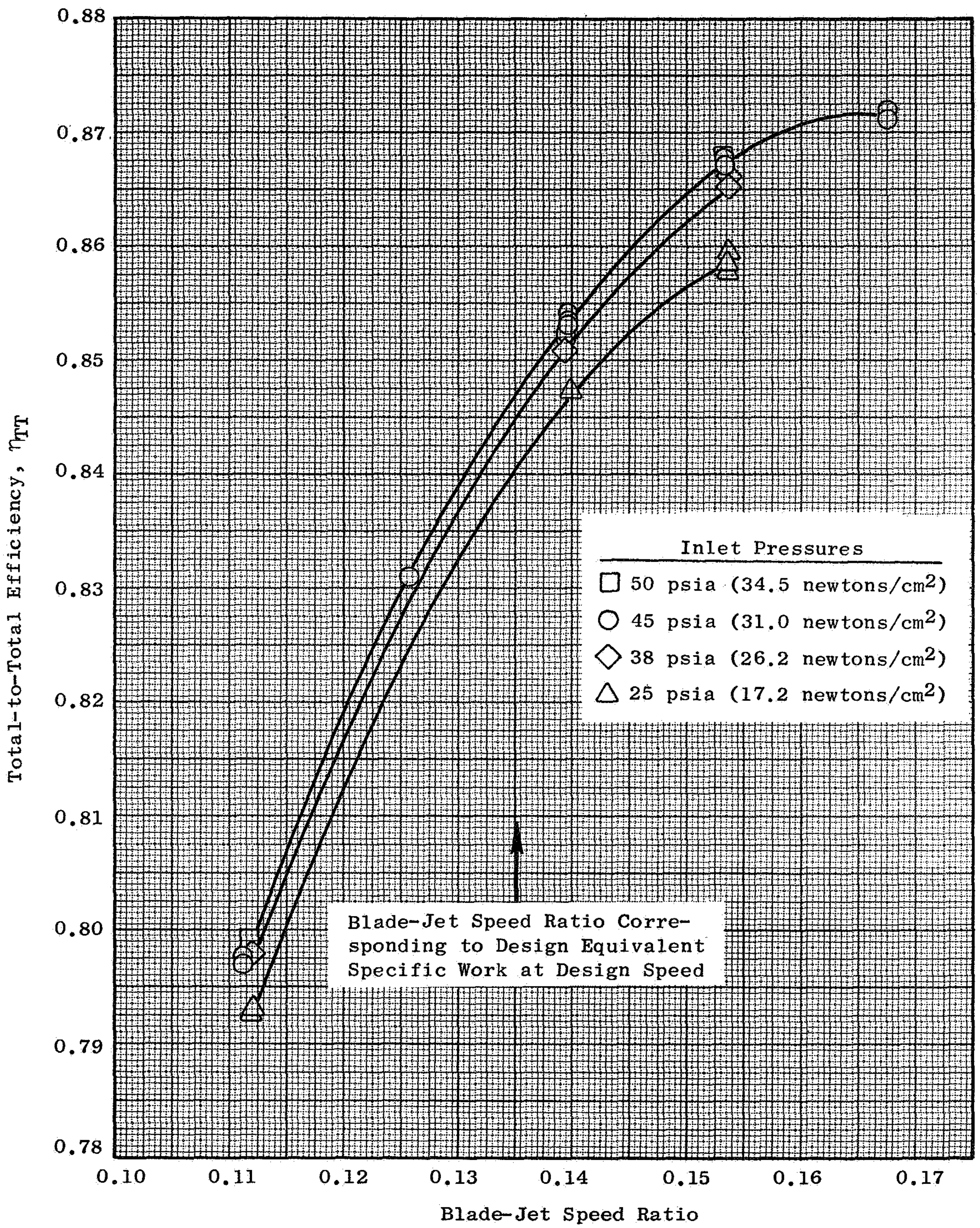

Figure 36. Total-to-Total Efficiency Vs. Blade - Jet Speed Ratio for Various Inlet Pressures.

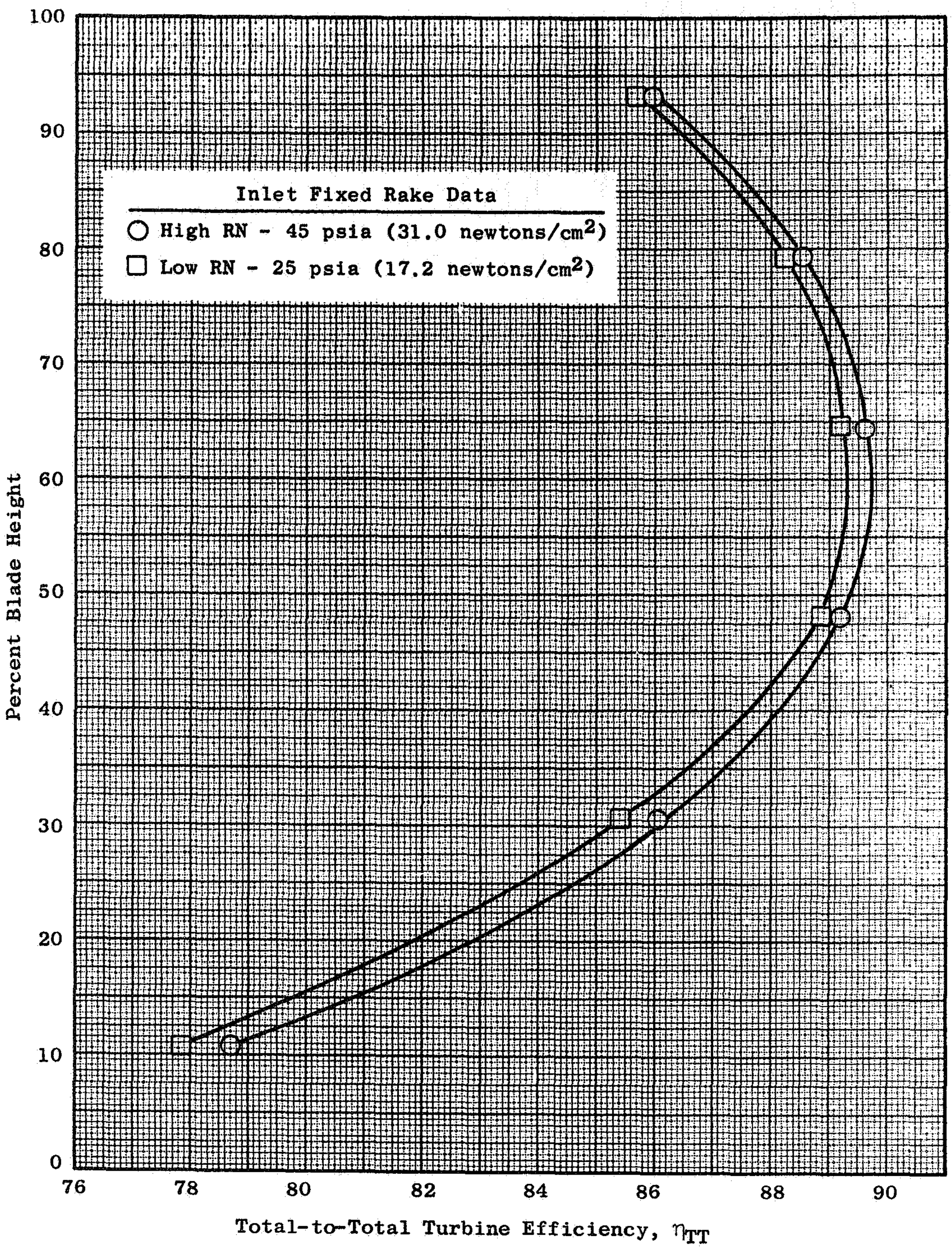

Figure 37. Radial Efficiency Profiles Based on Fixed Rake Data for High and Low Reynolds Numbers

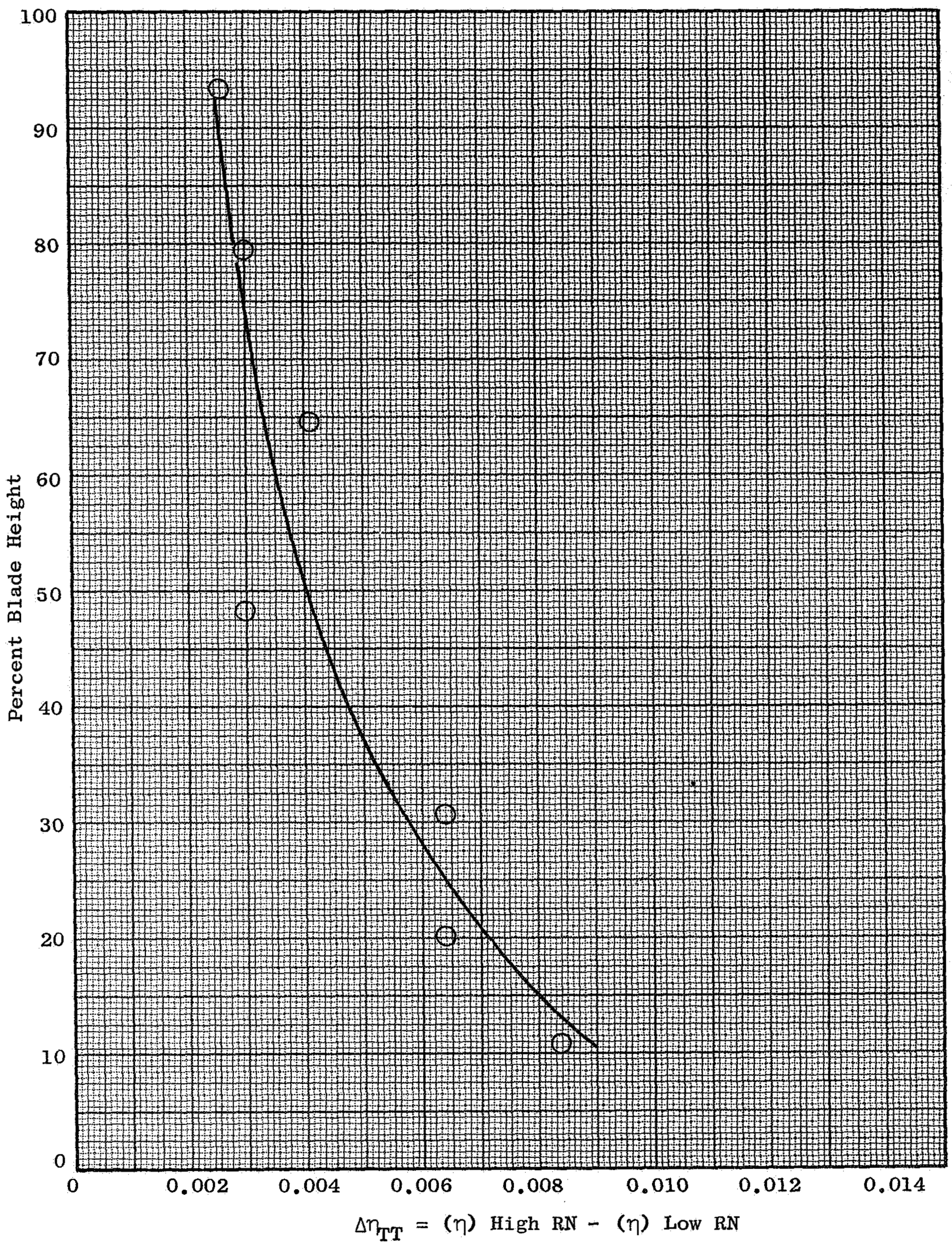

Figure 38. Percent Blade Height Vs. Change in Efficiency for High and Low Reynolds Numbers.

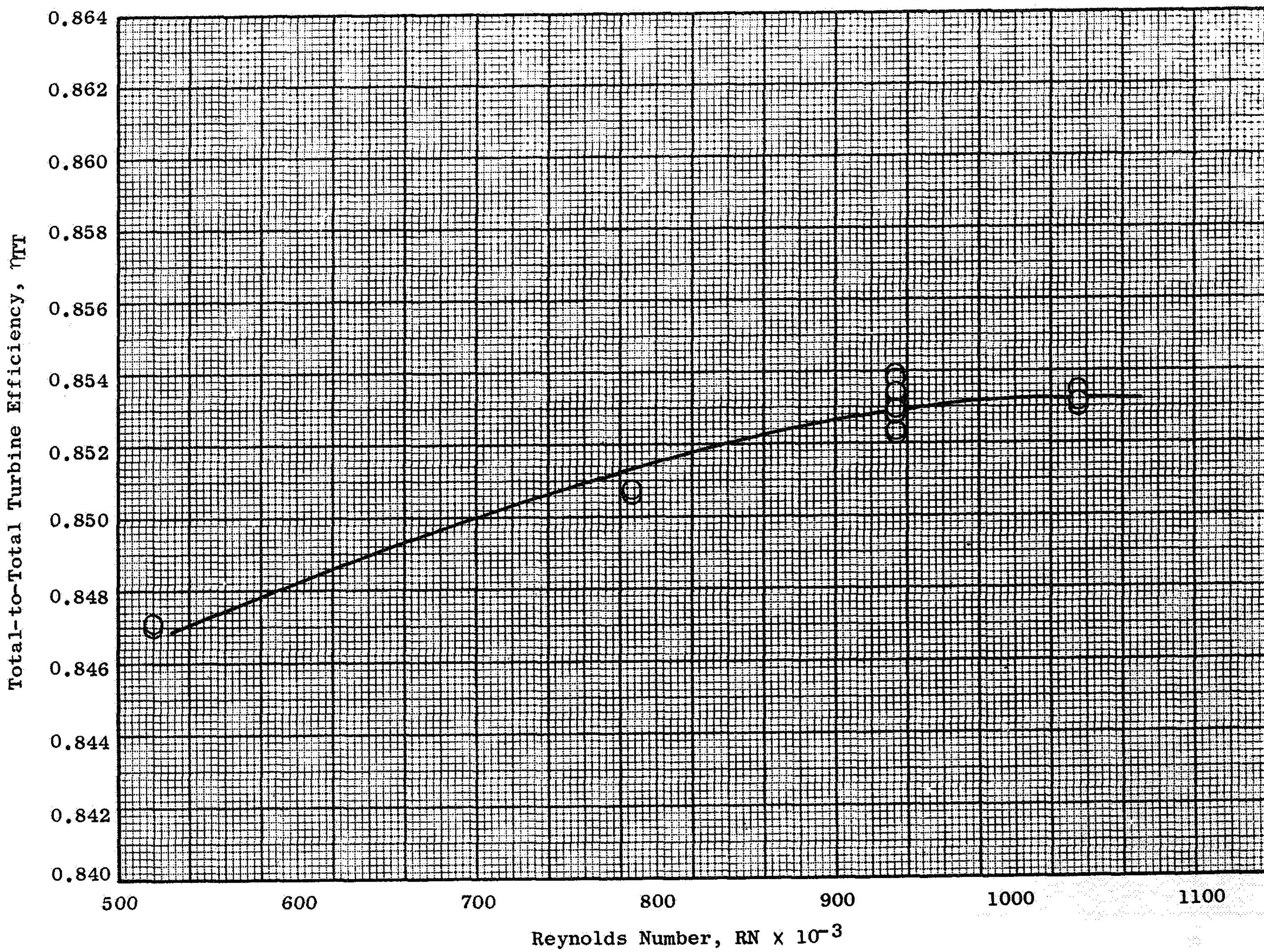

Figure 39. Total-to-Total Turbine Efficiency Vs. Reynolds Number at Design Equivalent Speed.

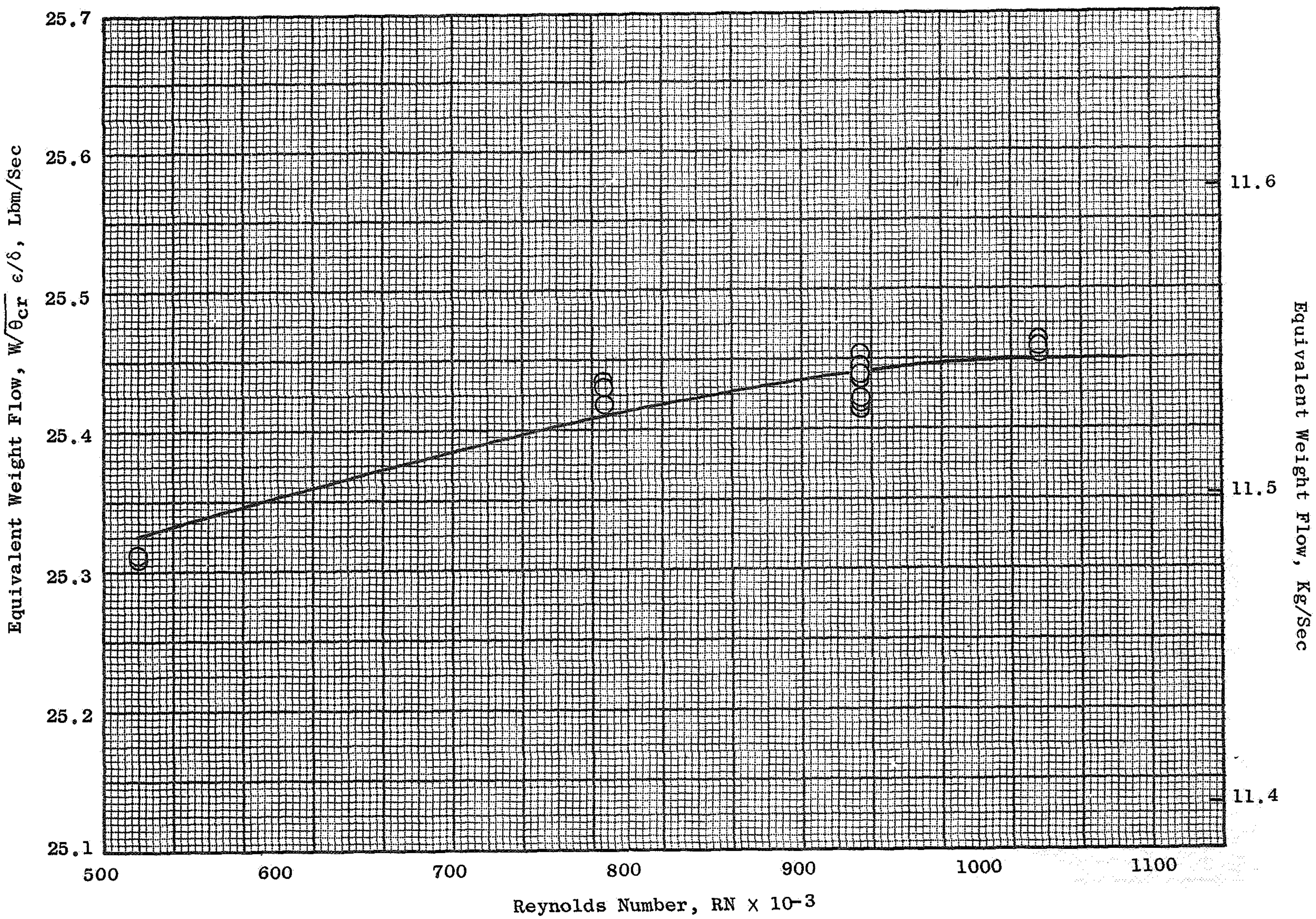

Figure 40. Equivalent Weight Flow Vs. Reynolds Number at Design Equivalent Speed.

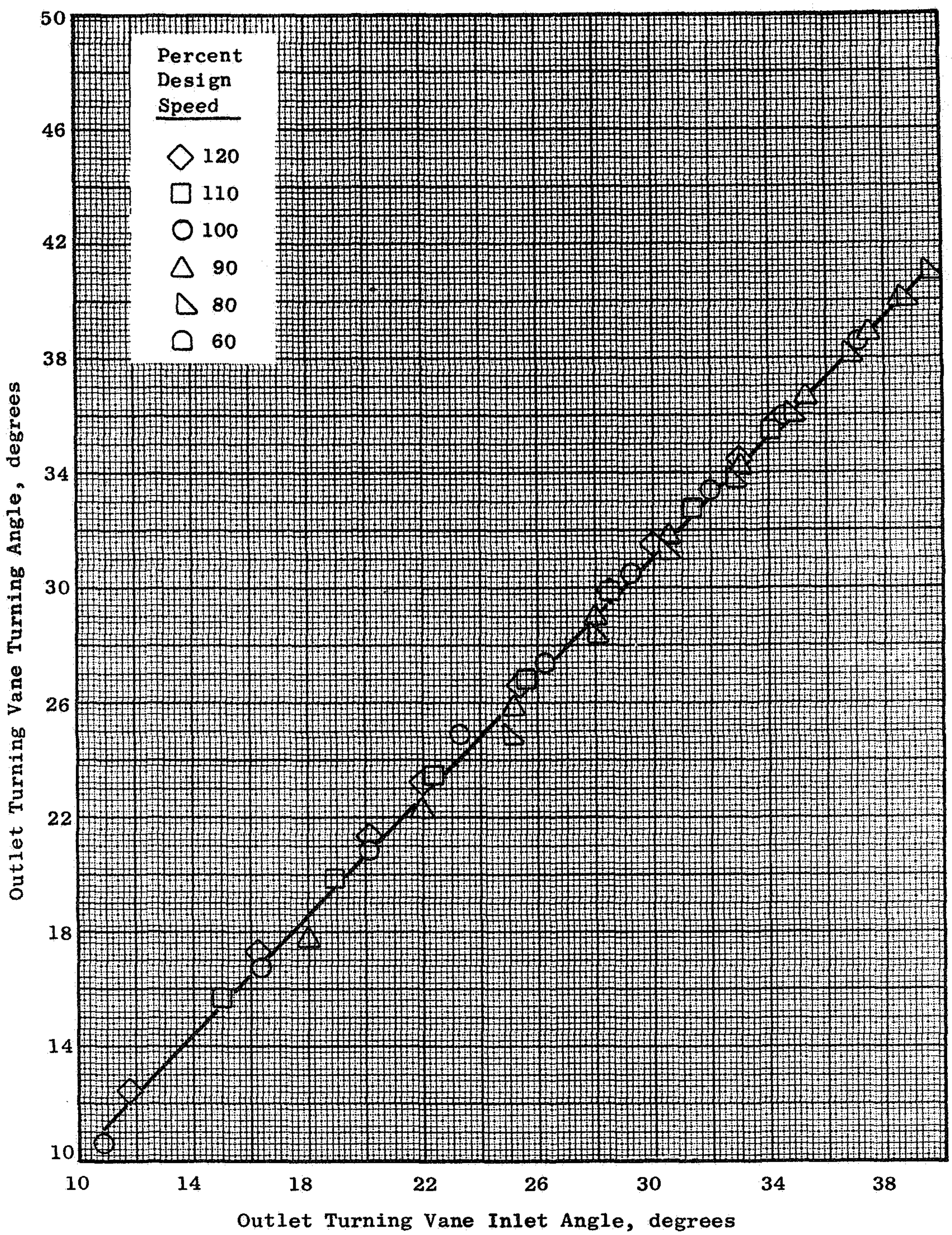

Figure 41. Outlet Turning Vane Turning Angle Vs. Outlet Turning Vane Inlet Angle at the Pitchline.

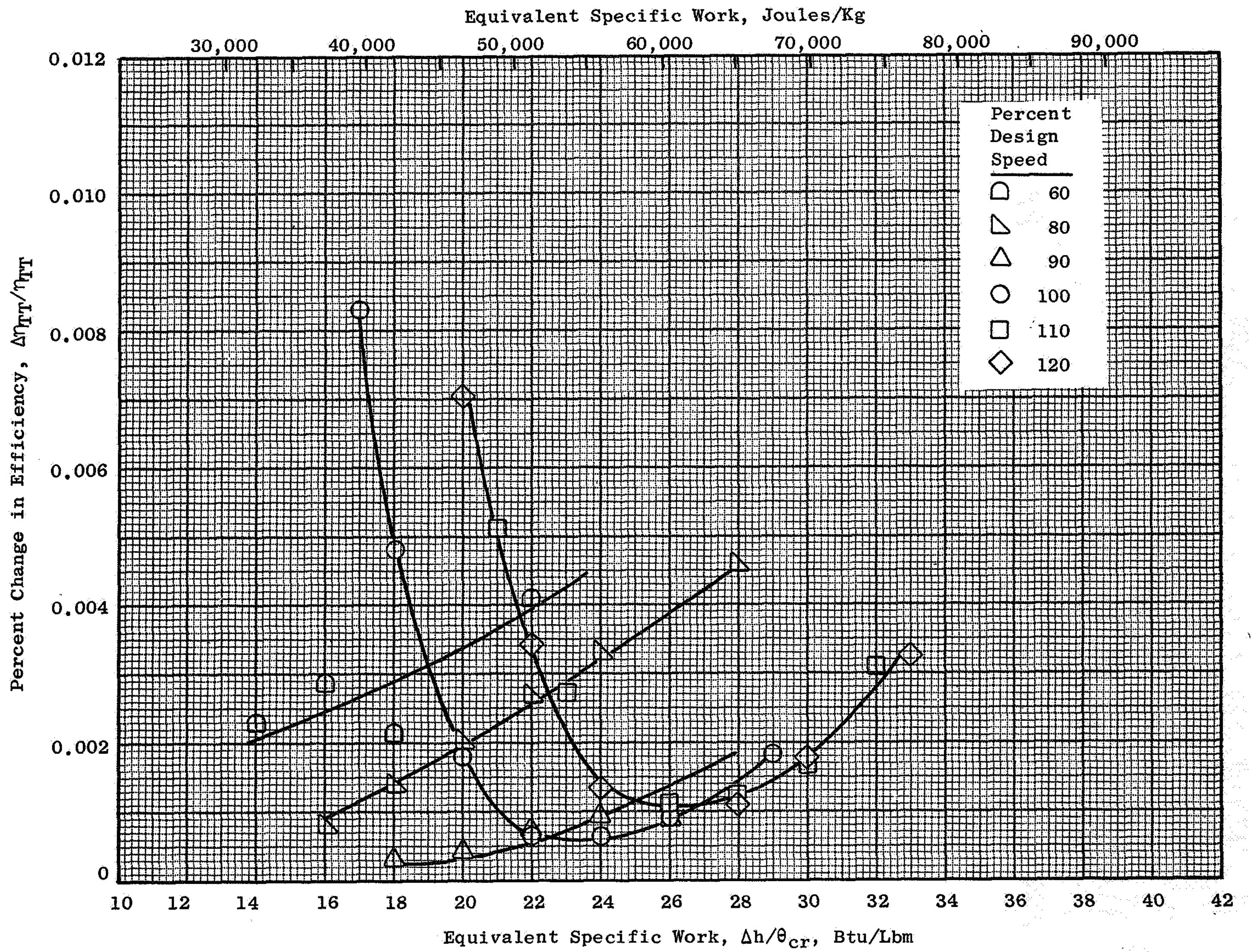

Figure 42. Performance Comparison of 4- and 4-1/2-Stage Turbines, Based on Calculated Exit Total Pressure.

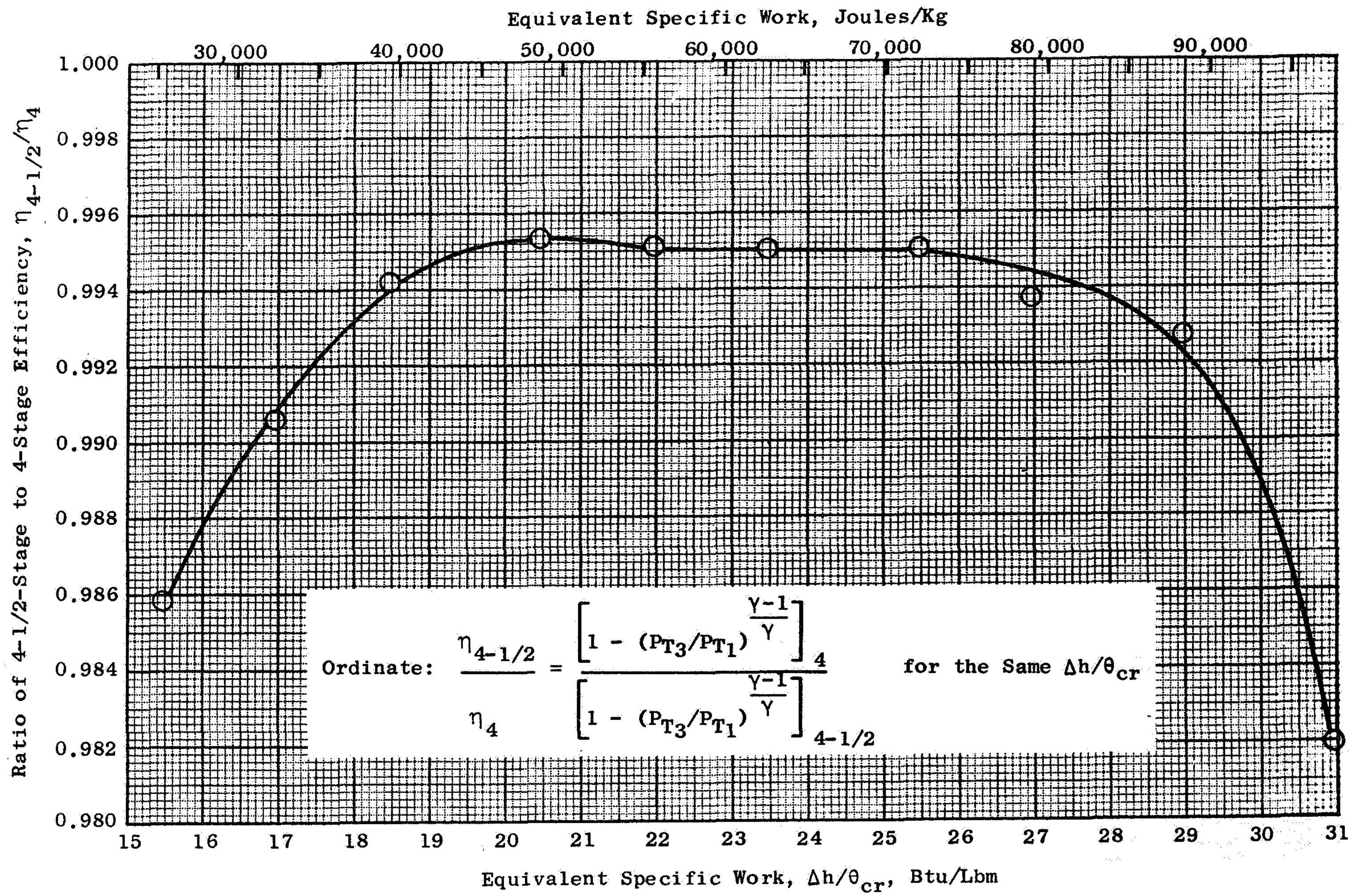

Figure 43. Performance Comparison of 4- and 4-1/2-Stage Turbines, Based on Measured Exit Total Pressure for 100% Design Speed.

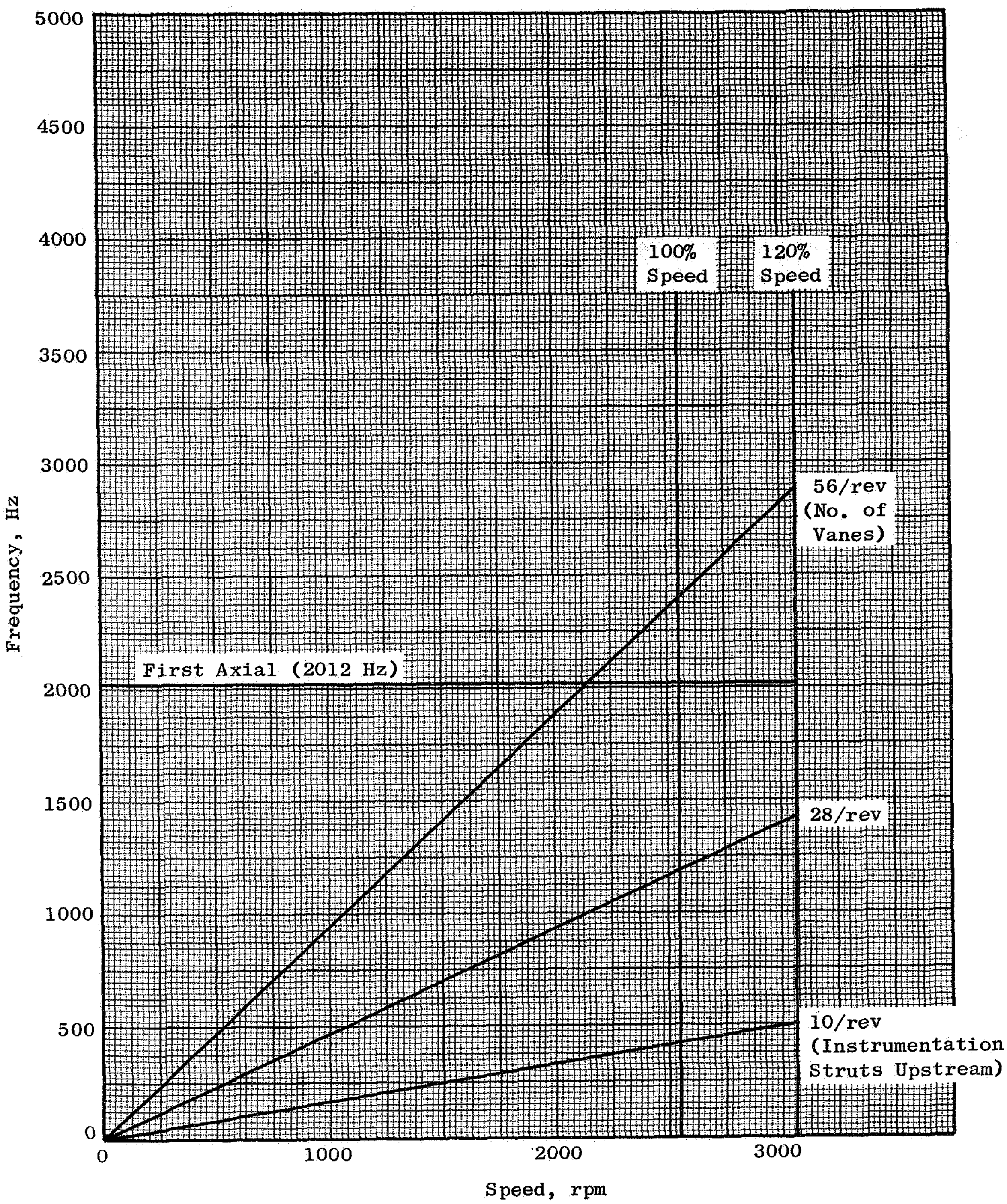

Figure 44. Most Probable Modes of Vibration, Stage One Blade.

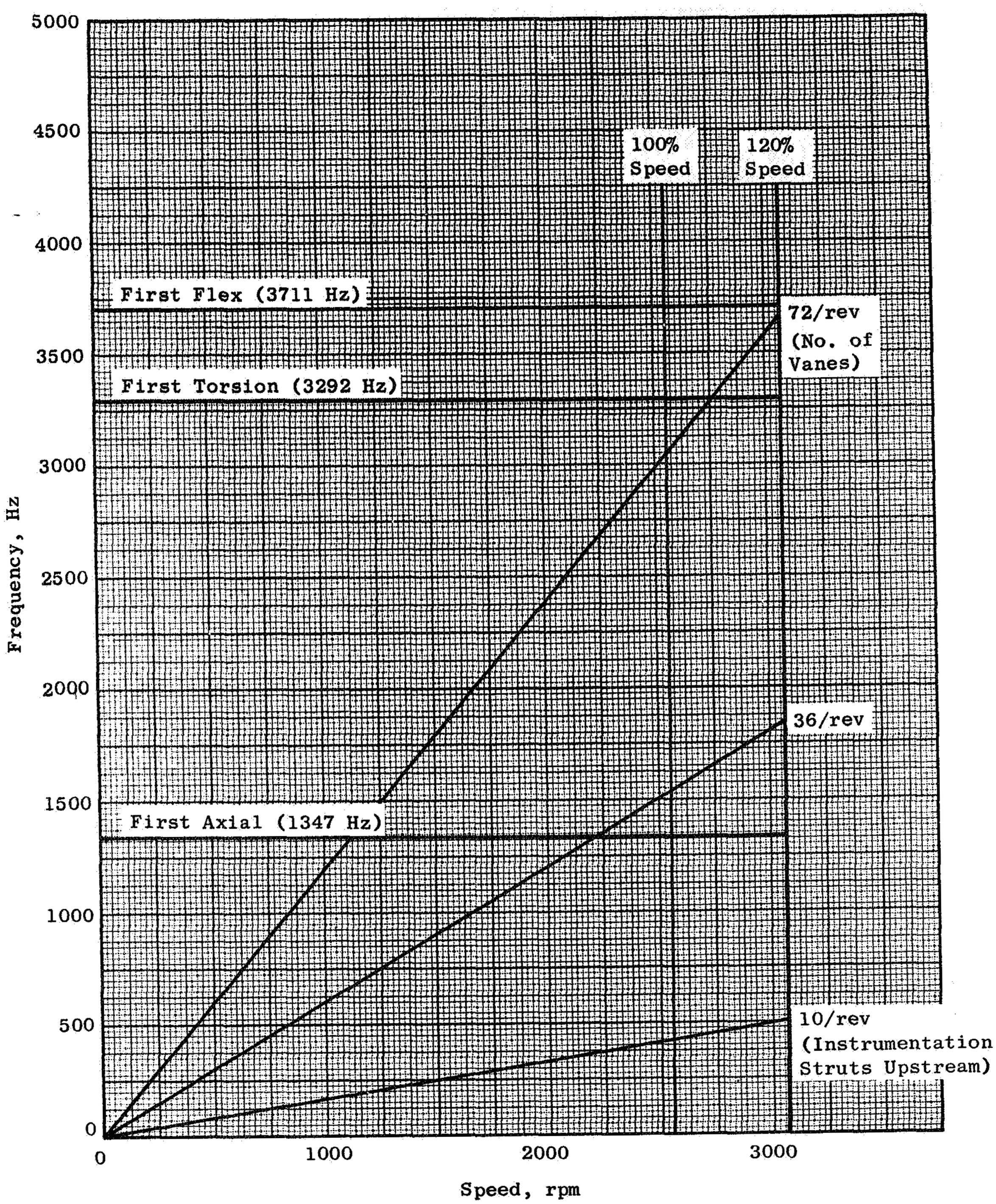

Figure 45. Most Probable Modes of Vibration, Stage Two Blade.

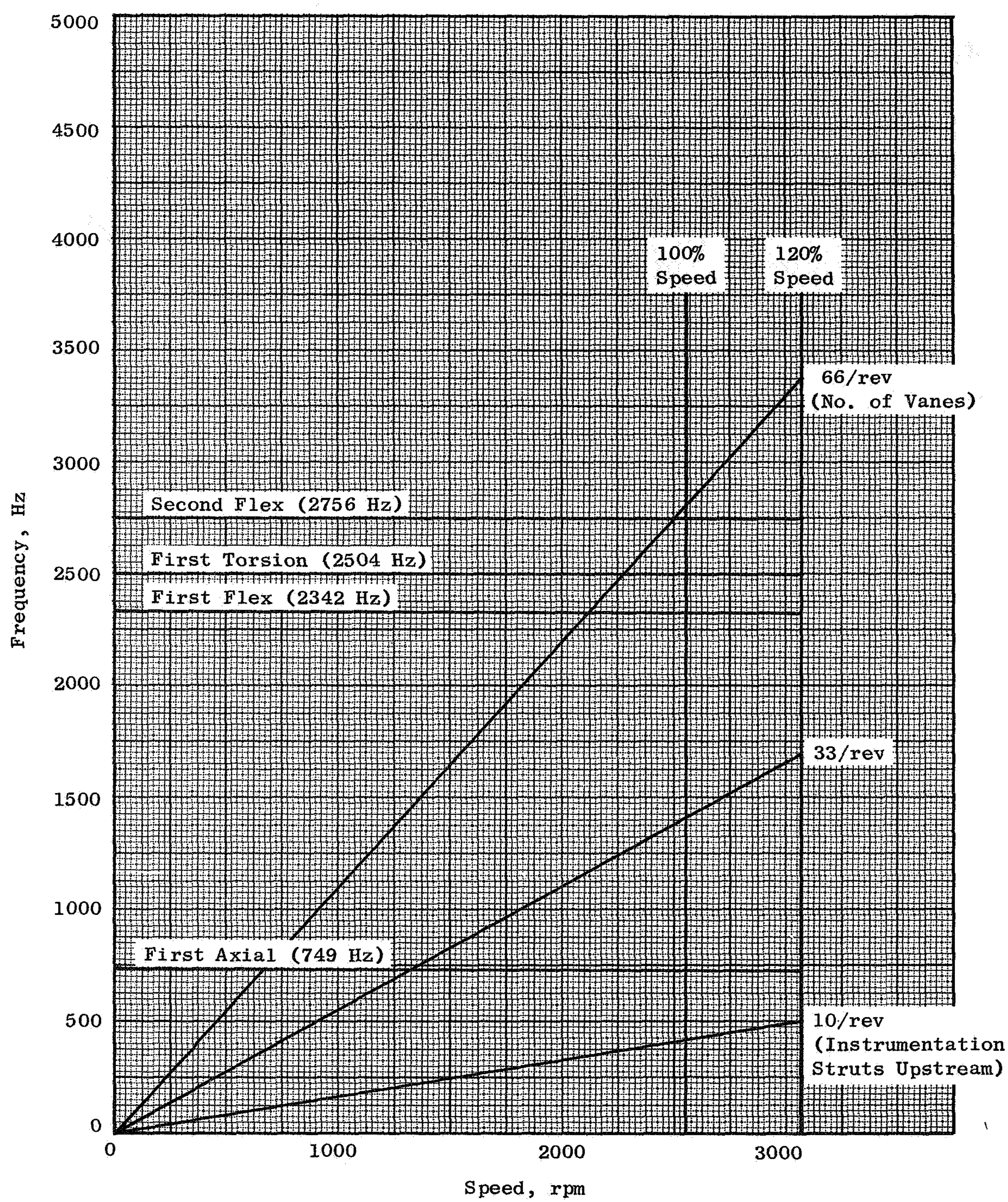

Figure 46. Most Probable Modes of Vibration, Stage Three Blade.

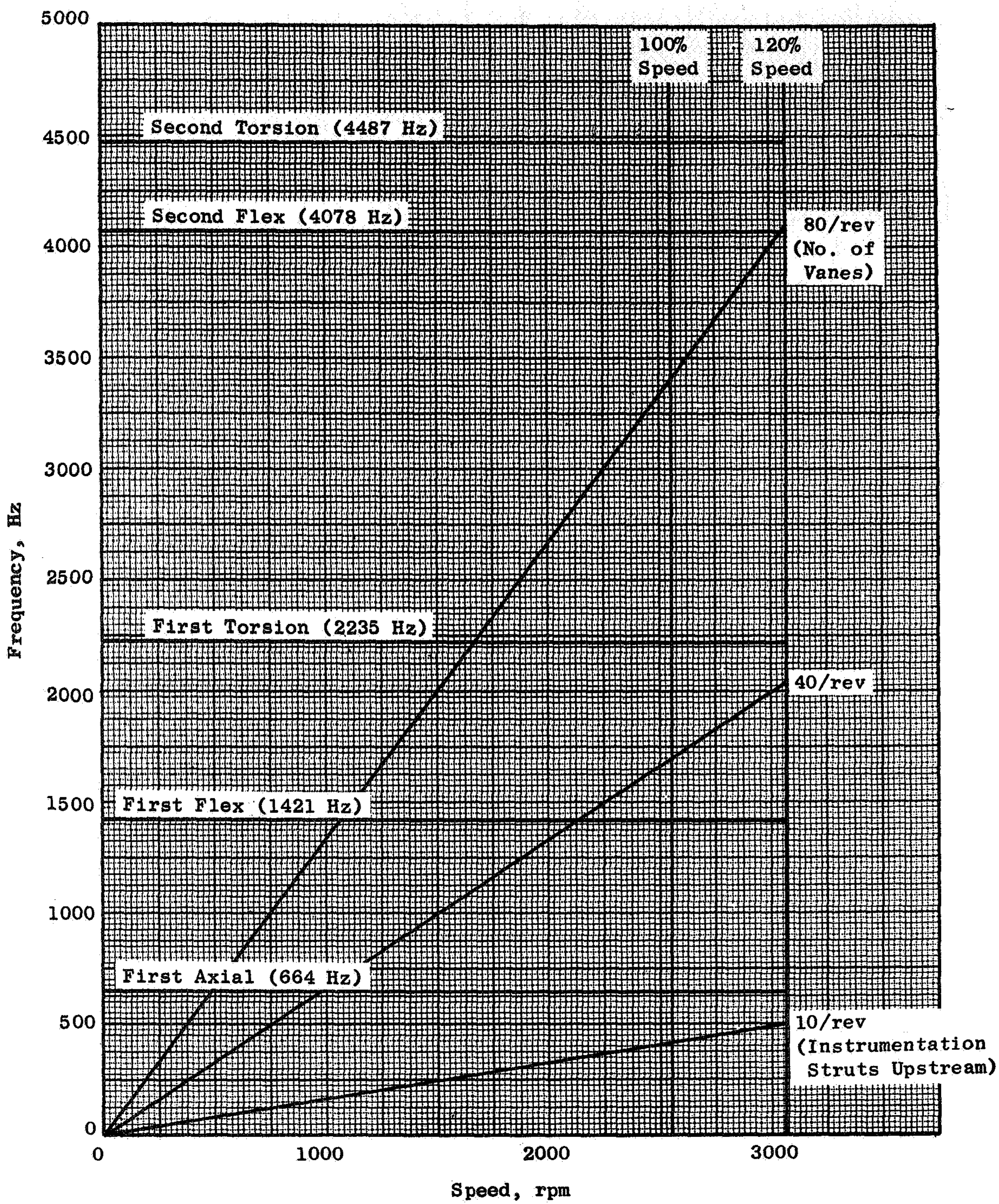

Figure 47. Most Probable Modes of Vibration, Stage Four Blade.

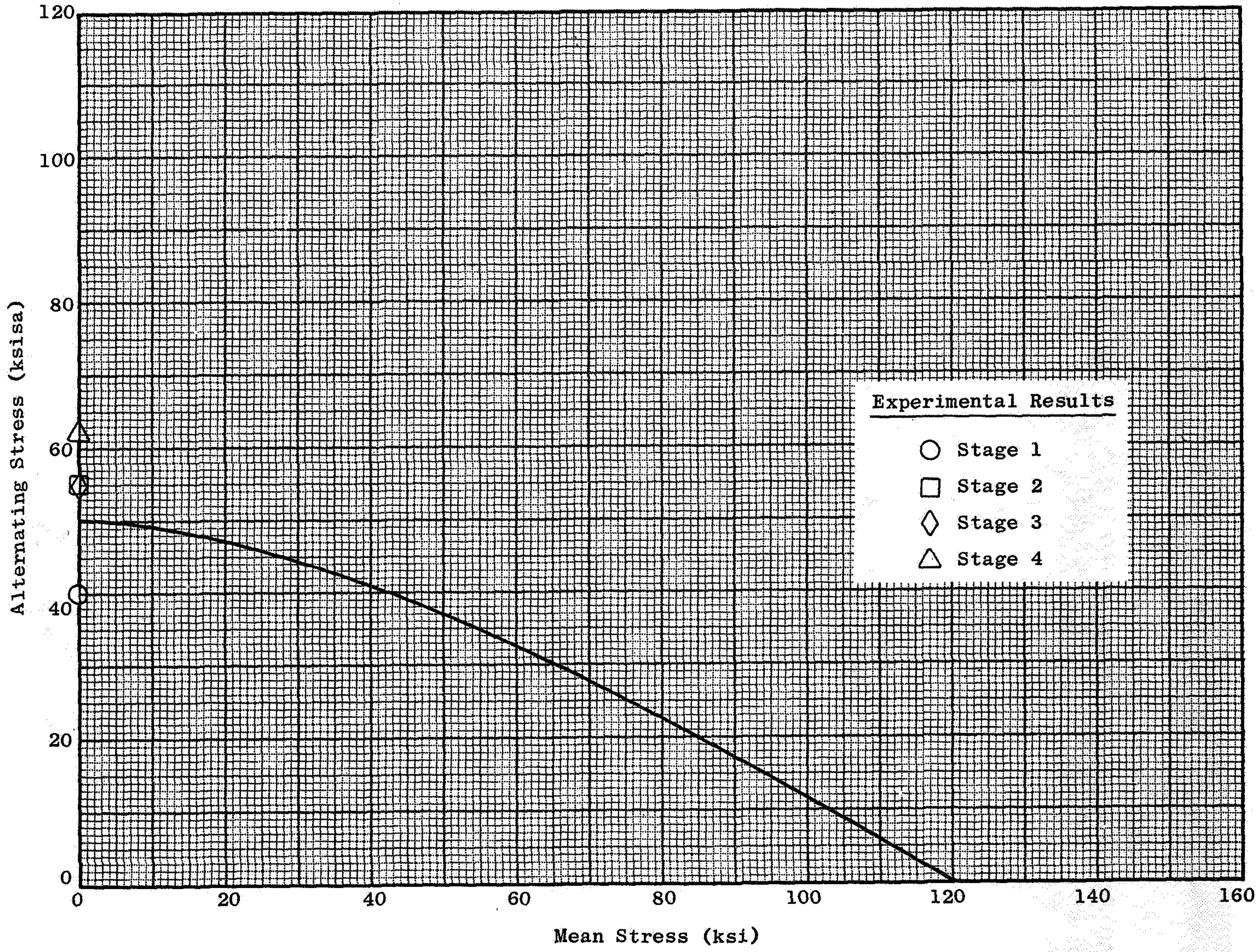

Figure 48. Goodman Diagrams for 410 Stainless Steel.

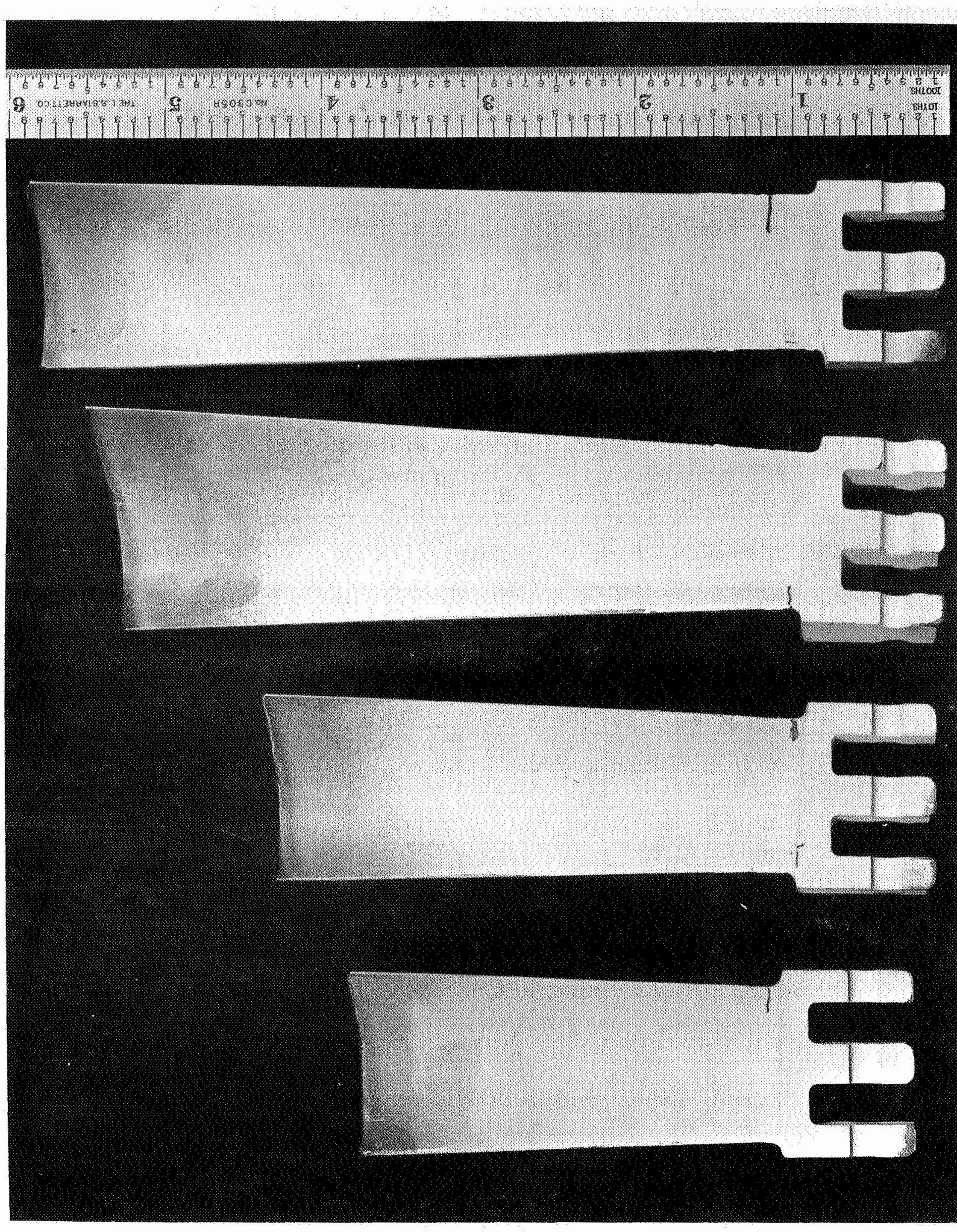

Figure 49. Fatigue Endurance Test Blade Failures.

NASA-Langley, 1974 E-7721

NATIONAL AERONAUTICS AND SPACE ADMINISTRATION
WASHINGTON, D.C. 20546

OFFICIAL BUSINESS
PENALTY FOR PRIVATE USE $300

SPECIAL FOURTH-CLASS RATE
BOOK

POSTAGE AND FEES PAID
NATIONAL AERONAUTICS AND
SPACE ADMINISTRATION
451

U.S.MAIL

POSTMASTER: If Undeliverable (Section 158 Postal Manual) Do Not Return

"The aeronautical and space activities of the United States shall be conducted so as to contribute . . . to the expansion of human knowledge of phenomena in the atmosphere and space. The Administration shall provide for the widest practicable and appropriate dissemination of information concerning its activities and the results thereof."

—NATIONAL AERONAUTICS AND SPACE ACT OF 1958

NASA SCIENTIFIC AND TECHNICAL PUBLICATIONS

TECHNICAL REPORTS: Scientific and technical information considered important, complete, and a lasting contribution to existing knowledge.

TECHNICAL NOTES: Information less broad in scope but nevertheless of importance as a contribution to existing knowledge.

TECHNICAL MEMORANDUMS: Information receiving limited distribution because of preliminary data, security classification, or other reasons. Also includes conference proceedings with either limited or unlimited distribution.

CONTRACTOR REPORTS: Scientific and technical information generated under a NASA contract or grant and considered an important contribution to existing knowledge.

TECHNICAL TRANSLATIONS: Information published in a foreign language considered to merit NASA distribution in English.

SPECIAL PUBLICATIONS: Information derived from or of value to NASA activities. Publications include final reports of major projects, monographs, data compilations, handbooks, sourcebooks, and special bibliographies.

TECHNOLOGY UTILIZATION PUBLICATIONS: Information on technology used by NASA that may be of particular interest in commercial and other non-aerospace applications. Publications include Tech Briefs, Technology Utilization Reports and Technology Surveys.

Details on the availability of these publications may be obtained from:

SCIENTIFIC AND TECHNICAL INFORMATION OFFICE

NATIONAL AERONAUTICS AND SPACE ADMINISTRATION

Washington, D.C. 20546